UNCLASSIFIED

AD NUMBER

AD841518

NEW LIMITATION CHANGE

TO

Approved for public release, distribution unlimited

FROM

Distribution authorized to U.S. Gov't. agencies and their contractors; Critical Technology; 01 AUG 1968. Other requests shall be referred to Air Force Office of Scientific Research [Attn: SREP], 1400 Wilson Boulevard, Arlington, VA 22209.

AUTHORITY

AFOSR ltr dtd 12 Nov 1971

THIS PAGE IS UNCLASSIFIED

AD-A184 243

University of Utah

Department of Chemical Engineering

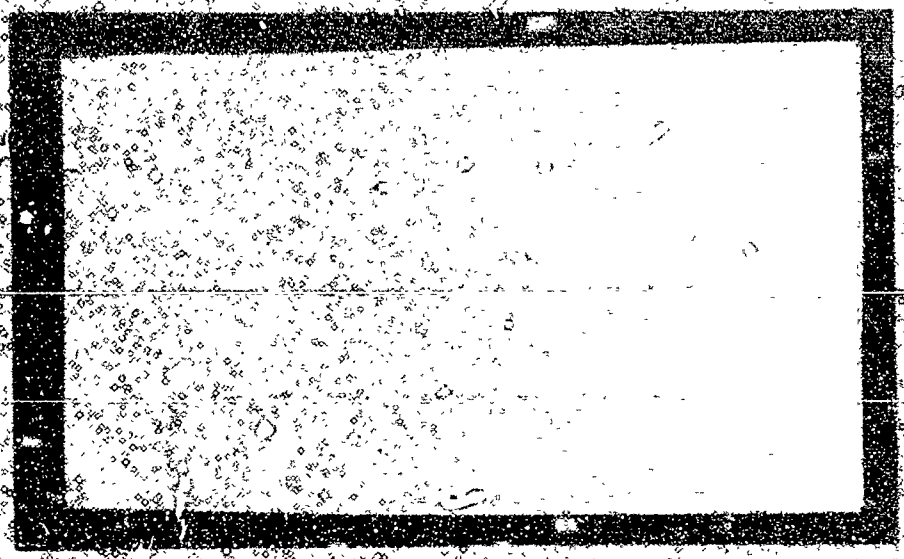

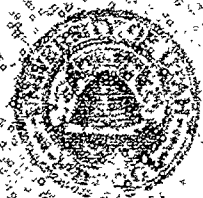

D D C
RECEIVED
OCT 8 2 1987
C

Salt Lake City, Utah

Technical Report

on

AMMONIUM PERCHLORATE-BASED PROPELLANT IGNITION BY LOW CONVECTIVE HEAT FLUXES

Under Air Force Grants 40-67 and 67-40A

August 1, 1968

This research under Grants AF AFOSR 40-67 and 67-40A, Project Task No. 9711-01, for the periods January, 1967 through June, 1968, was sponsored by the Air Force Office of Scientific Research Office of Aerospace Research, United States Air Force.

The Technical Supervisor for this program is Dr. Bernard T. Wolfson, Project Scientist Propulsion Division, Directorate of Engineering Sciences, Air Force Office of Scientific Research.

This report was prepared by C. P. Richardson, N. W. Ryan, and A. D. Baer.

Report approved by

A. D. Baer, Principal Investigator

TABLE OF CONTENTS

Page

ACKNOWLEDGMENTS iii

LIST OF FIGURES vi

LIST OF TABLES ix

ABSTRACT x

CHAPTER I: INTRODUCTION 1

CHAPTER II: APPARATUS AND PROCEDURE 11

A. Convective Heat-Flux Furnace 12
B. Propellant Sample Preparation. . . . . .
C. Ignition-Test Procedure. 16
D. Infrared-Detection System. 17
E. Polymer-Decomposition Test Procedure 19
F. Heat-Transfer Test Procedure 22

CHAPTER III: PRELIMINARY ANALYSIS OF IGNITION DATA 25

A. Ignition Model 26
B. Experimental Data. 32
C. Propellant-Ignition Test Data. 38

CHAPTER IV. FINAL ANALYSIS AND RESULTS OF IGNITION DATA. 45

A. Heat-Transfer Study. 46
B. Propellant-Ignition-Experimental Data. 51
C. Results and Interpretation of Ignition Data. 51

CHAPTER V: SUPPLEMENTARY STUDIES 59

A. Determination of the Time of the "Runaway" Reaction. . . 60
B. Long Sample-Ignition Studies 63
C. Rapid Heating of Polymeric-Fuel Binders. 66

1. Polybutadiene-Acrylic Acid-Copolymer-Decomposition Studies. 66
2. Polyurethane-Polymer-Decomposition Studies. 75
3. Polyflurocarbon-Polymer-Decomposition Studies . . . 75
4. Use of Convective Heat-Flux Furnace for Polymer-Decomposition Studies. 77

TABLE OF CONTENTS (continued)

Page

CHAPTER VI: CONCLUSIONS AND RECOMMENDATIONS 80

A. Measurement of Ignition Times 81
B. Convective Heat-Flux Furnace 82
C. Effect of Heat-Transfer Interpretation on Correlation of Ignition Data 82
D. Interpretation of the Ignition Test Data. 83
E. Ignition Tests of Relatively Long Propellant Samples. . . 85
F. Surface Temperature Measurements of Polymeric-Fuel Binders During Rapid Convective Heating. 85

LIST OF REFERENCES. 87

APPENDIX A: CALIBRATION OF THE FLOW CONTROL ORIFICE 93

APPENDIX B: MEASUREMENTS OF CRITICAL SYSTEM PARAMETERS. 95

A. Time Delay of Hot Gas Flow. 95
B. Gas Temperature Measurements. 97
C. Pressure in the Test Section During Tests 97

APPENDIX C: HEAT-TRANSFER STUDY EMPLOYING PLATINUM FILM RESISTANT THERMOMETERS. 100

A. Heat-Flux Gage Construction and Calibration 100
B. Heat-Flux Tests 102

APPENDIX D: HEAT-TRANSFER STUDY WITH THE INFRARED DETECTION SYSTEM. 106

A. Calibration of the Infrared Detection System. 106
B. Heat-Transfer Measurement Tests 111
C. Thermal Responsivity Measurements of Simulated Propellant 111
D. Calculation of the Heat-Transfer Coefficients 113

APPENDIX E: TABLES OF DATA. 116

APPENDIX F: THE HEAT-TRANSFER COMPUTOR PROGRAM. 145

A. Program Description 145
B. Definition of Program Variable Names. 145

APPENDIX G: NOMENCLATURE. 150

LIST OF FIGURES

Figure		Page
1.	Convective-Heat Flux Furnace Apparatus.	.13
2.	Cross-Sectional View of the Convective Heat-Flux Furnace.	.14
3.	Cross-Sectional View of the Test Section.	.15
4.	Test Section and Accessories.	.18
5.	Typical Oscilloscope Records of Ignition Tests.	.20
6.	Cassegraine system.	.21
7.	Electrical Circuitry of the Infrared-Detection System . .	.23
8.	Idealized Surface-Temperature History of a Semi-Infinite Slab of Propellant Undergoing Simple Thermal Ignition	.27
9.	Calculated Dimensionless Ignition Times as a Function of the Dimensionless Mean-Surface-Heat Flux.	.31
10.	Heat-Transfer Coefficients Calculated from Tests Where the Alumina Gage was Employed, Correlated in Terms of the Nitrogen Gas-Mass-Flow Rate	.34
11.	Heat-Transfer Coefficients Calculated from Tests Where the Alumina Gage was Employed, Correlated in Terms of the Helium Gas-Mass-Flow Rate	.36
12.	Correlation of the Heat-Transfer Coefficients in Terms of the Dimensionless-Parameters Nusselt Number . . .	.37
13.	Ignition Data of FM Propellant in Nitrogen with Mean-Surface-Heat Fluxes, Calculated From Alumina Gage Heat-Flux Study.	.39
14.	Ignition Data of FM Propellant in Nitrogen with Mean-Surface-Heat Fluxes, Calculated From Alumina Gage Heat-Flux Study, Illustrating Effect of Gas Temperature.	.40

LIST OF FIGURES (continued)

Figure		Page
15.	Ignition Data of FM Propellant in Nitrogen with Mean-Surface-Heat Flux Calculated from Alumina Gage Heat-Flux Study, Illustrating the Effect of Pressure	41
16.	Ignition Data of FM Propellant in Helium with Mean-Surface-Heat Flux Calculated from Alumina Gage Heat-Flux Study	43
17.	Heat-Transfer Coefficients for Different Gas Temperatures, Calculated from GAR Heat-Flux-Test Data, Plotted as a Function of Time	48
18.	Mean-Heat-Transfer Coefficients, Calculated from GAR Heat-Flux-Test Data at the Propellant Ignition Time and the Propellant Linear Ignition Temperature, Correlated as a Function of the Gas-Mass-Flow Rate	50
19.	Ignition Data of UA Propellant in Nitrogen with Mean-Surface-Heat Fluxes Calculated from the GAR Heat-Flux Study	52
20.	Ignition Data of FM Propellant in Nitrogen with Mean-Surface-Heat Fluxes, Calculated from the GAR Heat-Flux Study	53
21.	Ignition Data of G Propellant in Nitrogen with Mean-Surface-Heat Fluxes, Calculated from the GAR Heat-Flux Study	54
22.	Ignition Data of FM and UA Propellants in Nitrogen with Mean-Surface-Heat Fluxes, Calculated from the GAR Heat-Flux Study	56
23.	Typical Oscilloscope Records of AR-Propellant Ignition Tests, Illustrating Simultaneous Rise of the Photo-Diode Output and the Large Surface Temperature Rise	61
24.	Surface Temperature Histories of AR and Graphite-Coated AR Propellant Samples During Ignition Tests in Nitrogen	62
25.	High-Speed Photographs of the Ignition of Long FM Propellant Samples in Nitrogen	64

LIST OF FIGURES (continued)

26. Surface Temperature Histories of PC and Graphite Coated PC Polymer Samples During Rapid Heating Tests in Nitrogen at 760°C and 2.9 atm. . . . 67

27. Surface Temperature Histories of PC Polymer Samples During Rapid Heating Tests in Nitrogen at 1300°C and 2.9 atm 69

28. Photomicrographs (5X) of Surfaces of PC and A05 Polymer Samples After Rapid Heating Tests in Nitrogen. 71

29. Surface Temperature Histories of GAR and Graphite-Coated GAR Samples During Heat-Flux Tests in Nitrogen at 1000°C and 2.9 atm. 73

30. Surface Temperature Histories of GAR Samples in Nitrogen at 1300°C and 7.7 atm. 74

31. Surface Temperature Histories of PUC Polymer Samples During Rapid Heating Tests in Nitrogen at 1000°C and 2.9 atm 76

32. Surface Temperature Histories of PFC Polymer Samples During Rapid Heating Tests in Nitrogen at 1000°C and 2.9 atm 78

33. Typical Oscilloscope Records of Indicated GAR Surface Temperature Rise in millivolts. 96

34. Oscilloscope Records of Gas Temperature in the Channel of the Test Section 98

35. Electrical Circuitry Diagram for Temperature Measurements with Heat-Flux Gages 102

36. Sketch of Infrared Detection System Calibration Disc .107

37. Typical Oscilloscope Record of Infrared Detector Calibration Tests 108

38. Calibration Curve for the Infrared-Detection System. .110

39. Background Emissions from Polished and Graphite-Coated Brass Plug During Rapid Heating Tests. . .112

40. Program-Flow Chart of Heat Transfer Coefficient Calculations. 148

LIST OF TABLES

Table	Title	Page
I.	Composition of Propellants and Polymeric Fuel Binders.	117
II.	Thermophysical Properties of Propellants, Ingredients, and Polymer Fuel Binder at 60°C	119
III.	Flow Rates and Flow Control Orifice Data	120
IV.	Summary of FM Propellant Ignition Tests in Nitrogen.	121
V.	Summary of G Propellant Ignition Tests in Nitrogen	124
VI.	Summary of UA Propellant Ignition Tests in Nitrogen.	127
VII.	Summary of FM Propellant Ignition Data in Helium	130
VIII.	Summary of G Propellant Ignition Data in Helium.	132
IX.	Summary of UA Propellant Ignition Data in Helium	133
X.	Summary of Alumina Gage Heat-Transfer Study in Nitrogen.	134
XI.	Summary of Alumina Gage Heat-Transfer Study in Helium.	137
XII.	Heat-Transfer Study in Nitrogen Employing the Infrared-Detection System and Simulated Propellant GAR	138
XIII.	Summary of 1.9 cm-long Propellant Sample Ignition Tests in Nitrogen	141
XIV.	Polymeric Fuel Binder Decomposition Studies.	142
XV.	Data From GAR Thermal Responsivity Measurements.	144
XVI.	Listing of Heat-Transfer Program	146

ABSTRACT

The ignition response to convective heating of a series of ammonium perchlorate-based composite propellants was determined. Surface-heat fluxes in the range of 2-50 cal/(cm)^2(sec) were employed at pressures of 2-10 atmospheres of nitrogen or helium. Ignition times were determined by use of photoconductive detectors which indicated the appearance of first flame in the dark convective heating environment. The light signal was shown to correspond in time to the rapid rise of surface temperature measured by means of infrared radiation from the surface.

An electrically heated, pressurized furnace was constructed to supply hot gases to heat the propellant samples. The hot gases flowed from the furnace into a 0.2- x 0.4-inch rectangular channel. Razor cut propellant samples formed part of one of the 0.4-inch surfaces of the channel: and a quartz window, through which the sample was viewed, formed the opposing wall. The flow rate of the hot gas in the channel was determined by the aperture of a small nozzle placed on the outlet end of the flow channel. Flow through the channel was started by bursting a frangible diaphragm which covered the nozzle. Gas temperatures from 600-1350°C, at flow-Mach numbers from 0.02-0.29, were employed to yield reproducible ignition times from .02 to 20 seconds under essentially constant pressure conditions.

A satisfactory characterization of the transient heat-transfer process in the apparatus was found to be a difficult and most critical part of the study. An unsuccessful attempt to characterize the heat-transfer

rates, from the hot gas to the propellant, was made by the use of conventional heat-flux gages to obtain heat-transfer data. When surface temperature histories of propellant-like materials were measured by use of infrared radiation measurements, it was found that the apparent heat-transfer coefficients decreased as the surface temperature rose. Possibly, non-uniform gas-flow occurred in the assymetrically cooled channel with propellant on one side and the quartz window on the opposite side. When a heat-transfer characterization was developed which accounted for the change in the heat-transfer coefficients, it was possible to obtain meaningful interpretation of the ignition data.

The ignition times could be correlated as a function of the mean surface-heat flux; and, except for their measured effect on the heat-transfer rates, no effect of gas velocity, pressure, or gas composition on the ignition times was noted. Changes in surface texture resulting from the use of various sizes of oxidizer particles showed no significant effect on ignition times for the range of heating times employed in these tests.

Close agreement was found between ignition data derived from these tests when a gas temperature of 750°C was used and previously reported data from the thermal radiation heating of the same propellants. When convective heating-gas temperatures above 1000°C were used, it was found that the ignition times were about 80 per cent of the values observed at the same mean-heat flux for radiative heating and for tests at lower gas temperatures. In all cases, it was possible to represent the ignition data in terms of a thermal ignition model which considers a single, exothermic, Arrhenius type surface reaction. The indicated activation energy for this

reaction is 25-30 kcal/gm mole under all conditions; however, the pre-exponential factor is higher by a factor of five when the higher temperature convective heating gases were employed than under other conditions. It is postulated that reactions in the thin high-temperature boundary layer yield additional energy or reactive species which feed energy back to the surface. Since the activation energy is unchanged, it is presumed that the decomposition reaction of the ammonium perchlorate limits the initial reactive species.

CHAPTER 1

INTRODUCTION

Solid-propellant rockets have been much used by the military services as tactical weapons and as ballistic missiles and for many special applications in the exploration of space. For each specific rocket developed, a propellant-ignition system has to be designed, and as performance and reliability requirements are increased, the demands on the igniter-design engineer become greater. The design is subject, not only to constraints from cost and reliability considerations, but because of the desire to subject complex instrumentation and the propellant itself to predicted physical disturbances. Existing correlations must be improved and new correlations developed, and there is a need for a fundamental basis for rating igniter performances. As in the past, major improvements in design techniques will be developed as the result of empirical testing; however, fundamental information concerning the nature of the various processes which occur during ignition of a solid-propellant-rocket engine is essential to guide such tests. Eventually, when the processes involved in motor ignition are well understood, it may be possible to optimize the igniter design as part of the whole missile system.

The process of ignition of a solid-propellant motor may be divided into four aspects: (1) the characteristics of the igniter as a source of chamber-pressurizing gas and of energy transfer to the propellant surface; (2) the response of the propellant to the environment generated by the igniter; (3) the spread of the flame over the propellant surface; and (4) the pressurization of the rocket chamber to a steady-state condition. The relative importance of each step depends on the size and geometry of the motor. In a small motor, step (2) may be of prime importance; while, for a very large motor, step (3) may be most significant. The igniter per-

formance and the chamber-filling processes are closely coupled, and both are always important.

Igniter performance has been studied by several investigators [2, 12, 13, 25]. Keller [25] studied the effect on propellant ignition of environmental factors such as; (1) the type of convective gas employed, (2) the velocity of convective gas across the propellant surface, and (3) the magnitude of externally-applied heat flux. Allan and Bastress [2] correlated-experimental data with a theoretical model to predict heat transfer from igniter products to solid-propellant surfaces for head-end ignition systems.

The filling and pressurization of the rocket chamber is basically a mass and energy-balance problem. Adams [1] reports the ability to predict the effect of igniter-mass-discharge rate on the chamber-pressure transients by solving, numerically, the governing equations for the ignition element, motor chamber, and motor discharge.

The spread of flame over the propellant surface has been studied in several laboratories [24, 31, 36, 53]. The results of this study are difficult to generalize, since this process is related to the propellant response, the rocket-chamber conditions and the aerodynamic processes in the chamber. Lukenas, *et al.* [31] reports conditions under which the completion of flame spreading takes place after fifty per cent of the equilibrium-chamber pressure had been reached which indicates a need to consider a coupling of the two steps. If the igniter characteristics are well known, completion of flame spreading can be estimated from plots of chamber pressure versus time.

Since all the processes are coupled to the propellant response, this step is, perhaps, most important and is the process considered here. Good

experimental results may be obtained in laboratory tests, and these data can be correlated to lead to formal theories. Since the motivation for an interpretation of much of the experimental-ignition-response data is related to proposed ignition theories, a brief review of current theories is necessary for a discussion of prior experimental tests.

The controlling mechanism for the ignition of solid propellants is not thoroughly understood. There is a basic disagreement among the various investigators concerning the site of the precursor-exothermic-energy release which leads to steady burning of the propellant. There are three possible sites: (1) in the condensed phase, (2) at the surface, or (3) within the gas phase with energy feed back to the surface; thus, there are three separate theoretical models. The first model proposed was due to Hicks [30] and considers bulk-phase reactions to be of prime importance. If the reaction occurs at or very near the surface and the rate of the reactions is controlled by surface temperature, the model proposed by Baer and Ryan [8] may apply; and, if a hypergolic gas is present, a heterogeneous reaction, as proposed by Anderson and Brown [3, 5] will take place. If an oxidizing atmosphere exists, gas-phase reaction may take place between the gas and vaporized propellant as proposed by Summerfield and Mc Alevy [35]. These models and the critical assumptions required of each are summarized and discussed by Price, *et al.* [45].

It is desirable to formulate correlations which can describe propellant response for a wide range of igniter fluxes and environmental conditions. A great deal of effort has been directed to obtaining experimental data for such correlations. Tests have been made employing conductive, radiative, and convective modes of energy transport in neutral and reactive

environments at various pressures.

Conductive-heat-transfer methods were used in "hot wire" and "hot plate" propellant-ignition tests [4, 23, 27, 34, 39, 40]. Although the results of such tests are normally reproducible, interpretation of the data is difficult because of problems in accounting for pressure and gasification effects.

Radiant energy has been employed a great deal to ignite propellant samples. Thermal-radiation furnaces [7, 8, 39, 40, 49] have been used, and arc-image furnaces [11, 15, 18, 21, 46, 48, 52], in which high heat fluxes can be obtained almost independent of environmental conditions, have become almost a standard-test device. In the arc-image furnace, the applied heat fluxes may suddenly be applied and removed by a shutter to generate "go-no-go" ignition data. The main disadvantage for the arc-image furnace is that the gas phase adjacent to the propellant surface is cold; and, if gas-phase processes are critical, application of arc-image furnace data to the prediction of propellant response to a practical igniter output would be most difficult. Also, pyrolysis from the propellant surface may absorb some of the incident radiation; or, if the surface is swept clean by gas flow, convective-heat losses from the sample surface will arise. Radiation absorption in depth can severely alter the dependence of ignition time on the external-heat-flux density which is an effect not likely to be of importance for convective-heat fluxes [43].

Although practical igniters produce radiative and conductive-energy transfer from igniter products to the propellant surface; normally, the majority of the energy is transferred by a convective process. Most theories postulate the propellant response to be independent of the mode

of energy transport. However, this assumption must be investigated by comparing experimental results of propellant response where similar energy fluxes are transmitted by the two modes. In order to make this comparison, we must have experimental data in which convective methods were employed.

The Department of Chemical Engineering at the University of Utah has utilized a shock tube apparatus as an energy source of hot gas to convectively heat solid propellants [7, 25, 37]. In the shock tube, a diaphragm separates the pressurized-driver gas from the driven gas. When the diaphragm is punctured, an incident-shock wave moves through the undisturbed gas in the driven end of the tube. The incident-shock wave is reflected at the closed end of the tube and moves back through the gas, causing it to be stagnated, compressed, and heated. If initial conditions of pressure, temperature, and composition in the shock tube are carefully controlled, this hot, high-pressure gas behind the reflected wave can be tapped and allowed to flow through a test section past a propellant sample to produce ignition.

The major attributes of the shock tube are its ability to produce hot gases for ignition tests in a matter of microseconds, and to heat a variety of gases of diverse chemical compositions. However, in the shock tube, the available test time is limited. In Keller's work [25], a maximum heating time of 40 milliseconds was reported.

Keller [25] concluded that the slow process in ignition, after the heating of the propellant surface to its thermal-ignition temperature, was the rate of decomposition of the ammonium perchlorate used as an oxidizer in his propellants. He also states that the ignition time for a

given propellant is a function only of the applied-energy flux, the initial-propellant temperature, and the kinetics of the key-ignition reaction. If the parameters are made dimensionless to account for different propellant-thermophysical properties and for different values of the pre-exponential factor used in an Arrhenius-type equation describing energy flux to the surface from the key-ignition reaction, the ignition time and external-flux relationship is adequately described. In fact, Keller was able to correlate the experimental data for convective-heat fluxes in the range of 20 to 160 cal/(cm)^2(sec) with data where a radiant-energy source was used in the heat-flux range of 1 to 13 cal/(cm)^2(sec) [7]. This correspondence occurred only for the conditions in which the gas velocity across the propellant surface was quite high or where the propellant surface was relatively smooth.

Keller concluded that the environmental conditions of the gas, the temperature, linear velocity, and oxidizing species, affected only secondary-ignition reactions for rough-surfaced propellants, and that these secondary-ignition reactions augmented the heat flux externally applied to the propellant surface.

Bastress and Niessen [10, 42] used the combustion products of CO-O_2-N_2 and H_2-O_2 mixtures as energy sources for convectively heating solid propellants with fluxes of 20 to 200 cal/(cm)^2(sec). Variations in energy flux were attained by altering the pressure, the composition, and velocity of the combustion products. Energy fluxes were varied during an ignition test by use of a variable-area-nozzle device controlling the gas-flow rate over the propellant surface. The effect of test-chamber configuration on propellant-ignition times was studied. Also, ignition tests

were made where different materials such as brass, quartz, and propellant were positioned upstream from the sample.

Niessen and Bastress [42] concluded that effects of gas pressure on ignition time were small compared with the effect of the energy-flux level for convectively-applied fluxes. Furthermore, the ignition temperatures calculated for constant and variable flux conditions were in good agreement, thus enabling the conclusion that the constant-flux data may be used for the development of igniter-performance requirements.

Bastress, *et al.* [10], reported that under test conditions where the propellant sample width was less than that of the test chamber, ignition times were reduced when the chamber width was reduced. It was postulated that this effect was the result of a difference in the mass concentration of propellant decomposition products in the boundary layer. Bastress also observed that the use of an inert approach surface upstream from the propellant sample resulted in ignition times greater than those measured with propellant as the approach material. Propellant samples one- to two inches long in the direction of gas flow ignited away from the leading edge of the sample. An increase in gas-flow velocity also increased the ignition time of the propellant sample; but this effect was reduced when the approach surface consisted of propellant.

The results of the efforts of Keller and of Bastress and Niesse indicated a need for additional work in the area of propellant response to convective heat flows. The use of the shock tube as an energy source is time-limited because of the onrush of cold gas. Also, unless the driven end of the tube is evacuated to a low pressure, the operating conditions for tests are at relatively high pressures. In the use of combustion products

it is difficult to accurately measure the temperature of the hot gases, and therefore, it is most difficult to separate gas-temperature effects on ignition time from heat-flux effects.

There is a need for a good comparison between experimental-ignition data where both convective and radiative modes of heat transfer were used separately. Good experimental data, where low-convective-heat fluxes are employed, should be obtained in such a manner that effects of test-gas temperature, pressure, velocity, and composition and, also, propellant-surface roughness, can be separated from the effects of heat fluxes externally applied to the propellant surface.

The primary objectives of this study were:

(1) To obtain ignition data for ammonium perchlorate-based propellants, convectively heated at rates of 2 to 50 $cal/(cm)^2(sec)$, and to compare these data with existing experimental results in which radiant-energy-heating rates of 2 to 13 $cal/(cm)^2(sec)$ were employed.

(2) To study the effect of surface roughness on propellant-ignition response at lower heat fluxes and longer ignition times than those employed by Keller, and to compare these results with those reported where heat fluxes of 20 to 120 $cal/(cm)^2(sec)$ were employed.

(3) To overlap and extend the work of Keller [25] to longer ignition times, 0.0146 to 20.0 seconds, in order that a wide range of experimental results may be evaluated for the theoretical correlations.

(4) To investigate the phenomena reported by Bastress, *et al.* [10] concerning the position at which ignition occurred when long samples are used, and to explain this process.

In order to complete these objectives, it was necessary to construct

an apparatus capable of convectively heating with a variety of gas compositions, igniting the propellant, and measuring ignition times for heat fluxes from 2 to 50 cal/(cm)^2(sec). The apparatus constructed was to be suitable for measuring ignition times for ammonium perchlorate-based propellants at gas temperatures from 500 to 1500°C, pressure from 2.5 to 8 atm, and at various gas-flow rates.

Early experimental results, in which this convective-flux furnace was employed for igniting double-based and composite propellants, have been reported in References [28] and [47]. It was apparent from these results that a more thorough study of the heat-transfer processes would be necessary, and a major fraction of the effort reported here was to develop a reliable heat-transfer characterization.

As a subsidiary investigation, the infrared detection system, employed previously by Keller [27], was used to measure-propellant-surface temperatures during ignition tests. This system was also used to measure the surface temperature of several polymeric-fuel binders during rapid heating.

The next chapter, "Apparatus and Procedure," describes in detail the convective-heat-flux furnace, the test section, infrared surface-temperature measuring system, as well as the sample preparation and procedure of the ignition tests. A discussion of the theoretical concepts involved and the development of the scheme of interpretation for these experimental data is then presented. The Appendices contain sections on the calibration of the critical-flow-control orifices, on furnace-gas-temperature measurements, and a detailed section on the heat-transfer study. Tables of the propellant ingredients and thermophysical properties of ignition and heat-transfer data are collected in Appendix E.

CHAPTER II

APPARATUS AND PROCEDURE

A. CONVECTIVE HEAT FLUX FURNACE

The hot gases used for the propellant ignition studies were generated by an electrically heated furnace which is shown pictorially in Figure 1 and in a cross-sectional sketch in Figure 2. This furnace maintained a 4.6 cubic-foot volume of nitrogen at pressures of 8 atm and temperatures up to 1350°C. The walls were insulated with porous insulating fire-brick. The furnace temperature was kept within ± 10°C of the desired value by a controller whose input signal came from a platinum-platinum-rhodium (13 per cent) thermocouple located in the furnace center. The thermocouple temperature was periodically checked by use of a calibrated optical pyrometer. A half-inch nickel tube delivered hot gas from the center of the furnace, through the wall, to a test section which was bolted to the furnace shell.

The test section, shown in Figure 3, contained a four-inch long channel of 0.2- by 0.4-inch cross section. Exchangeable critical-flow-control orifices were fastened to the outlet end of the channel. In all, seven different sized orifices were used, and the procedure for the calibration is discussed in Appendix A. Gas-flow rates through the flow channel were varied from 0.941 to 45.9 $gm/(cm)^2(sec)$. Table IV shows the gas-flow rates and Mach numbers in the test section for the different orifices when flow occurred with furnace pressures of 2.9 atm and 7.7 atm, and standard temperatures of 760, 1000, and 1300°C. The pressure in the test section was measured by the Statham PG 401 or a Kistler Model 401 pressure transducer, and the transducer output was recorded by photographing the oscilloscope screen upon which the pressure signal was displayed.

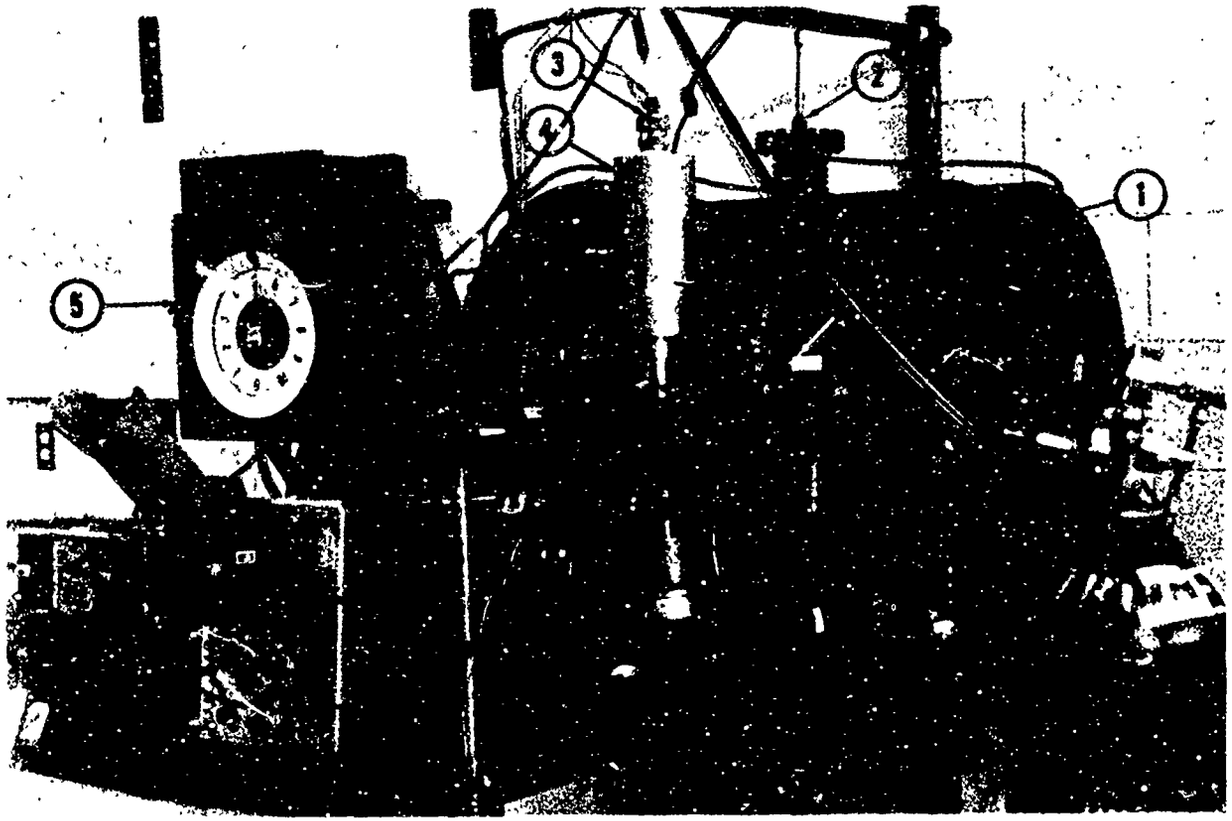

FIGURE 1. CONVECTIVE HEAT-FLUX FURNACE APPARATUS

(1) Furnace housing; (2) Thermocouple well; (3) Infrared detector; (4) Cassegraine focusing system; (5) Temperature controller; (6) Solenoid needle; (7) Slide valve; (8) Test section; (9) Pressure transducer; (10) Oscilloscope.

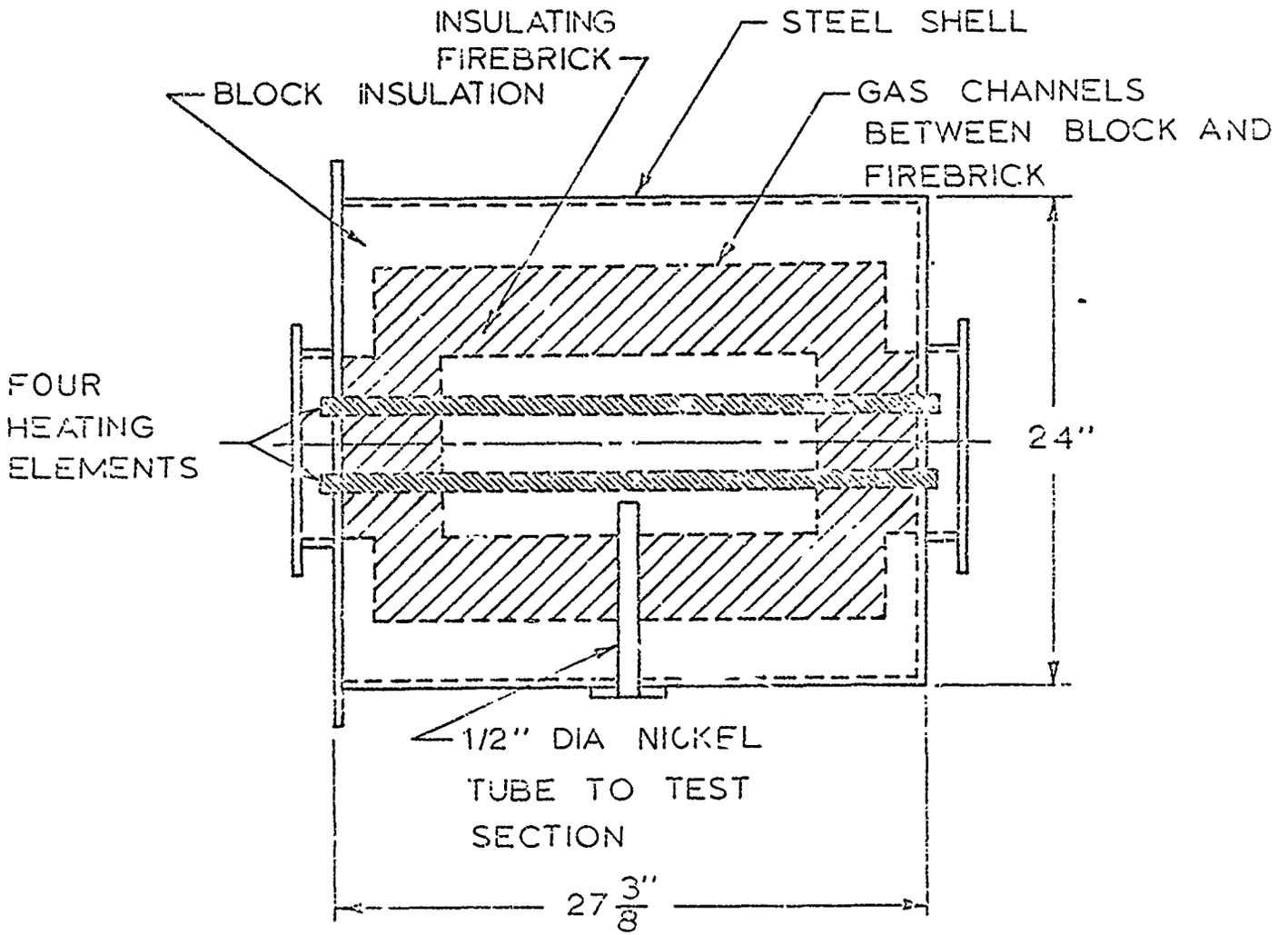

FIGURE 2. CROSS-SECTIONAL VIEW OF THE CONVECTIVE HEAT-FLUX FURNACE.

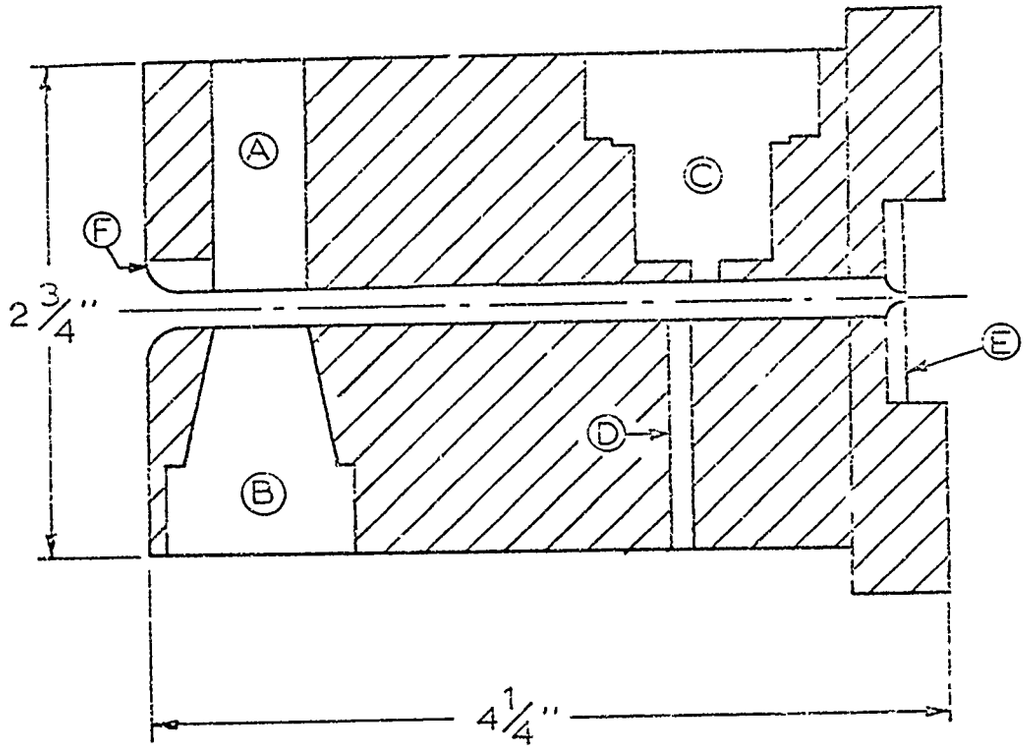

FIGURE 3. CORSS-SECTIONAL VIEW OF THE TEST SECTION.

Hot gas from the furnace flows from left to right through the 0.4-inch-wide by 0.2-inch-high center channel, past the propellant sample at (A), and through the control orifice (E) to the atmosphere. The sample surface, which is flush with the channel wall, is viewed by a IP-40 photocell through a quartz window (B). A pressure transducer mounts at (C), and cold gas for filling the test section to the furnace pressure enters at (D).

Propellant cast in the sample holders were mounted in the test section (Figure 3) so that the propellant surface formed part of the 0.4-inch wide channel wall. A quartz window, through which the sample could be observed, was installed opposite the propellant. The inlet region of the flow channel, which was upstream of the propellant sample, was constructed of fired pyrophylite.

A removable rectangular orifice, slightly smaller than the test section channel, was inserted just ahead of the inlet of the test section to insure a turbulent boundary layer across the propellant surface.

A solenoid-driven needle was used to rupture a friable diaphragm positioned across the downstream end of the test section. Disintegration of the diaphragm initiated the flow of hot gas past the sample surface. The first light of ignition was detected by an IP40 photocell, and the photocell output was displayed and photographed on the screen of a Tektronix Model 502 oscilloscope. The oscilloscope sweep was triggered simultaneously with activation of the solenoid-driven needle which ruptured the diaphragm.

B. PROPELLANT SAMPLE PREPARATION

The propellant and polymer fuel binders used in this study were mixed in the Department of Chemical Engineering at the University of Utah. Tables I and II show the composition and properties of the various propellants and fuel binders used.

Polymer and propellant mixtures containing Philblack E, a carbon black added to reduce the transmissivity of the polymers, were blended for

15 minutes in an Osterizer and then extruded through a small batch homogenizer. The polymers were cast directly into sample holders and then were held under a vacuum for an hour before curing. Propellants and polymers containing glass beads were mixed in a laboratory-sized sigma blade mixer under 0.7 psia of air pressure for forty minutes. The mixed propellants and glass-filled polymers were placed into sample holders, which were intentionally overfilled, and then the surfaces of the samples were tamped while under vacuum. All the samples were then cured at 80°C for seven days.

Sample holders, shown in Figure 4, were constructed of mild steel and contained cylindrically-shaped pieces of propellant about 1 cm in diameter and 1 cm deep. In some tests, propellant samples, which were 1.9 cm long, measured in the direction of gas flow, were prepared by casting into special holders (also shown in Figure 4). In all cases, the maximum propellant width was about 0.015 cm less than the test-section channel width.

C. IGNITION TEST PROCEDURE

Prior to each ignition test, a sample was prepared by cutting away the excess propellant with a new razor blade to give a smooth, flat surface. The sample was then fitted into the test section so that the propellant formed part of the channel wall.

A cellulose-acetate diaphragm was positioned on the test section; and during pressurization, cold gas was allowed to enter the test section at a pressure equal to that in the furnace, thus, protecting the sample from hot furnace gas. The flow of the hot gas was initiated by rupturing the diaphragm with a solenoid-driven needle and the oscilloscope was

FIGURE 4. TEST SECTION AND ACCESSORIES.

(1) Diaphragm holder; (2) Diaphragm; (3) Test section; (4) Slide valve; (5) Long sample holder filled with propellant; (6) Sample holder filled with propellant; (7) Pyrex heat-flux gage; (8) Alumina heat-flux gage; (9) Gas flow-control orifice.

triggered. Photocell and pressure transducer outputs were photographed on the oscilloscope. A typical oscilloscope record is shown in Figure 5. The rupturing of the diaphragm is indicated by the sudden drop in pressure; and the first flame of ignition is detected by the sudden rise in the IP40 photocell output.

Long propellant samples were ignited in a test section which was fitted with an observation window equal in length to the sample. During these ignition tests, a Fastax Motion Picture Camera was used to photograph the propellant surface through the window at a framing rate of 2000 per second; and the position of the first visible flame of ignition and the nature of the flame spread were observed.

D. INFRARED DETECTION SYSTEM

An infrared-detection system was constructed to record surface temperature histories of convectively-heated propellant samples, simulated propellants, and polymer fuel binders. The center portion of the heated surface was focused on to the sensitive element of an infrared detector by a Cassegraine system (Figure 6) through an Irtran 2 window mounted in the test section in the position normally occupied by the quartz window. The Cassegraine system contained only first surface mirrors. The Philco Model GPC-201A gold-doped-germanium photoconductive detector was filled with liquid nitrogen and the gas was evacuated to obtain a temperature near 63°K, the nitrogen triple point. The change in detectivity per unit change in temperature at 63°K is much less than at 77°K, the normal boiling point of nitrogen, and the lowered temperature was employed to produce

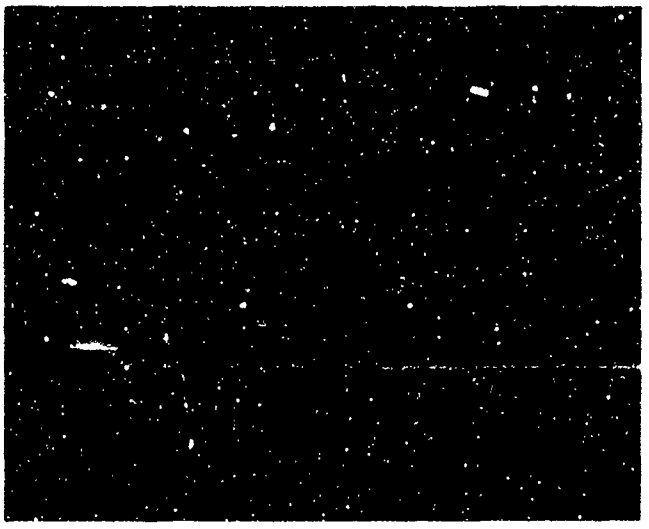

Pressure Scale:	+0.825	Time Scale:	0.02 sec/div
Propellant:	UA	Orifice Number:	3
Gas Temperature:	1303°C	Initial Pressure:	7.7 atm

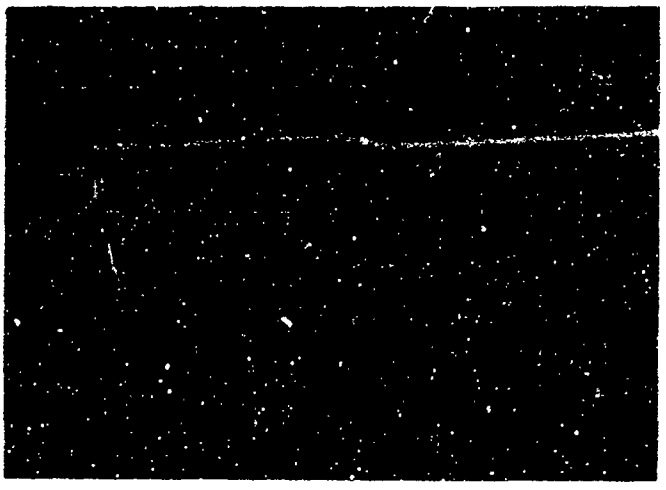

Pressure Scale:	-0.403 atm/div	Time Scale	0.1 sec/div
Propellant:	UA	Orifice Number:	12
Gas Temperature:	758°C	Initial Press:	7.7 atm

FIGURE 5. TYPICAL OSCILLOSCOPE RECORDS OF IGNITION TESTS

The time sweep is from left to right and the pressure trace starts on the lower left of each picture. The jump in pressure indicates the bursting of the diaphragm. The essentially horizontal trace is the output from the photocell observing the propellant surface. The steep rise indicates the propellant ignition.

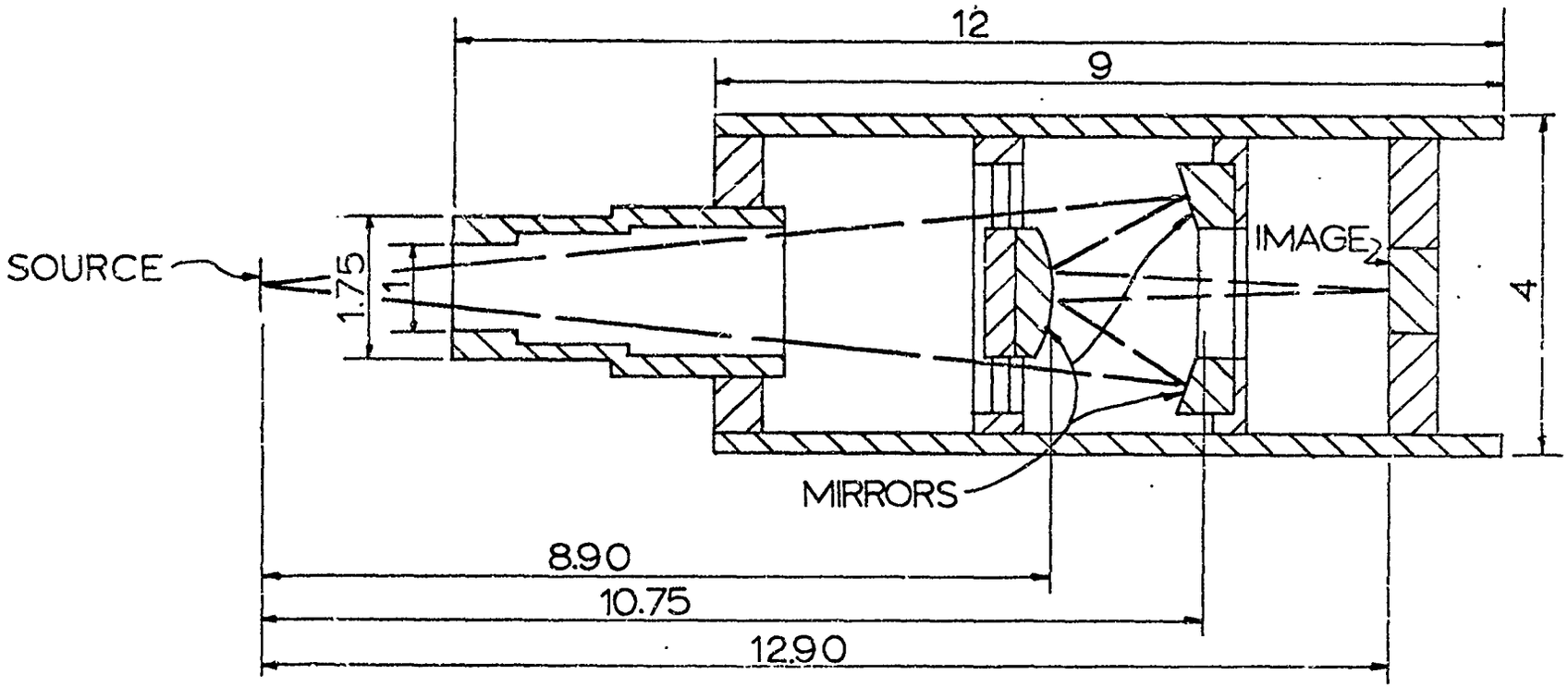

FIGURE 6. CASSEGRAINE SYSTEM.

The propellant sample located at the "source" is focused on the infrared detector at the "image" by the mirrors.

a more stable operating condition. At 63°K, and for wave-lengths in the range of 2 to 10 microns, the gold-doped-germanium detector has a detectivity of about 1.05×10^{10} cm/watt.

An electrical circuit was constructed (Figure 7) to enable the infrared detector output to be displayed on a Tektronix Model 502 oscilloscope. The voltage to the oscilloscope from the detector circuit was suppressed by an adjustable counter-potential so that, at the start of each test, the displayed voltage was zero with a current of 25 μ amps through the detector. Calibration of the infrared-detection system, by use of an electrically-heated copper disc mounted in the sample position, is discussed in detail in Appendix D.

E. POLYMER DECOMPOSITION TEST PROCEDURE

Polymer fuel binders were subjected to rapid heating in a manner similar to the ignition test samples. The infrared-detection system was employed to monitor the surface temperature of the polymer during the heating. The detector output in millivolts was displayed and photographed on the screen of an oscilloscope. Appendix D contains details of the procedure used to convert detector output in millivolts to surface temperature in degrees centigrade.

F. HEAT TRANSFER TEST PROCEDURE

Two methods were used to characterize the heat-transfer processes of the convective-heat-flux furnace. Tests were made in which platinum-film-resistant-thermometer heat-flux gages replaced propellant samples in the test section. Appendix C contains a discussion on the construction,

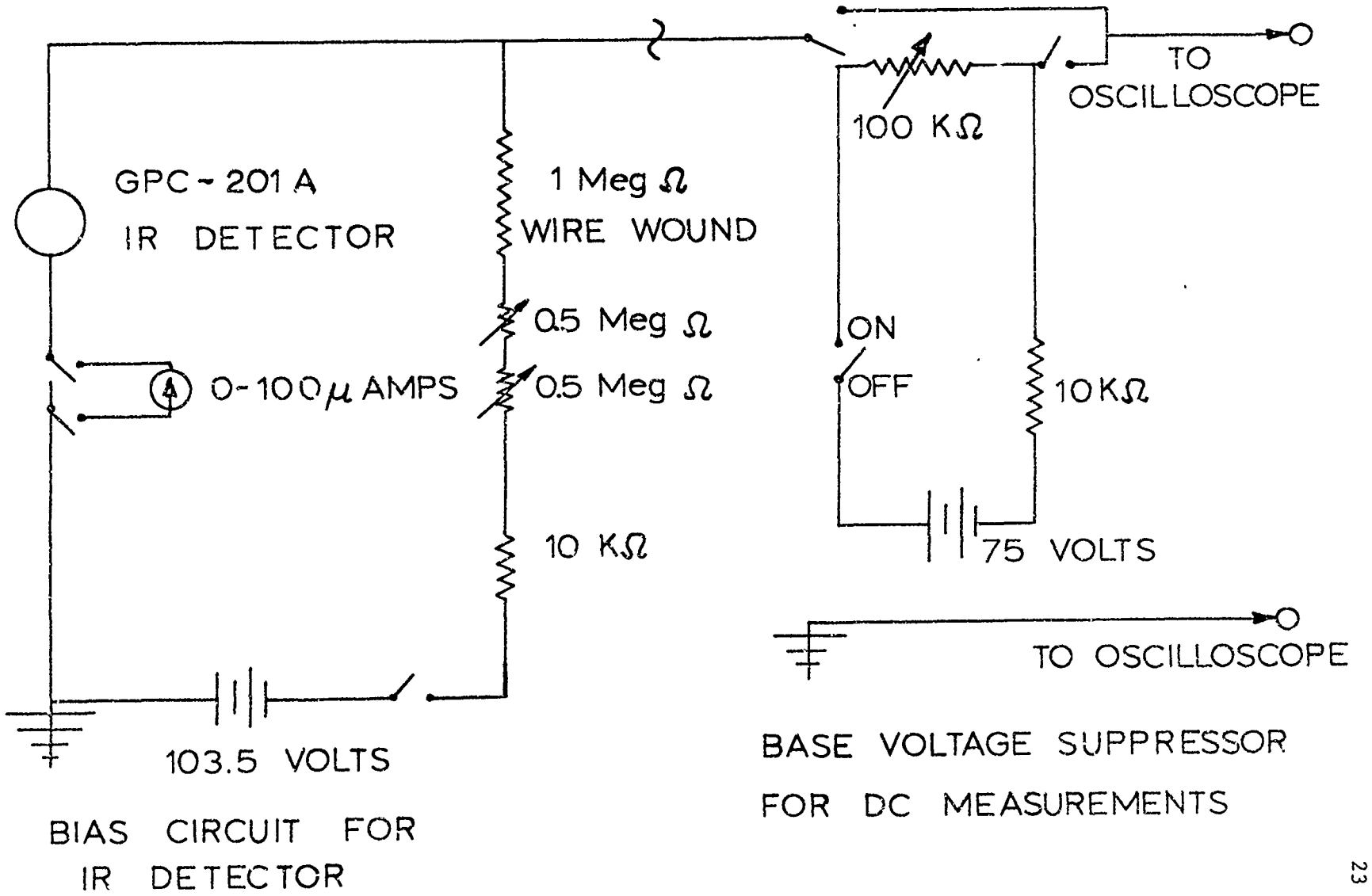

FIGURE 7. ELECTRICAL CIRCUITRY OF THE INFRARED-DETECTION SYSTEM.

calibration, and use of the heat-flux gage to obtain heat-transfer coefficients. The infrared-detection system was employed to measure surface temperatures of simulated propellant subjected to rapid heating and these data were also used to characterize the heat-transfer rates in the apparatus. Appendix D contains a detailed development of the calibration and use of the infrared-detection system in this study.

CHAPTER III

PRELIMINARY ANALYSIS OF IGNITION DATA

A. IGNITION MODEL

The analysis of the ignition data obtained in this study is most conveniently presented by reference to the "simple thermal-ignition model" for composite propellants proposed by Baer and Ryan [8]. This model has been found to adequately correlate data from a thermal-radiation furnace [8] and from high-convective-flux-ignition tests in a shock tube [25], and, thus, differences between results obtained in this study and predictions of this model are also differences with prior experimental results for the same propellants.

Physically, this model envisions the propellant as a constant thermal property, semi-infinite solid subjected to a surface-heat flux. A single Arrhenius type reaction controls the transition from ignition to burning. The site of the reaction was postulated to be at or near the propellant surface; and it was found that, when the energy released by the reaction reached rates comparable to that of the externally-applied energy, a "runaway" reaction occurred. Since the model describes ignition in terms of propellant temperatures, it is by definition a "thermal-ignition model." Figure 8 illustrates the type of propellant-surface-temperature history expected. Mathematically, the model was described by the following partial-differential equation:

$$\frac{\partial T}{\partial \tau} = \alpha \frac{\partial^2 T}{\partial x^2} \quad . \tag{1}$$

The boundary conditions are, when

$$x = 0, \; F_t(0,t) = -k \frac{\partial T}{\partial x} = F_s + Be^{-E_a/RT}, \tag{2}$$

$$x = +\infty, \; T(t) = T_o \text{ for all } t, \text{ and}$$

$$t = 0, \; T(x) = T_o \text{ for all } x;$$

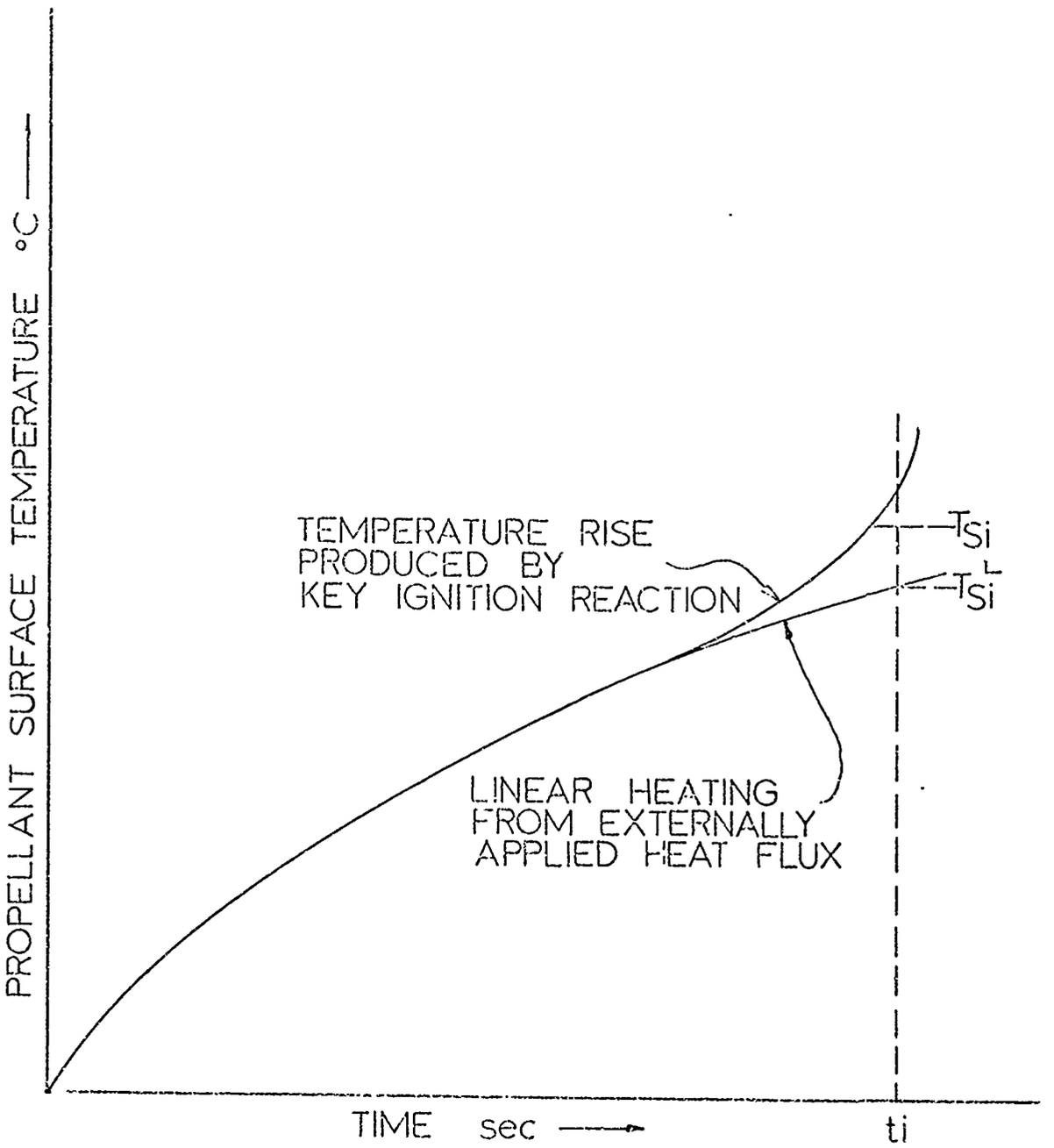

FIGURE 8. IDEALIZED SURFACE TEMPERATURE HISTORY OF A SEMI-INFINITE SLAB OF PROPELLANT UNDERGOING SIMPLE THERMAL IGNITION.

here

T is the temperature;

t is the time;

F_t is the total energy flux at the surface;

F_s is the externally applied energy flux;

E_a is the activation energy of the rate-controlling-surface reaction; ;

R is the universal-gas constant; and

B is the product of the frequency factor, Z, and the energy release at the surface per unit area, Q_s.

Numerical solutions to Equation (1) were obtained for various assumed values of the parameters, F_s, B, E_a, T_o, and the thermal properties to yield ignition times as a function of these parameters and the external flux [9]. The parameters of this ignition model have physical significance and have been determined by "best fit" to prior ignition data for the propellants considered in this study. The model predicts that experimental data should yield a straight line as a log-log plot of the square root of ignition time, $t_i^{\frac{1}{2}}$, versus the mean-surface-heat flux, $\bar{F}_s$. The slope of this line is related to the activation energy of the rate-controlling surface reaction by

$$S = 4.2 \frac{RT_o}{E_a} - 1.0 \quad . \tag{3}$$

The characterization of the propellant-ignition data in terms of $t_i^{\frac{1}{2}}$ and $\bar{F}_s$ suggests a convenient means by which most experimental data may be compared for all modes of energy transport. In the cases of the arc-image and radiation furnaces, the mean-surface-heat flux is very nearly constant

throughout the period of heating and the mean-heat flux is easily evaluated. However, when convective heating is employed, the heat flux varies during the test; and a mean-heat flux must be defined.

The required definition of the mean-heat flux is obtained by the use of the linear-ignition temperature, which is found to be a convenient correlating parameter. The linear-ignition temperature is calculated to be the surface temperature of the propellant at the ignition time if the propellant had acted as a passive solid. For constant-flux heating from an initial-uniform temperature, the linear ignition temperature, T_{si}^{L}, is found from the well known relationship [14]

$$T_{si}^{L} - T_o = 2F_s \Gamma \sqrt{t_i/\pi} \tag{4}$$

where T_o is the initial temperature and

$$\Gamma = \sqrt{k\rho c} \quad .$$

In the case of heating through a constant convective heat-transfer coefficient, h, from a gas at T_G,

$$T_{si}^{L} - T_o = (T_G - T_o)(1 - e^{N^2} \operatorname{erfc} N) \tag{5}$$

where

$$N = \frac{h t_i^{\frac{1}{2}}}{\Gamma} \quad .$$

The mean-heat flux is now defined as that constant-heat flux which would bring the propellant-surface temperature to the linear-ignition temperature in the ignition time. The linear-ignition temperature is calculated by whatever analytical representation most closely approximates the experimental-heating conditions, and the ignition time is determined from experimental data. Proof that such a definition is meaningful requires the assumption of the validity of an ignition model. The range

of validity of this definition for the "simple thermal-ignition model" has been obtained. Numerical solutions to Equation (1) with the surface boundary condition of

$$F_T(0,t) = -k\frac{\partial T}{\partial x} = h(T_G - T_s) + B_e^{-E_a/RT} \qquad (6)$$

were obtained to give ignition times as a function of h and T_G [9]. The linear-ignition temperature was then obtained by use of Equation (5) and the mean-heat flux was calculated from Equation (4) in the form

$$F_s = \frac{(T_{si}^{L} - T_o)}{2\Gamma}\sqrt{\pi/t_i} \qquad (7)$$

where the ignition time, t_i, was from the numerical calculations. A comparison between ignition times calculated on the basis of a constant-surface flux to the ignition times calculated for constant h and T_G, but correlated in terms of the defined mean-heat flux, gives the criterion for evaluation of the usefulness of this mean-heat flux. Figure 9 shows such a comparison. Calculated-ignition times correlated in terms of a true constant flux and the mean-heat flux are found to be identical for all ignition times of interest, except when the gas temperature is lower than the surface temperature at which the "runaway" surface reaction occurs. In such a case, the energy is actually transferred from the surface of the solid to the gas during the later stages of the process. In the propellants tested and for the ignition times of interest in this study, thi effect of gas temperature is not predicted since the minimum temperature employed was 750°C and a significant effect should be noted only for gas temperatures less than 400-500°C. The mean-heat flux,

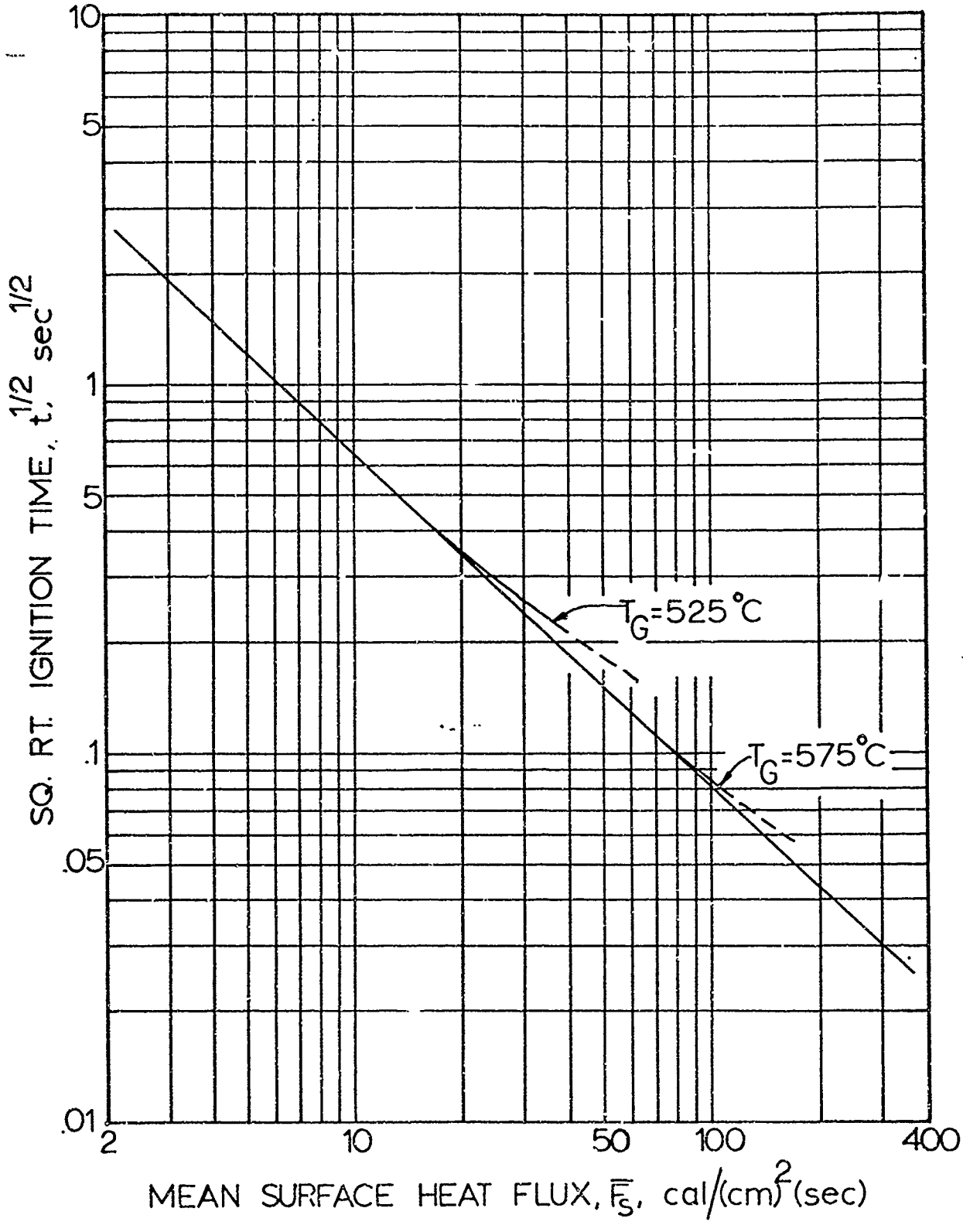

FIGURE 9. CALCULATED IGNITION TIMES AS A FUNCTION OF THE MEAN-SURFACE-HEAT FLUX.

The straight line is for a constant surface-heat flux. The curves breaking from this line are for convective heat by gas at the indicated temperature.

as defined above, should be an adequate correlation parameter if the "simple thermal-ignition model" is valid. Other possible time-flux relationships have been considered, and the mean-heat flux is found to be valid in all cases considered [16]. Likely, this defined mean flux is a general-correlation parameter for all reasonable conditions.

B. EXPERIMENTAL DATA

Experimental-ignition data of double base and composite propellants were obtained by use of the convective-ignition apparatus and are reported in References [28] and [47]. In this preliminary work, heat-transfer tests were made in which pyrex heat-flux gages were employed, and truly meaningful values of the heat-transfer coefficient were not obtained. Reproducibility and consistency of the results were less than adequate for the purposes of the study. The heat-flux gages, mounted in the propellant position, were located in the inlet flow region of the test section; and it was suspected that an irregular transition from a laminar to a turbulent-boundary layer occurred during flow across the gage surface. Also, it was observed that the heat-transfer coefficients, h, dropped about 25 per cent during the period of a test. It was not known whether this effect was real or was related to unknown property changes of the pyrex gages since, during these tests, the surface of the pyrex gage reached temperatures much greater than the maximum temperature employed in characterizing the gages. This is discussed further in Appendix C.

The ignition data obtained in this prior study [28] [47] reflected the uncertainties in the heat-transfer characterization. Although the

ignition times were about those observed for the propellants in other test devices, under supposedly comparable conditions, it was difficult to draw firm conclusions concerning the observed convective-ignition results and prior data and interpretations. Since the later heat-transfer study lead to significant modification of the apparatus, it was necessary to obtain new ignition data for the several propellants originally investigated.

Based upon this earlier experience, the convective ignition apparatus was improved prior to further ignition tests. In order to insure that the boundary layer across the propellant sample was always turbulent, a sharp-edged orifice was placed upstream from the sample to trigger the transition. For the new heat-transfer study, the pyrex heat-flux gages were replaced by an alumina gage whose surface temperature always remained in the range of its calibration. Nitrogen temperatures of 1000°C and 1300°C and pressures of 2.9 and 7.7 atm were used in this heat-transfer study; and the heat-transfer coefficients were found to be constant during the test.

Figure 10 is a correlation of the heat-transfer coefficients, h, with the mass flow rates of the hot gas, G, obtained when using the turbulence trip and an alumina gage. A temperature term, T^*, equal to 1273°K divided by the gas temperature in degrees Kelvin, was multiplied by h values in order to make an approximate temperature correction for the variation in gas thermophysical properties (see Reference [25]). The data were well represented by a straight line of slope 0.683 and the following equation.

$$h(T^*)^{0.4} = 0.00251\ (G)^{0.683} \qquad (8)$$

where h is in cal/(sec)(cm)^2 and G in gm/(sec)(cm)^2.

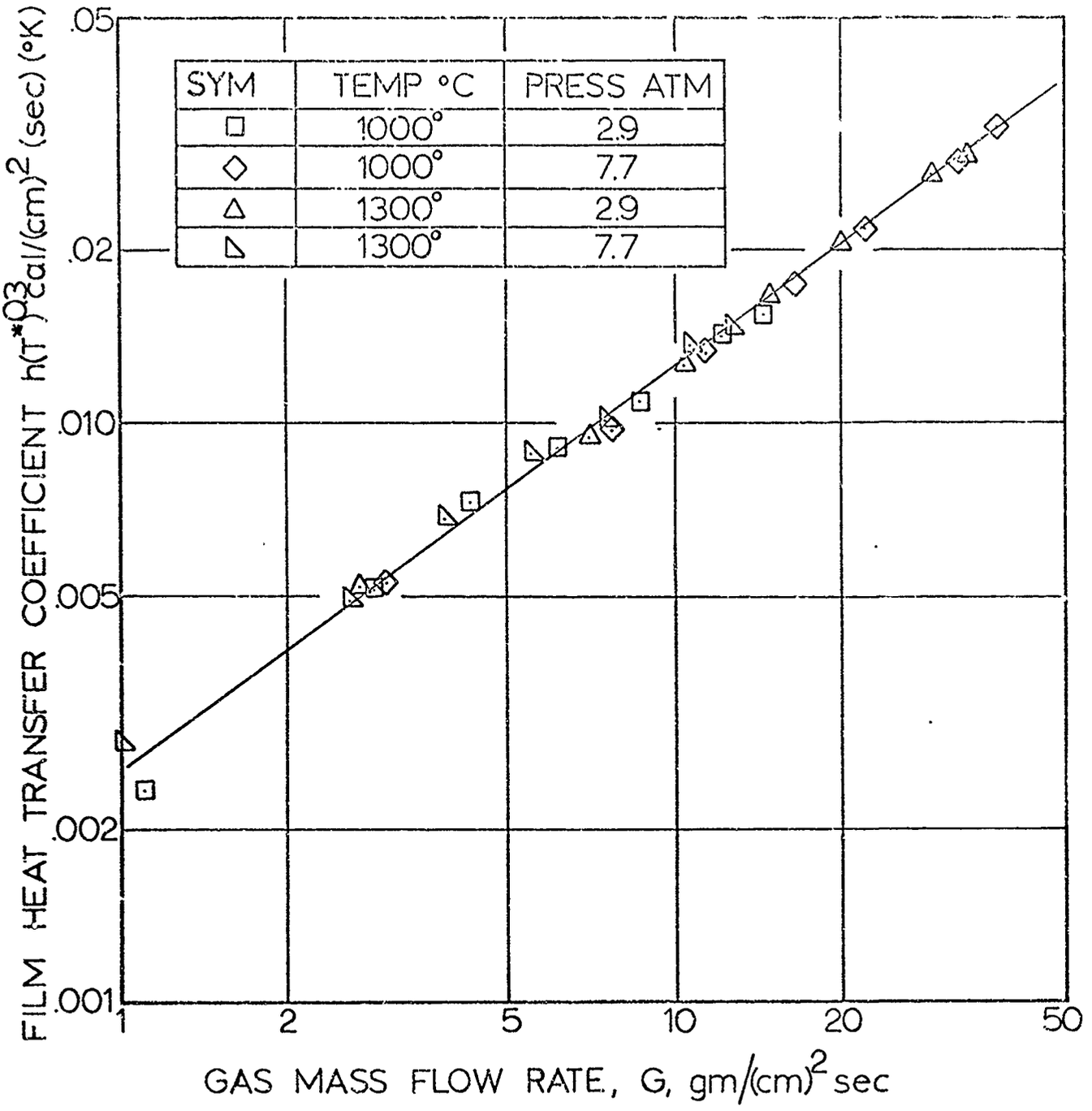

FIGURE 10. HEAT-TRANSFER COEFFICIENTS CALCULATED FROM TESTS WHERE THE ALUMINA GAGE WAS EMPLOYED, CORRELATED IN TERMS OF THE NITROGEN GAS-MASS-FLOW RATE.

A heat-transfer study was also conducted with helium gas as the media at temperatures of 750°C and 1000°C, and pressures of 2.9 and 7.7 atm. Heat losses from the electrically heated furnace limited the maximum-helium temperature to 1000°C. Heat-transfer coefficients were again plotted, on log-log coordinates, as a function of the mass-flow rates of the gas (see Figure 11). The equation of the line representing these data is:

$$h(T^*)^{0.3} = 0.0114(G)^{0.690} \qquad (9)$$

The thermal conductivity of helium is about five times greater than for nitrogen. For this reason, when using a specific-gas temperature, the helium will give higher heat fluxes than the nitrogen. By use of this fact, the fluxes could be extended from around 30 cal/(cm)^2/sec) with nitrogen at 1300°C to 50 cal/(cm)^2(sec) with helium at 1000°C.

The heat-transfer coefficients calculated from the heat-transfer data for both nitrogen and helium atmospheres were represented in Figure 12 by a dimensionless log-log plot of $Nu/Pr^{0.3}$ versus Re, where Nu is the Nusselt number, Pr is the Prandtl number, and Re is the Reynolds number. The slope of the line best representing these data was 0.695. For comparison, the Dittus-Boelter equation [17], which is applicable to steady-state turbulent flow, is also shown in Figure 12. Since the alumina gage was positioned in the inlet-flow region of the test section, and the thermal boundary layer was developing during tests, it is not anticipated that the data would agree well with the steady-state correlation. The plot of $Nu/Pr^{0.3}$ versus Re correlate the experimental data extremely well, however, it must be noted that the alumina gage experienced temperature rises of about 75°C while propellant ignition takes place for temperature rises in

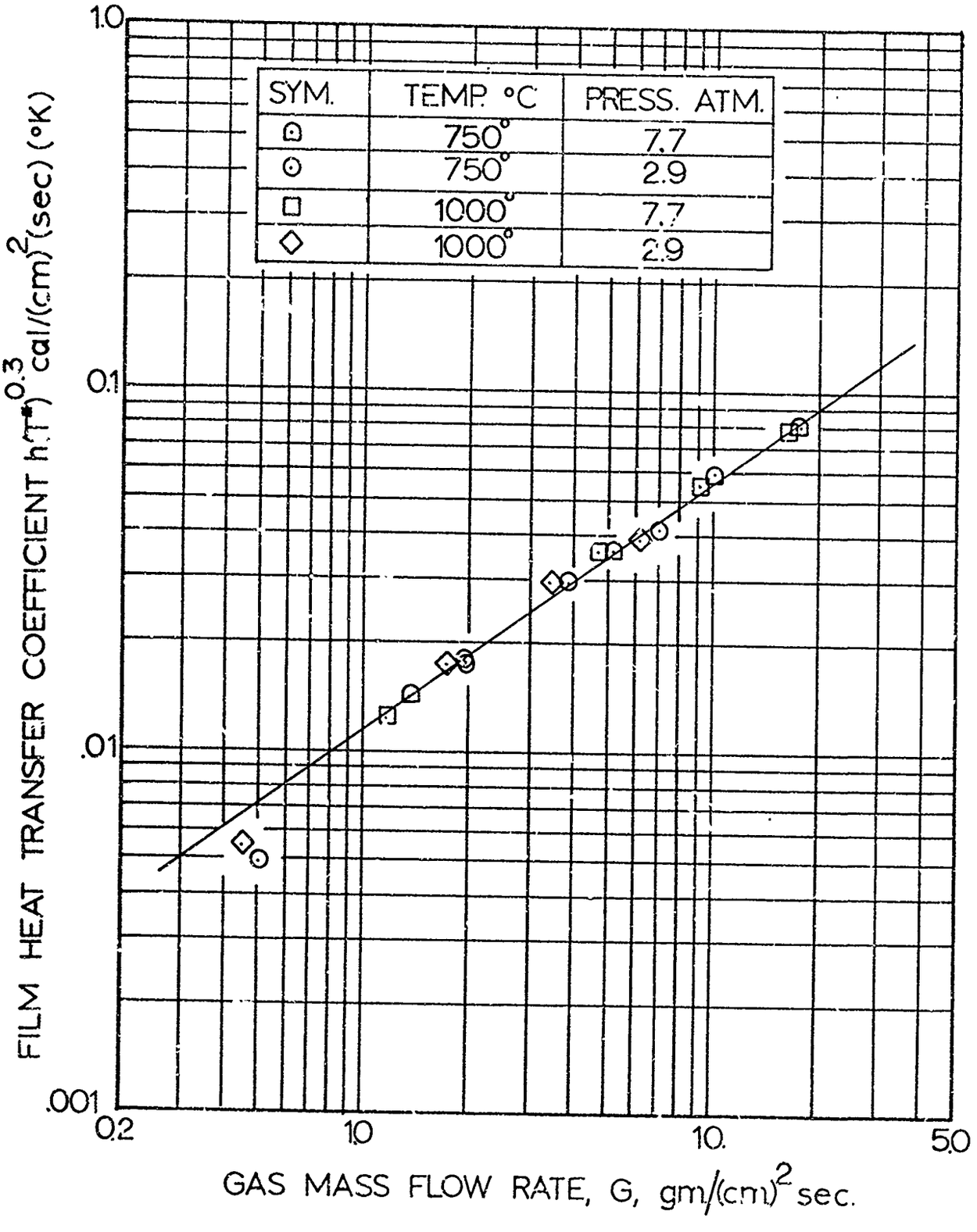

FIGURE 11. HEAT-TRANSFER COEFFICIENTS CALCULATED FROM TESTS WHERE THE ALUMINA GAGE WAS EMPLOYED, CORRELATED IN TERMS OF THE HELIUM GAS-MASS-FLOW RATE.

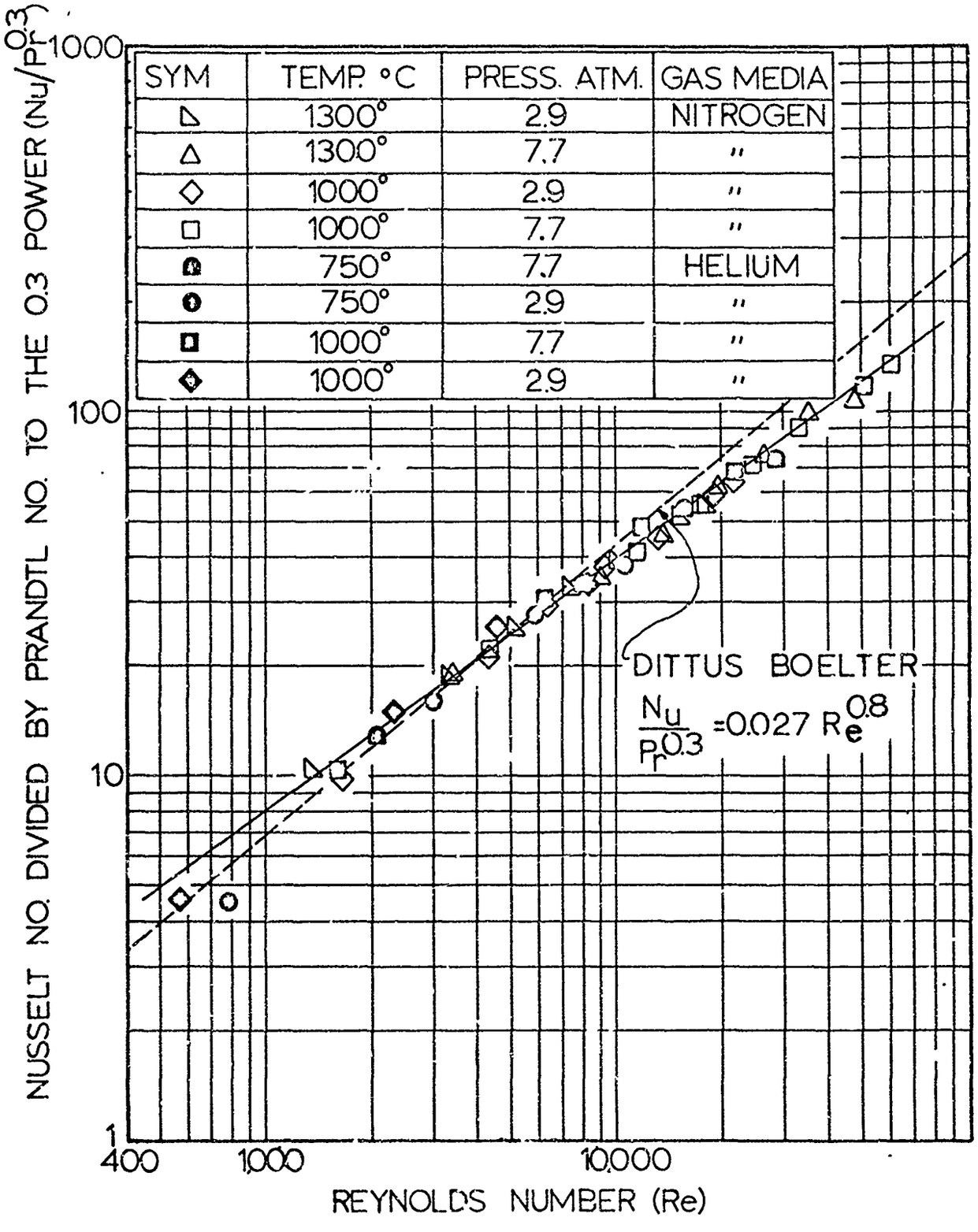

FIGURE 12. CORRELATION OF THE HEAT-TRANSFER COEFFICIENTS IN TERMS OF DIMENSIONLESS-PARAMETERS.

excess of 300°C. This difference in surface temperature could affect the film heat-transfer coefficients, and this point will be discussed again in the next chapter.

C. PROPELLANT IGNITION TEST DATA

Ignition tests were conducted using FM, G, and UA propellants in nitrogen and helium atmospheres. These propellants are similar in composition. They are all ammonium perchlorate (AP) oxidized with a PBAA fuel binder (see Table I). Fine grain-ammonium perchlorate (75 weight per cent) was used in the UA propellant, which also contained a "copper chromite" burning-rate catalyst. FM propellant also contained 2 per cent catalyst but was formulated from a bimodal blend of coarse and fine AP at an 80 per cent level. The G propellant was like the FM except that additional AP replaced the catalyst. Nitrogen at a temperature of 760, 1000, and 1300°C was used as was helium at 760°C and 1000°C. Both gases were employed at furnace pressures of 2.9 and 7.7 atm.

Figure 13 is a log-log plot of the square root of ignition time, $t_i^{1/2}$, for the FM propellant, versus the mean surface-heat flux, $\bar{F}_s$. Mean-surface heat-fluxes for the measured-ignition times were calculated using Equation (7) with h values taken from correlation Equation (8). Although these data tend to scatter about the "simple thermal-ignition" line they also appeared to be formed into groups according to the gas temperature and pressure, and straight lines drawn through the ignition times for specific-gas temperatures and pressures represented the data well. These temperature and pressure effects are further illustrated in Figures 14 and 15. An increase in gas temperature appears to result in lower ignition times at a constant

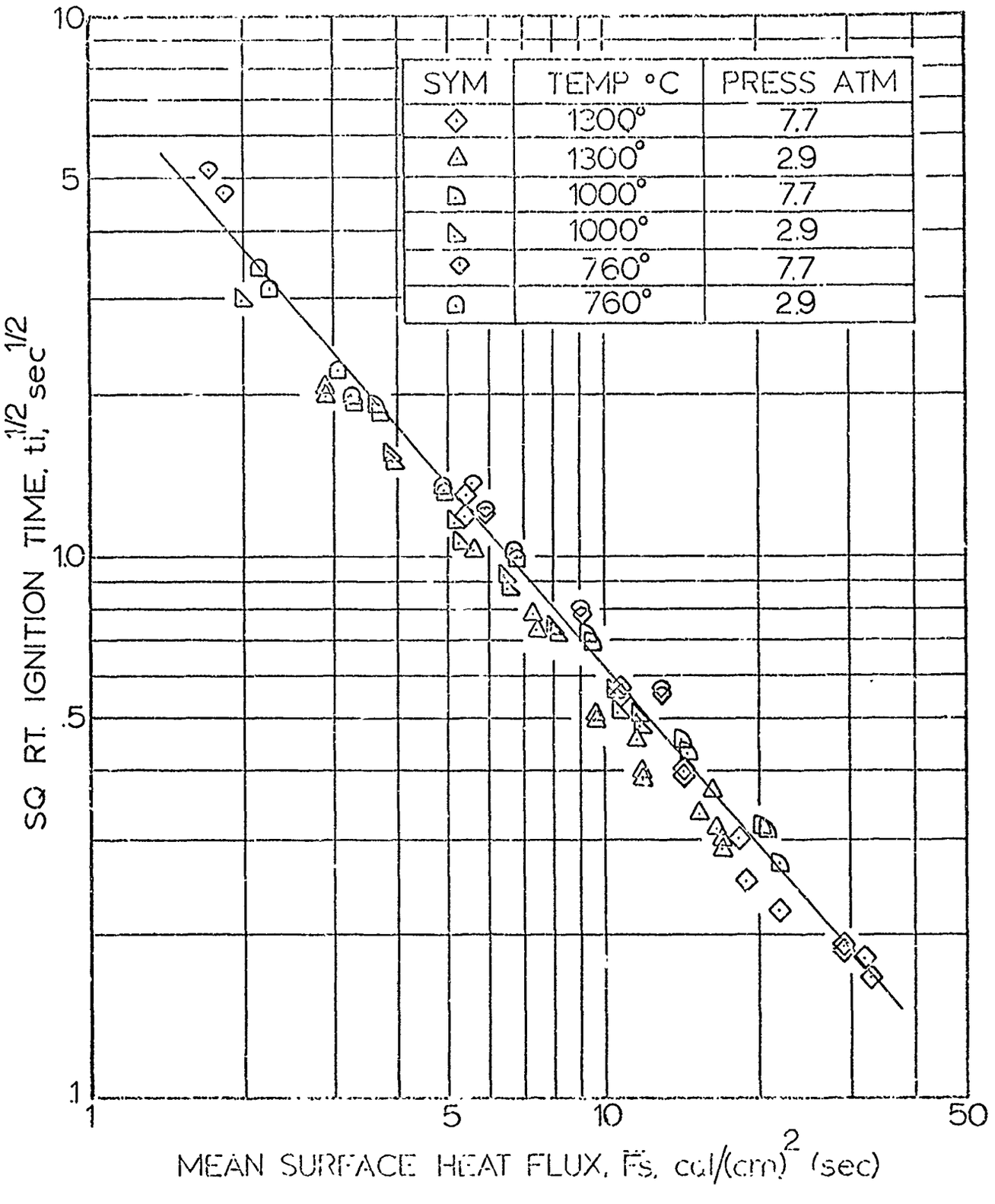

FIGURE 13. IGNITION DATA OF FH PROPELLANT IN NITROGEN WITH MEAN-SURFACE-HEAT FLUXES, CALCULATED FROM ALUMINA GAGE HEAT-FLUX STUDY.

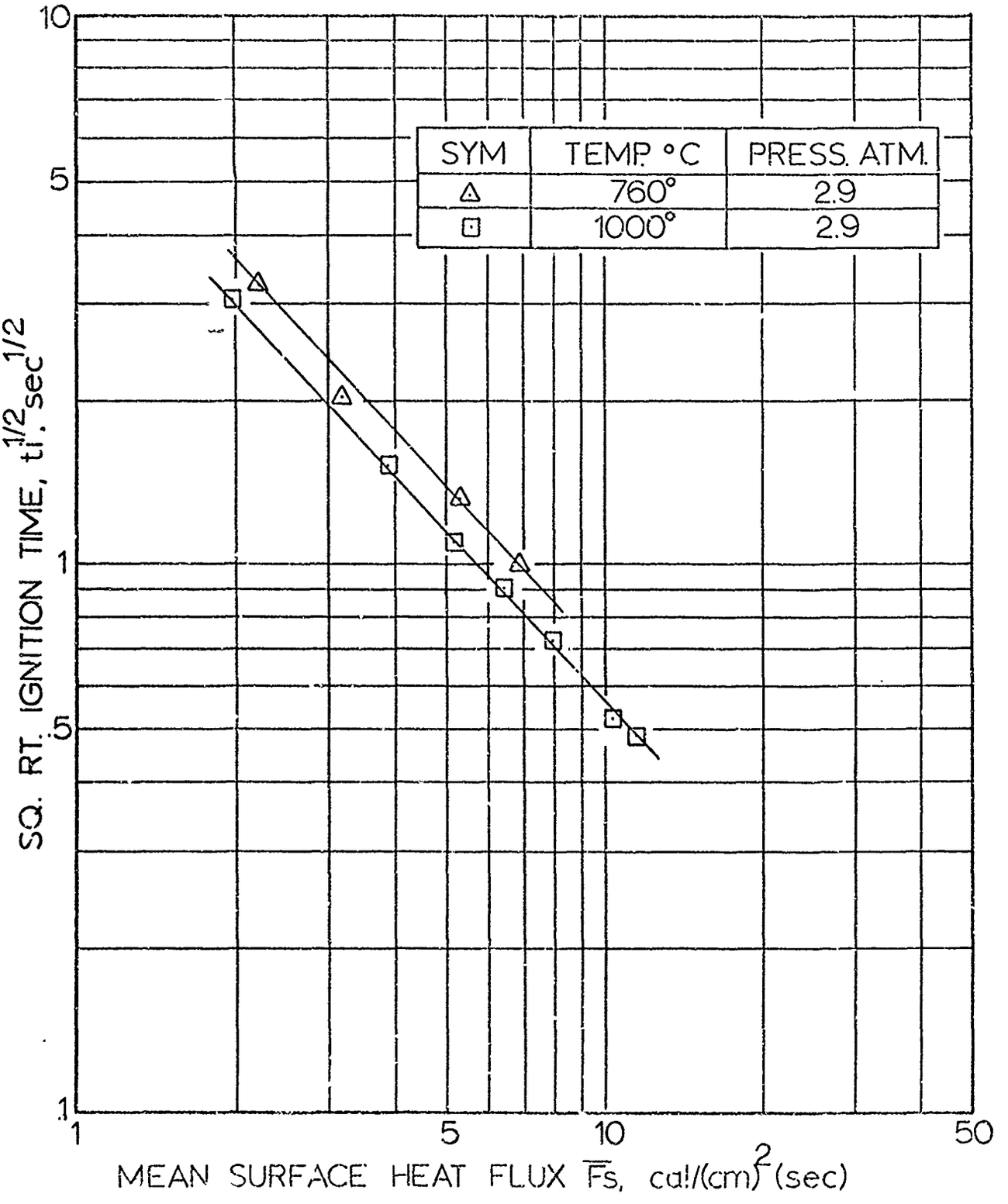

FIGURE 14. IGNITION DATA OF FM PROPELLANT IN NITROGEN WITH MEAN-SURFACE-HEAT FLUXES, CALCULATED FROM ALUMINA GAGE HEAT-FLUX STUDY, ILLUSTRATING EFFECT OF GAS TEMPERATURE.

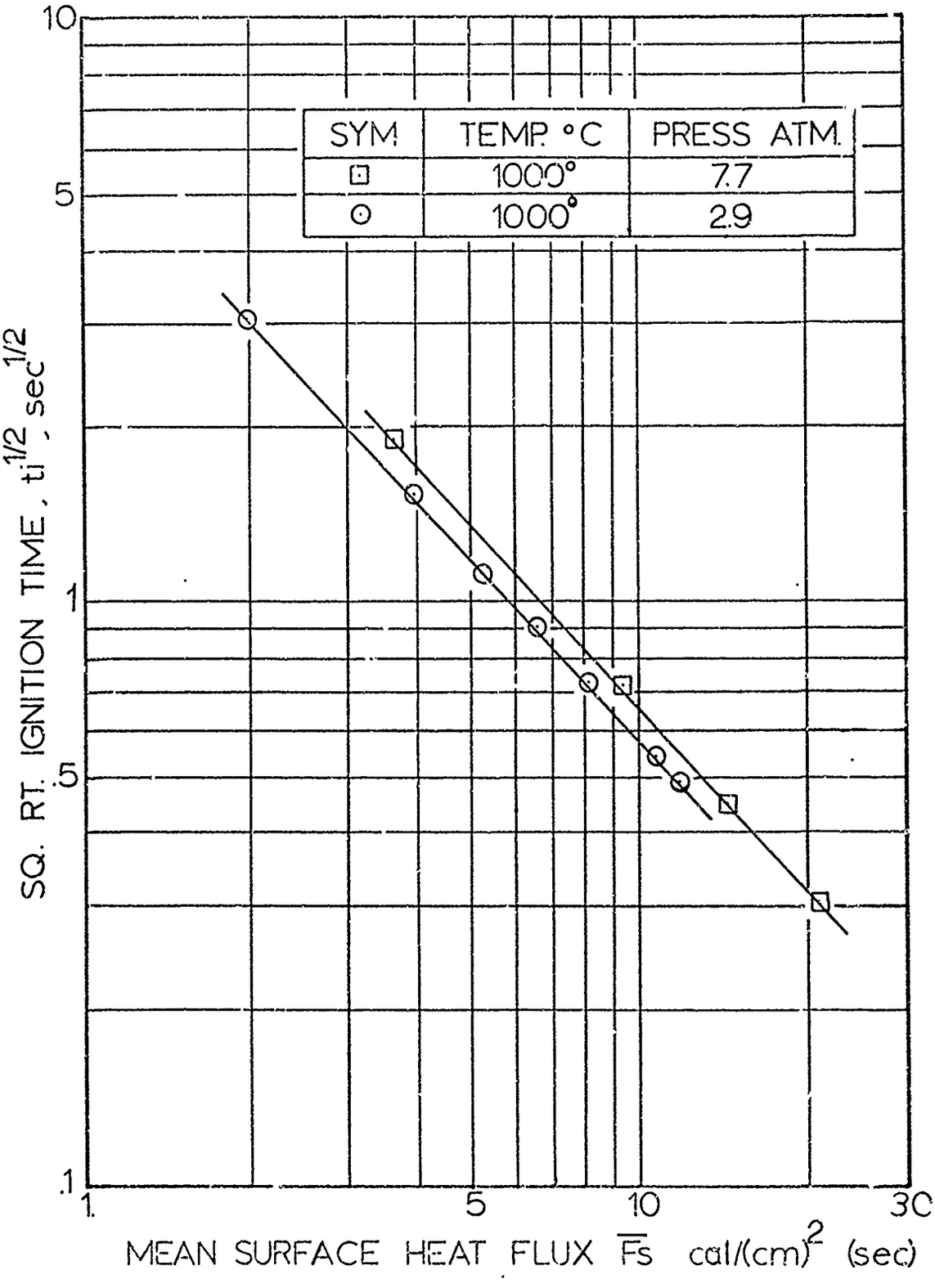

FIGURE 15. IGNITION DATA OF FM PROPELLANT IN NITROGEN WITH MEAN-SURFACE-HEAT FLUX CALCULATED FROM ALUMINA GAGE HEAT-FLUX STUDY, ILLUSTRATING THE EFFECT OF PRESSURE.

mean-heat flux; but an increase in pressure, contrary to all expectations, appears to increase ignition times. Similar results were obtained for UA and G propellants and these data are presented in Tables V and VI.

The results of the ignition test for FM propellant, where a helium atmosphere was employed, were also correlated by a log-log plot of $t_i^{\frac{1}{2}}$ versus $\bar{F}_s$ and are illustrated in Figure 16. The mean-surface-heat-flux values were calculated using Equation (7) and values taken from the helium heat-transfer data. In the case of helium as the heat-transfer media, the ignition times appeared to be affected by the gas temperature in the same manner as in nitrogen, but no pressure effect is indicated.

Straight lines drawn through the ignition times, for a given gas temperature, as shown in Figures 13 and 16 have slopes near -1.06. These data represent ignition tests in which different gas velocities were used, and it is assumed that the propellant ignitability was not affected by the gas velocity. The slope of the lines indicated that the activation energy of the rate-controlling reaction, calculated from Equation (3), was negative in value. This obviously is incompatible with the ignition model proposed.

The dilemma presented by the data shown in Figures 13 and 16 is that either the convective system in this apparatus is basically different from the process in other test devices or else these data are subject to a systematic error in measurement or in interpretation. Since previous work has been well described by the model, a further investigation of the possible errors in the ignition time or heat-transfer characterization appeared necessary. The ignition times of the exposed propellants were measured as the time lapsed between the initiation of the flow of the hot

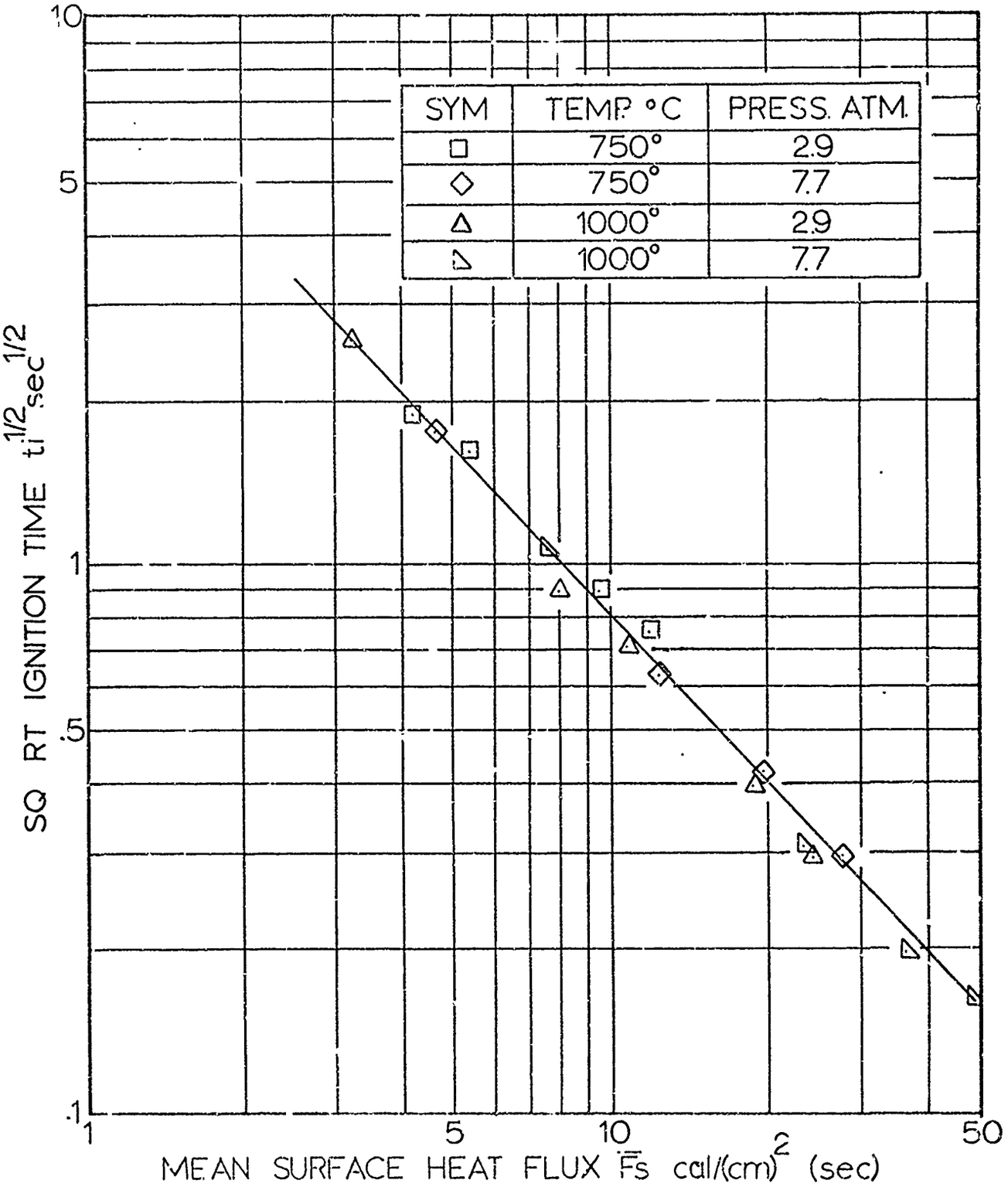

FIGURE 16. IGNITION DATA OF FM PROPELLANT IN HELIUM WITH MEAN-SURFACE-HEAT FLUX CALCULATED FROM ALUMINA GAGE HEAT-FLUX STUDY.

gas and the first trace of light from the propellant surface. It was possible that this light signal did not coincide with the occurrence of the "runaway" reaction postulated in the thermal ignition model. This possibility was checked by simultaneously monitoring the propellant-surface temperature with an infrared-detection system to detect the "runaway" reaction and the light emission seen by the photocell during ignition. Coincidence of the two phenomena was observed. The results are discussed further in Chapter V.

The heat-transfer characterization was suspect partly as the result of an unexplained difference noted between heat-transfer coefficients calculated from the pyrex and alumina gage tests. This difference appeared to be the result of the difference in surface temperature obtained under a given set of test conditions. For conditions which would yield ignition times of the propellant sample, the alumina gage rose about 75°C and the pyrex gage rose about 220°C. The propellant sample surface temperature would be in excess of 325°C. It was not known what effect the differences in boundary layer temperature would have on heat-transfer coefficients. Also, the quartz window opposite the propellant would not rise above 200°C, and a large difference in temperature would exist across the narrow flow channel. For these reasons, it was decided that an additional heat-transfer study should be made to again characterize the convective heat-flux furnace. In this study, a substance having thermophysical properties near to those of the actual propellants should be used.

CHAPTER IV

FINAL ANALYSIS AND RESULTS OF IGNITION DATA

A. HEAT TRANSFER STUDY

As a result of the arguments presented in the last chapter, it was found necessary to conduct a third heat-transfer study which would hopefully permit a satisfactory estimation of energy transfer rates from the hot gas to the propellant. The results from this study were intended to yield a more meaningful interpretation of the propellant ignition data. The gas temperature and pressure effects noted in the prior interpretation could be verified or denied. Also, more realistic values of the activation energies obtained from these data by use of Equation (3) might be obtained from additional and, perhaps, modified heat-transfer data.

A novel approach was taken to further investigate the heat-transfer characteristics of the convective heat-flux furnace. A dummy propellant, GAR, was fabricated from the PBAA polymer, carbon black, and glass beads such that its thermophysical properties were similar in value to those of the propellant investigated. An infrared-detection system was constructed which monitored the surface temperature of the GAR samples while undergoing mock ignition tests. During a test, the surface temperature of this dummy propellant rose about 260°C; whereas, propellant samples experienced temperature rises of about 350°C for comparable-heat-exposure conditions. Since the alumina heat-flux gage measured surface temperature rises of only about 75°C, the GAR test conditions more nearly resembled the actual ignition test conditions. Appendix C contains a detailed explanation of the heat-transfer study conducted employing the heat-flux gages, and Appendix D discusses the calibration and use of the infrared-detection system used in obtaining heat-transfer data.

During simulated-ignition tests, conducted in a nitrogen atmosphere of 760, 1000, and 1300°C, and 2.9 and 7.7 atm, surface-temperature histories of the GAR samples were obtained for exposure times about equal to the propellant ignition times under the same conditions. The technique for converting the intrared-detector output to surface temperatures of the GAR samples is discussed in Appendix D. Instantaneous heat-transfer coefficients, h, were calculated from these temperature histories and previously determined thermophysical properties of the material [25]. For gas temperatures of 760°C, instantaneous heat-transfer coefficients, calculated at times near propellant ignition times, were approximately 30 per cent lower than the values calculated at earlier times. The coefficients obtained early in the runs correspond almost exactly to those obtained from the prior heat-transfer study. In the tests where the gas temperature was 1000°C, the coefficients dropped by about 10 per cent; but when the gas temperature was 1300°C, the heat-transfer coefficients were found to remain relatively constant throughout a run. Figure 17 illustrates this effect for a typical set of conditions. The heat-transfer coefficients were apparently a function of time and gas temperature. This being the case, the results of the heat-flux study in which the alumina gage was employed would not be expected to adequately describe the heat t transfer from hot gas to the propellant surface for a given set of conditions. However, if mean-heat-transfer coefficients, $\bar{h}$, were defined, which would predict the GAR surface temperature at the propellant ignition times, these heat-transfer coefficients should be essentially the values which apply for

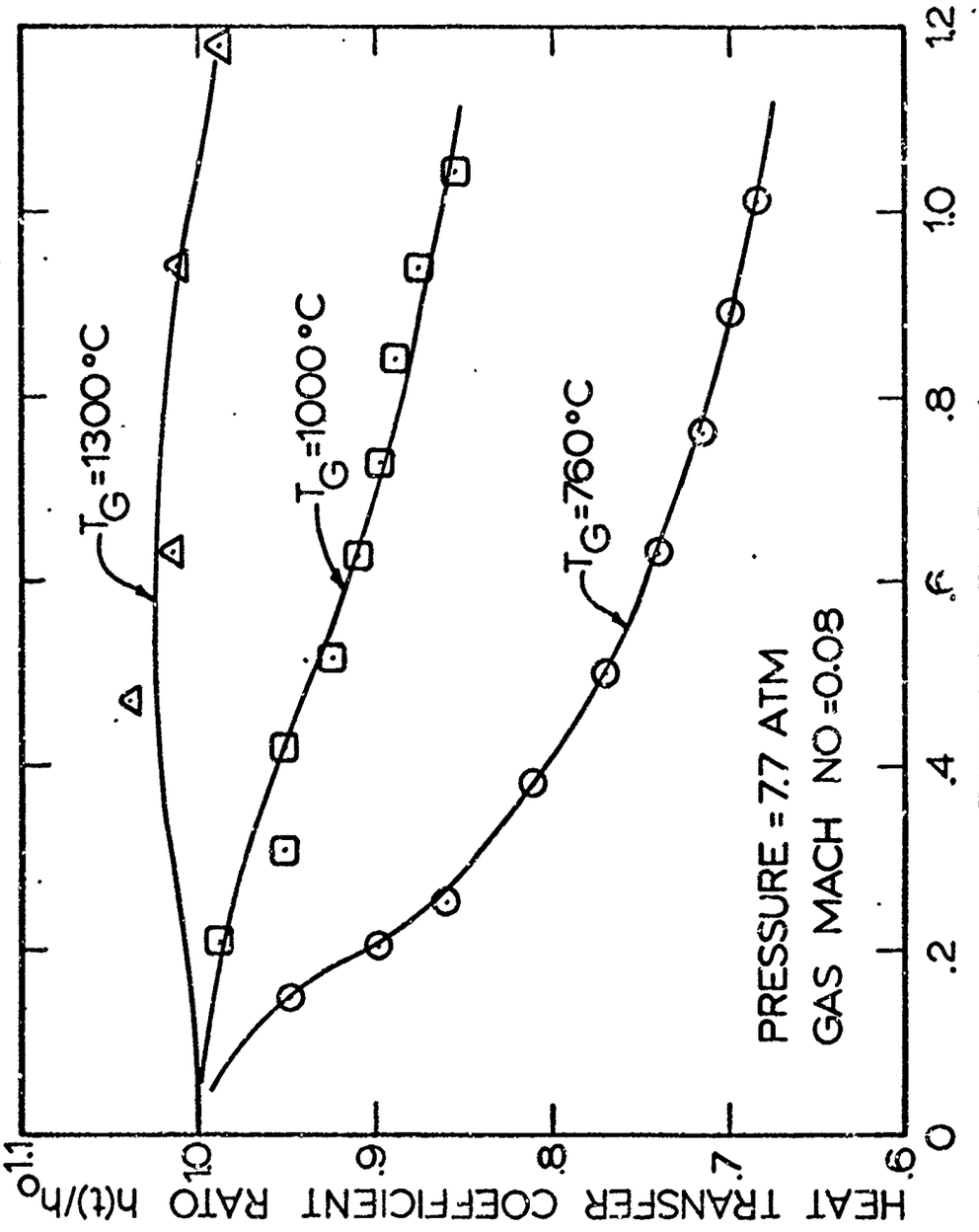

FIGURE 17. HEAT-TRANSFER COEFFICIENTS FOR DIFFERENT GAS TEMPERATURES, CALCULATED FROM GAR HEAT-FLUX-TEST DATA, PLOTTED AS A FUNCTION OF TIME.

heating the propellant surfaces. Figure 18 is a log-log plot of such mean heat-transfer coefficients versus gas mass flow-rates for the various gas temperatures employed. The coefficients generally lie below the values based on the alumina heat-flux gases, but the values where the gas temperature was 1300°C are quite near the alumina gage values.

The dummy propellant, GAR, was intentionally formulated to have a higher thermal responsivity than the actual propellants; therefore, during simulated ignition tests, the GAR surface temperature did not reach a temperature equal to the propellant-linear-ignition temperature. Decomposition of the PBAA polymer was thus avoided, and a single gage could be used for several tests. At some time, t_e, which was later than the ignition time, t_i, (see Equation D-8 in the Appendices) the GAR surface temperature would reach the propellant-linear-ignition temperature. Normally the temperature at this time, t_e, could be obtained by extrapolation of the surface-temperature history of the GAR. Heat-transfer coefficients, $\bar{h}^+$, were calculated using time t_e and the GAR-surface temperature extrapolated to the propellant-ignition temperature, and these results are also summarized in Figure 18. The thought here is that the correct mean-transient heat-transfer coefficient might require evaluation at the same surface temperatures. Evaluation of the ignition data by use of the "equal surface temperature" mean heat-transfer coefficients yields essentially the same results as evaluation at the same exposure time; and since, in this later case, extrapolation of the data is avoided, the only mean heat-transfer coefficients subsequently considered are those from the GAR tests in which equal exposure times are used.

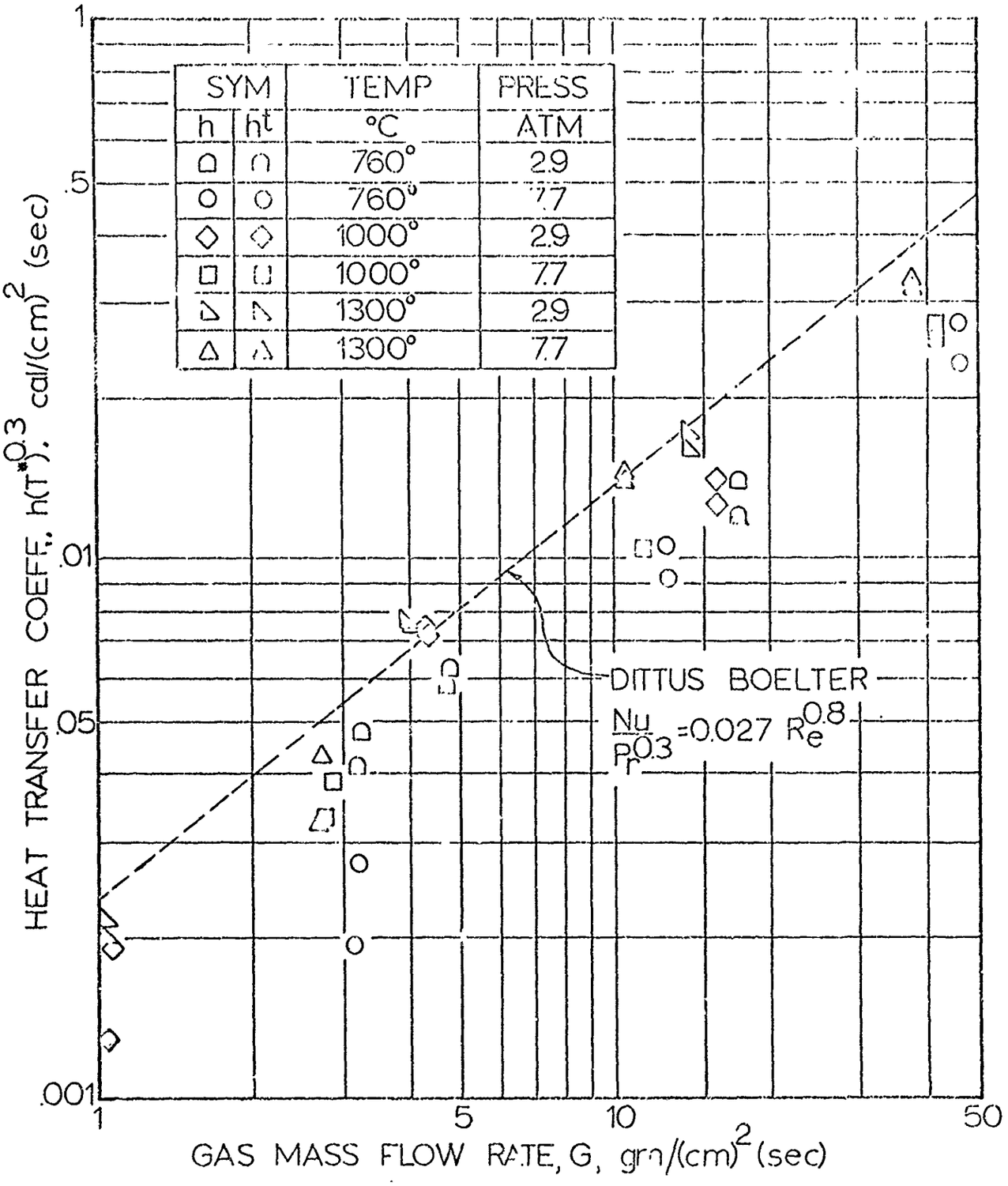

FIGURE 18. MEAN-HEAT-TRANSFER COEFFICIENTS, CALCULATED FROM GAR HEAT-FLUX-TEST DATA AT THE PROPELLANT IGNITION TIME AND THE PROPELLANT-LINEAR-IGNITION TEMPERATURE, CORRELATED AS A FUNCTION OF THE GAS-MASS-FLOW RATE.

The blackened values represent the extrapolated data where propellant-linear-ignition temperatures were used.

B. PROPELLANT IGNITION EXPERIMENTAL DATA

Mean surface heat-flux values, $\bar{F}_s$, for propellant ignition tests were calculated using Equations (4) and (7) with $\bar{h}$ values from Figure 18. In Figure 19, the ignition times of UA propellant are represented as a function of $\bar{F}_s$. When the test gas temperature was 760°C, the ignition times were well correlated by the thermal ignition line. This thermal ignition line represents data obtained by use of the radiation furnace [7] with gas temperatures ranging from 722°C to 1540°C. The ignition times, where gas temperatures of 1000°C and 1300°C were employed, were well represented by a line parallel to the ignition data where 760°C test gases were used. Similar results were seen from ignition tests of FM and G propellants and these data are represented in Figures 20 and 21. The same thermal ignition correlation exists for the catalyzed UA and FM propellants. The ignition times for the uncatalyzed G propellant are about 20 per cent longer.

C. RESULTS AND INTERPRETATION OF IGNITION DATA

The propellant ignition data, shown in Figure 19, indicated that the ignition times obtained by using gases having temperatures of 1000°C or greater were about 80 per cent of the ignition times of samples subjected to gas temperatures of 760°C. This effect will receive further comment later. When correlated as $t_1^{\frac{1}{2}}$ versus $\bar{F}_s$, these data indicate no effect on ignition times when the pressure was varied from 2.9 atm to 7.7 atm. Since different sized flow-control orifices were used so that the gas flow Mach number across the surface was varied from 0.02 to 0.292, no effect was

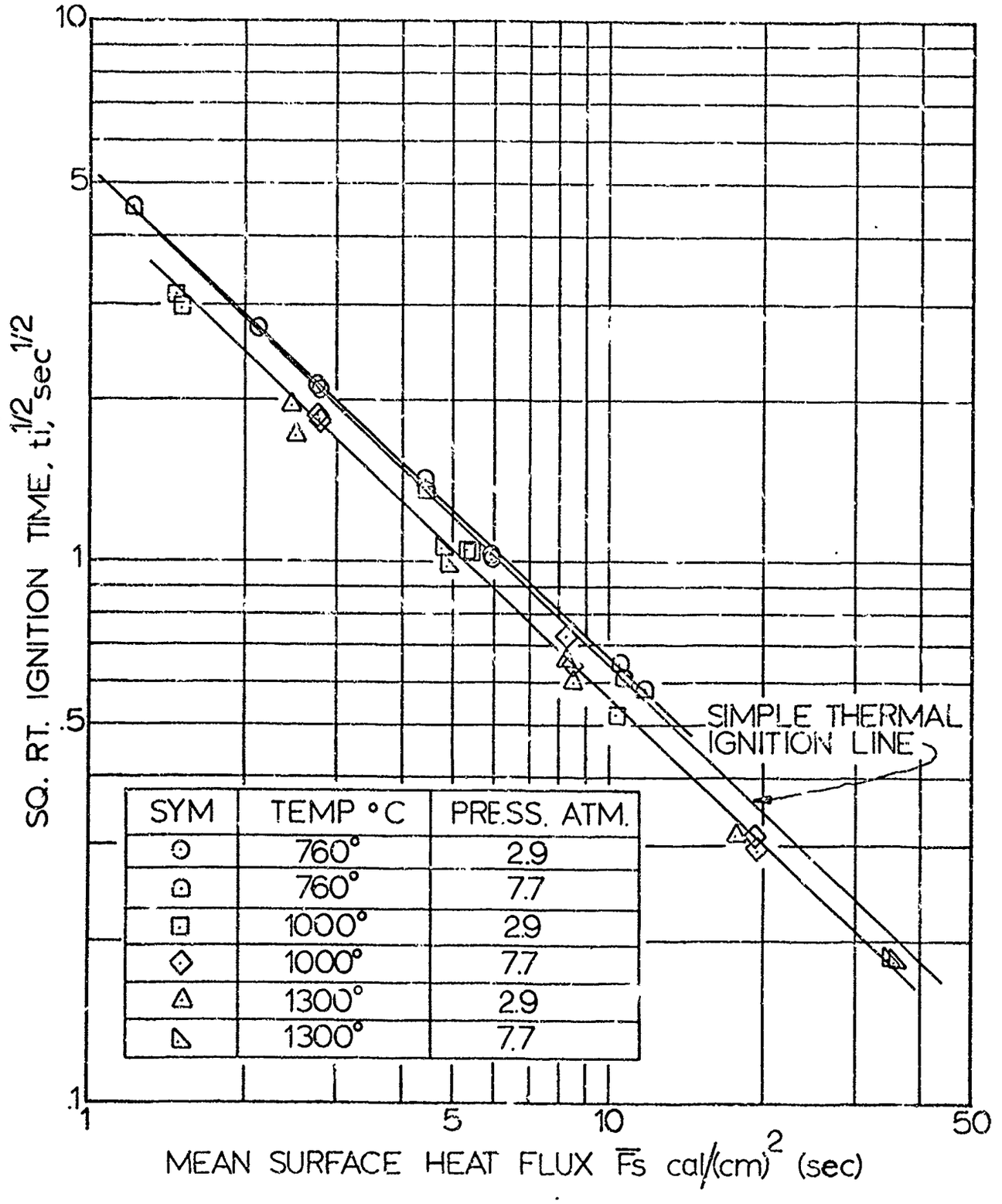

FIGURE 19. IGNITION DATA OF UA PROPELLANT IN NITROGEN WITH MEAN-SURFACE-HEAT FLUXES CALCULATED FROM THE GAR HEAT-FLUX STUDY.

The experimental data where 760°C gas temperatures were employed are well represented by the thermal ignition line, and a line through the high temperature data is very nearly parallel to this line.

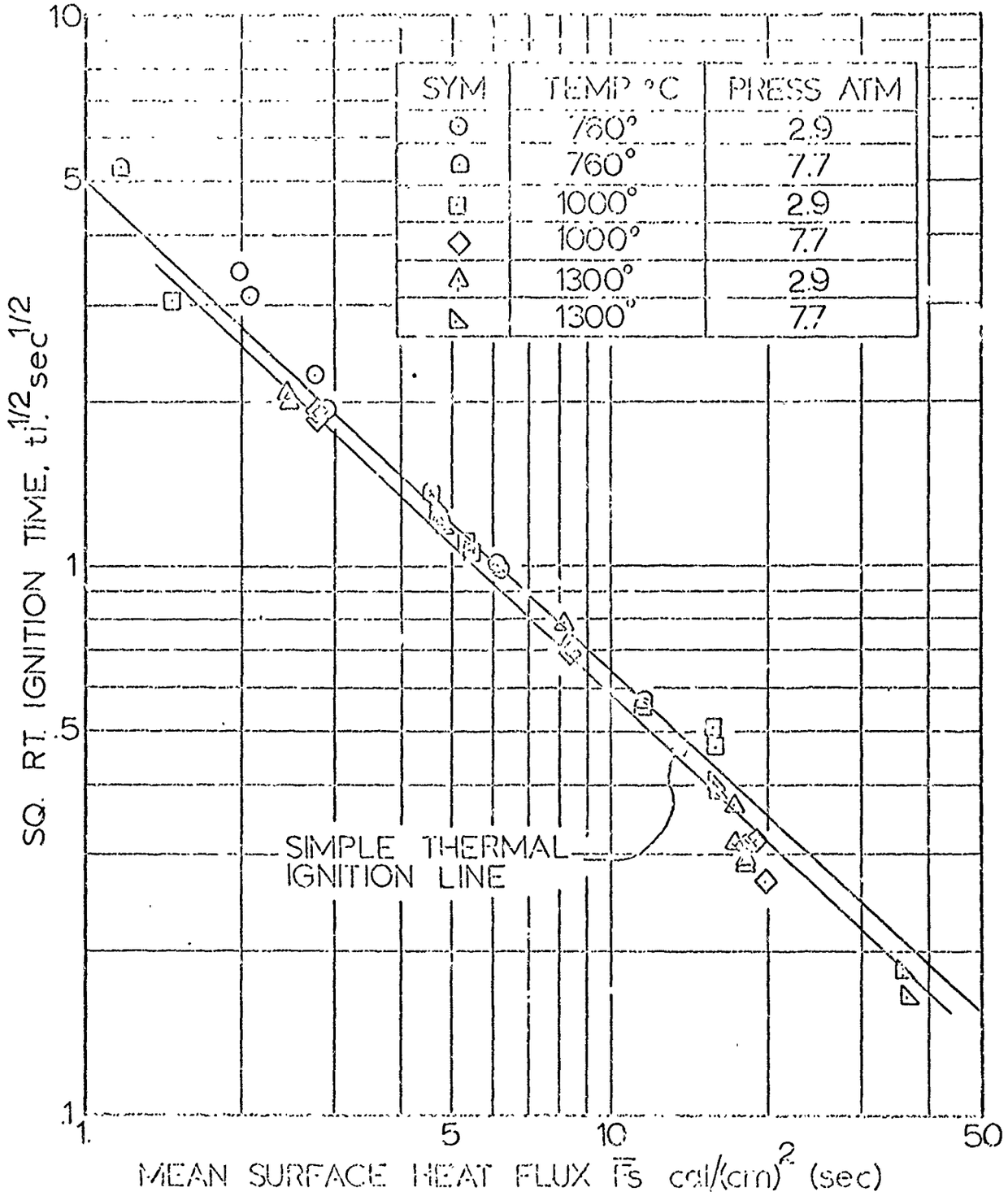

FIGURE 20. IGNITION DATA OF FM PROPELLANT IN NITROGEN WITH MEAN-SURFACE-HEAT FLUXES, CALCULATED FROM THE GAR HEAT-FLUX STUDY.

The experimental data where 760°C gas temperatures were employed are well represented by the thermal ignition line, and a line through the high temperature data is very nearly parallel to this line.

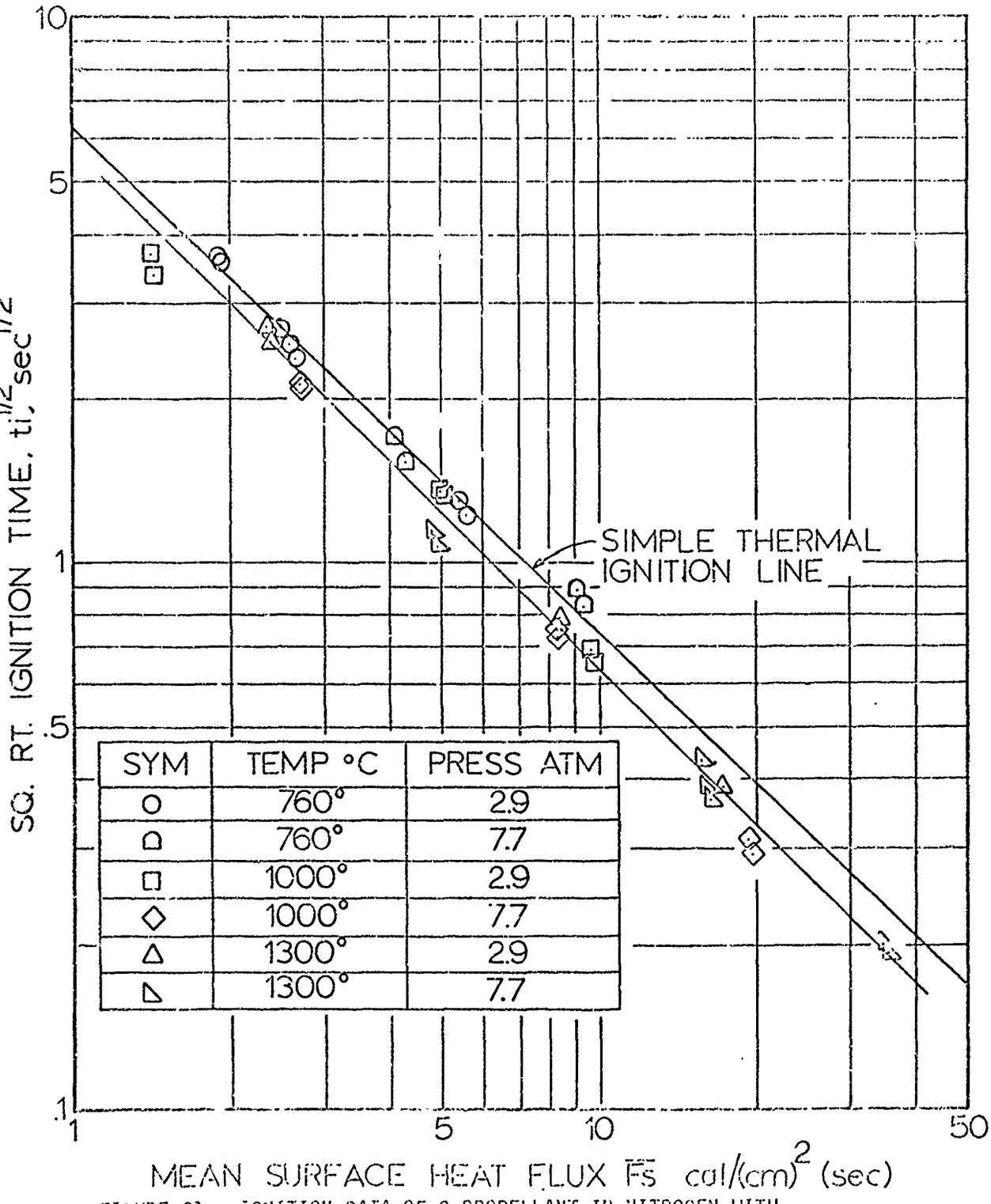

FIGURE 21. IGNITION DATA OF G PROPELLANT IN NITROGEN WITH MEAN-SURFACE-HEAT FLUXES, CALCULATED FROM THE CAR HEAT-FLUX STUDY.

The experimental data where 760°C gas temperatures were employed are well represented by the thermal ignition line, and a line through the high temperature data is very nearly parallel to this line.

noted on propellant ignitability due to differences in gas velocity for heat fluxes ranging from 2 to 30 cal/(cm)^2(sec).

Figure 22 is a log-log plot of $t_i^{1/2}$ versus $\bar{F}_s$ for FM and UA propellants. The results taken from the UA propellant ignition tests were indistinguishable from the FM test. Therefore, since the propellants differ mainly in the perchlorate crystal size, which presumably manifests itself as a change in surface texture, no effects of surface roughness on ignition times were indicated. Thus, the surface roughness effect noted by Keller [25] at high convective fluxes was not seen. Extrapolation of Keller's results into the lower flux region indicates that such a surface effect should have been detectable in this study. This discrepancy has not yet been resolved.

The data shown in Figure 20 indicated a heating-gas-temperature effect on the ignition process. This effect is not the result of the gas temperature approach to the surface-ignition temperature predicted by the model and illustrated in Figure 9. The gas temperature is too high; the ignition times are too long; and there is not even qualitative agreement since the ignition times are uniformly affected. Parallel lines may be drawn through the data points; one for the 1000 and 1300°C gas temperature, and a second through the data for 760°C gas. Although the slopes of these lines could be varied some, the best fit lines through the data have slopes of -0.905. By use of this value, activation energies of the rate-controlling reactions can be calculated by use of Equation (3) to be about 25,000 cal per mole in each case. It appears that the pre-exponential factor, B, of Equation (2) was the sole term affected by differences in gas temperatures. Values of t_i, $\bar{F}_s$, and E_a from the results

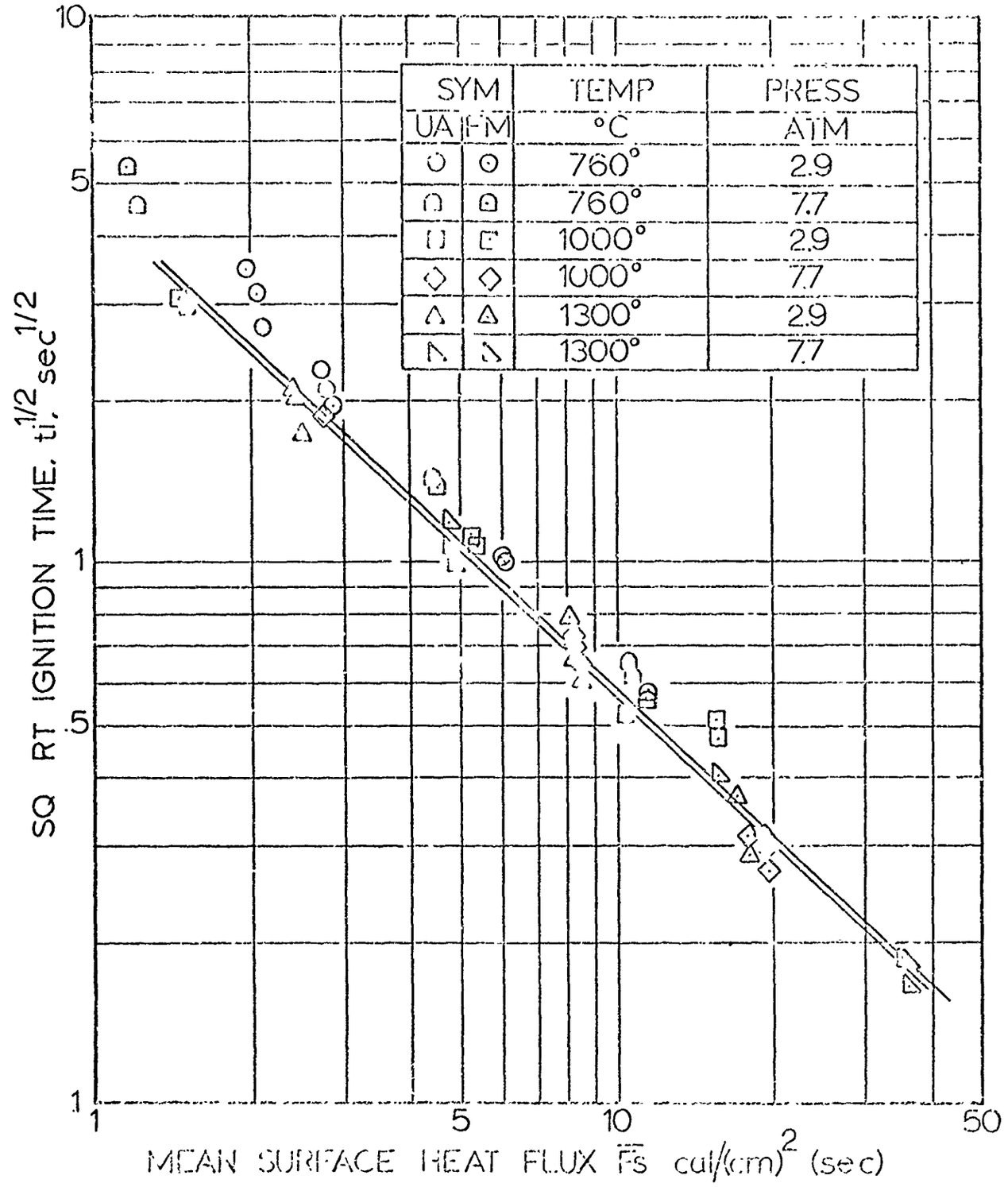

FIGURE 22. IGNITION DATA OF FM AND UA PROPELLANTS IN NITROGEN WITH MEAN-SURFACE-HEAT FLUXES, CALCULATED FROM THE GAR HEAT-FLUX STUDY.

of the UA propellant ignition tests were used to calculate pre-exponential factors of $1.5 \times 10^{}$ and $6.6 \times 10^{}$ cal/(cm)^4(sec) for gas temperatures of 760°C and above 1000°C, respectively.

At least two explanations of this gas temperature effect are apparent. It is possible that the low gas temperature results in a slow gas-phase step and limits the rate of the ignition process. However, it appears likely that such a slow step would effectively increase the ignition time by an essentially uniform time for occurrence of these gas-phase processes. Thus, the fractional increase in ignition time should be greater for shorter ignition times, and this is not the effect noted. The second explanation is suggested by the fact that the ignition times where gas temperatures of 760°C were used are in good agreement with the ignition data from the radiation furnace. This similarity would be expected if the effect of the gas-temperature conditions near the surface were comparable in the two cases. It is postulated that, for the heating by a low temperature gas, the boundary layer gas was too cold to permit rapid exothermic reactions near the surface; and, in the low-pressure radiative environment, the free convective-thermal boundary was too thick to permit rapid reaction near enough to the surface to be effective. However, for convective gas temperatures greater than 1000°C, the temperature in the boundary layer near to the surface would be significantly higher than in the radiation furnace tests. The reactions occurring in the gas phase would take place rapidly, and, significantly, energy would be fed back to the surface from the reactions or, perhaps, indirectly in the form of reactive species. The reactions could involve further reaction of the products of

decomposition of ammonium perchlorate.

The fact that the slopes of the correlating lines through the ignition data, for all temperatures at all pressures, were virtually the same, implies that the same reaction was rate-controlling for all of the conditions; only the energy yield per unit of reaction was changed. Therefore, even though there may be gas species returning to the propellant surface when environmental conditions are of 1000°C or greater, solutions to Equations (1) and (2) still describe the ignition response of ammonium-perchlorate-based propellant as a function of the externally-applied-heat flux and the propellant-thermophysical properties.

It should be noted that this postulate is feasible but only qualitative. No attempt has yet been made to confirm the existance of post-decomposition reactions in the gas phase, and the explanation is presented, since it appears to be consistent with all observations. Alternative interpretations of these results may be possible.

CHAPTER V

SUPPLEMENTARY STUDIES

A. DETERMINATION OF THE TIME OF THE "RUNAWAY" REACTION

The infrared detection system was employed for surface temperature measurements of AR propellant during ignition tests. This propellant consists of a fine grain, ammonium perchlorate, like the UA propellant, but it also contains Philblack E added as a blackening agent to reduce the transmissivity of the polymer to the infrered radiation. Figure 23 is a typical oscilloscope record from these tests, which illustrates the behavior of the propellant surface during heating. The rapid surface temperature rise which is determined from the change in millivolt output from the infrared sensor, starts one to two milliseconds before flame is detected by the photodiode. The maximum rate of surface temperature rise, which is related to the occurrence of the "runaway" reaction, is essentially simultaneous with "first light" seen by the photodiode. Thus, the use of a light sensitive device gives an accurate measurement of the time of the "runaway" reaction for the tests conducted in this study. The surface-temperature histories measured during the ignition process were similar to those measured by Keller. Figure 24 illustrates typical data obtained by use of AR propellant samples with razor-cut surfaces and carbon-coated surfaces. These temperature histories agree, in general, with the predictions based upon the heat-transfer studies and the thermal-ignition theory.

An attempt was made to measure AR propellant-surface temperatures throughout the complete-ignition transient. The largest flow-control orifice (flow Mach number equal to 0.292 at a furnace pressure of 7.7 atm) was employed in an effort to reduce radiation from the flame. When a constant steady-state-surface temperature was indicated, it was found that this temperature was near 750°C or about 200-250°C above the anticipated value.

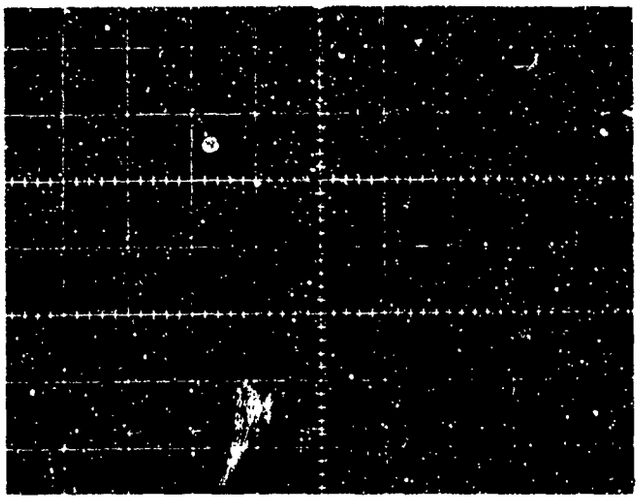

Propellant:	AR	Orifice Number:	12
Gas Temperature:	1300°C	Time Scale:	0.01 sec/div vvv
Initial Pressure:	7.7 atm	Detector Sens:	-1000 mv/div

(conditions for both records)

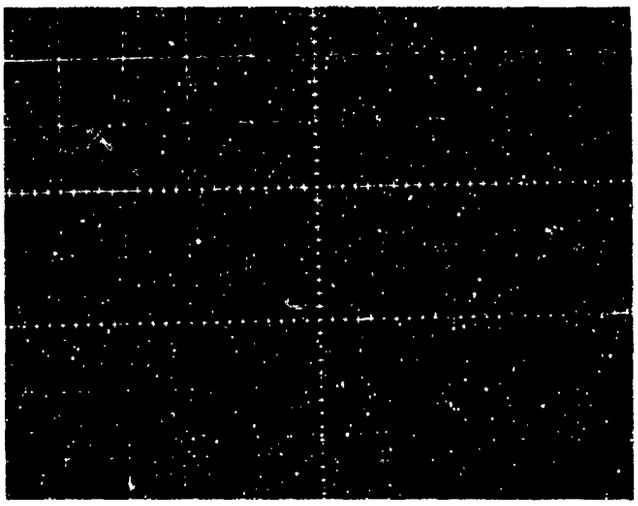

FIGURE 23. TYPICAL OSCILLOSCOPE RECORDS OF AR-PROPELLANT IGNITION TESTS ILLUSTRATING SIMULTANEOUS RISE OF PHOTO DIODE OUTPUT AND THE LARGE SURFACE TEMPERATURE RISE.

The time sweep is from left tc right. The upper trace is the infrared detector output and the lower trace is the output from the photo diode observing the propellant surface.

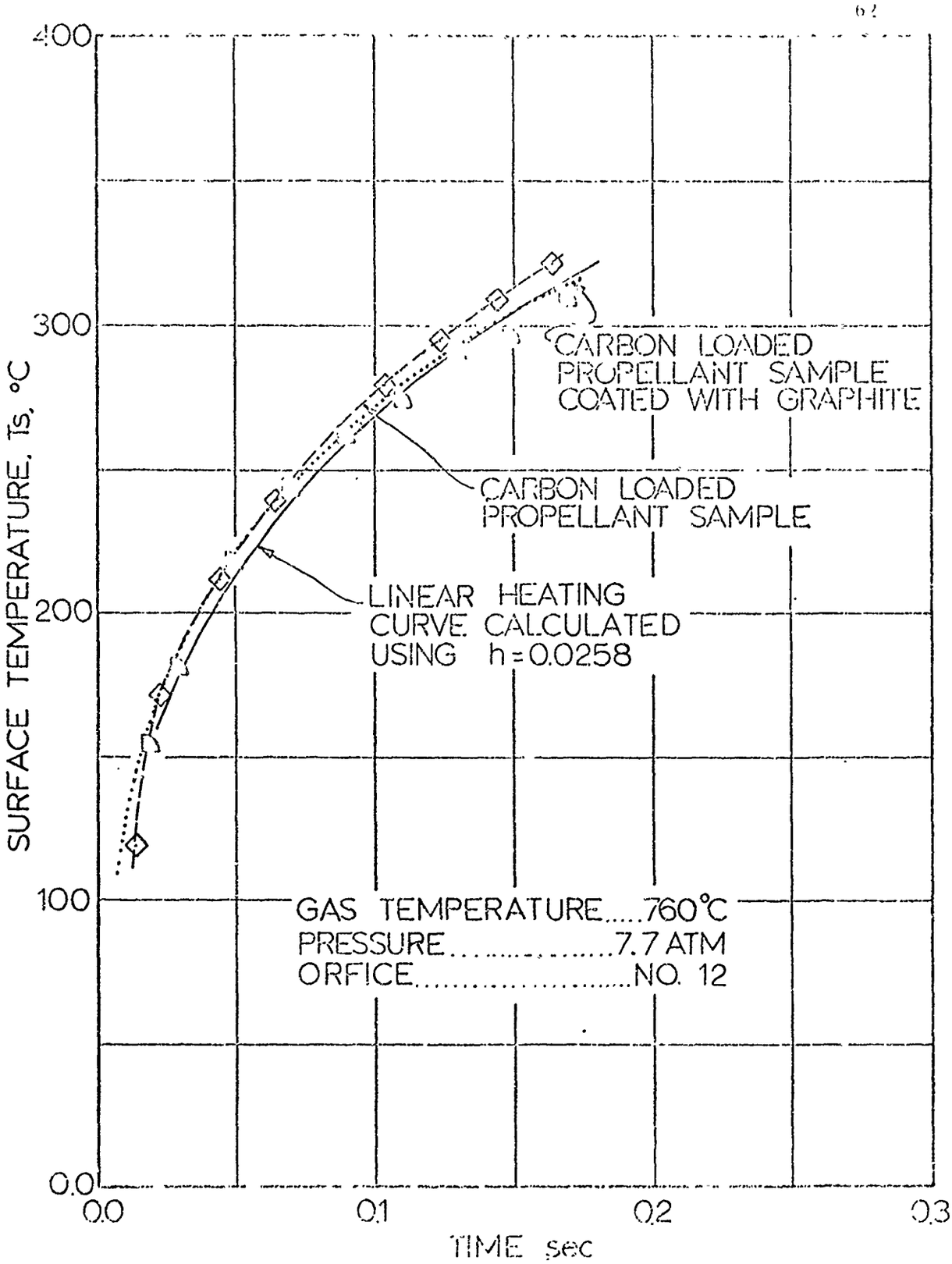

FIGURE 24. SURFACE TEMPERATURE HISTORIES OF AR AND GRAPHITE-COATED AR-PROPELLANT SAMPLES DURING IGNITION TESTS IN NITROGEN.

Apparently, radiation from the thin flame zone was significant, and the infrared detector output was not indicative of the surface temperature after the flame appeared. Tests could be conducted with no flow-control orifice, and this would possibly cut down on the radiation from the flame zone.

B LONG SAMPLE IGNITION STUDIES

In order to investigate the phenomena reported by Bastress [10] concerning ignition occurrence away from the leading edge of a convectively heated sample, a new test section was designed to enable ignition tests to be made using relatively long propellant samples. Samples in these tests were 1.9 cm long, measured in the direction of gas flow; whereas, the normal circular sample surfaces were 1 cm in diameter. Presumably, the flow structure was quite uniform over the last one-half to three-fourths of the sample contacted by the gas. The results of these tests are summarized in Table XIII.

During ignition tests, the surfaces of the propellant samples were photographed using a Fastax Model WF 17 T motion picture camera operating at 2000 frames per second. The position of the "first light" of ignition on the sample surface was located by review of the developed motion pictures. Also, the spread of the flame across the sample surface was observed. A typical ignition sequence is shown in the series of photographs presented as Figure 25.

Samples of the coarse-grain, FM propellant ignited in a nitrogen atmosphere consistently showed ignition to begin near the leading edge of the sample. Since the heat flux near the leading edge is normally higher

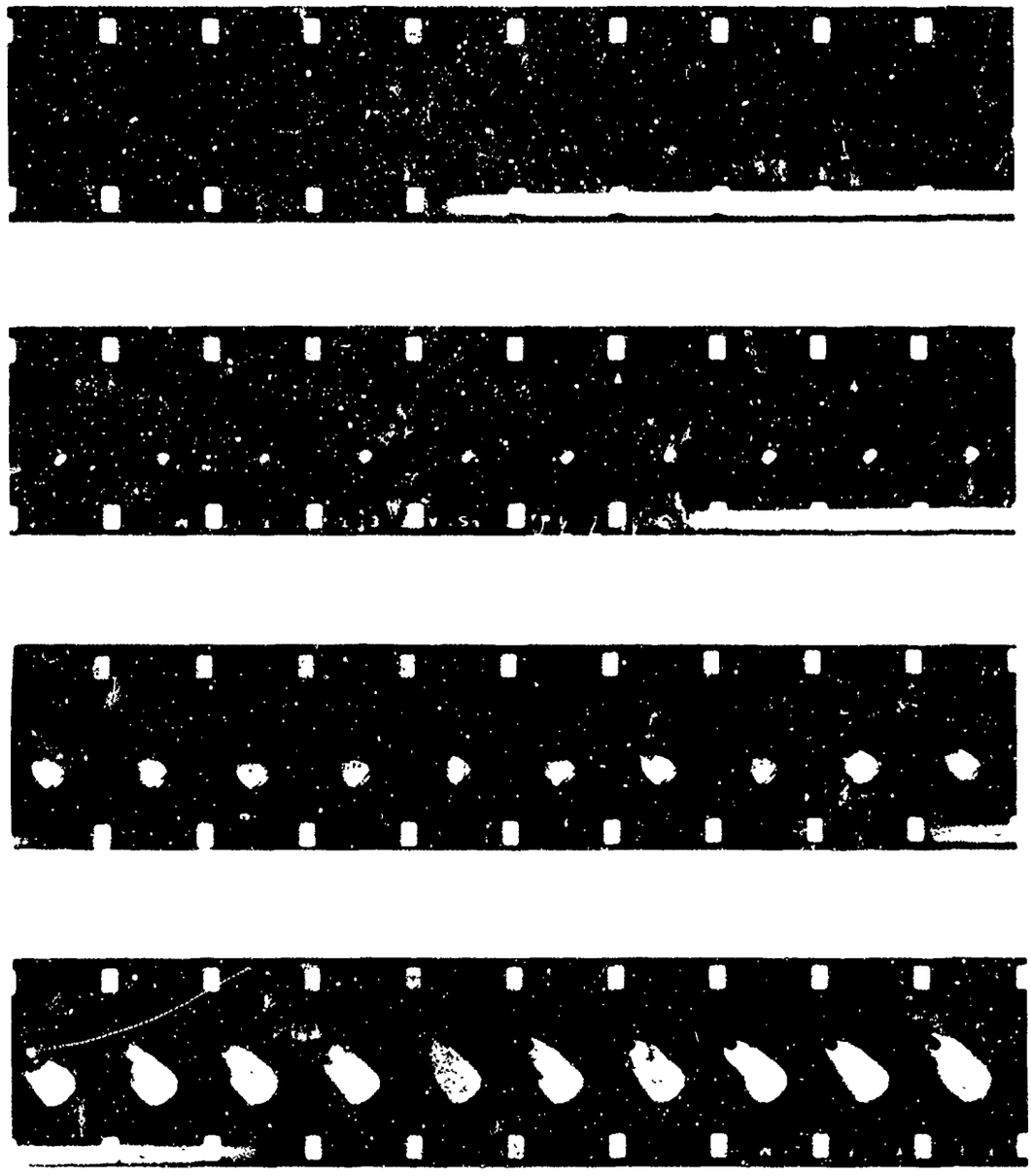

FIGURE 25. HIGH SPEED PHOTOGRAPHS OF THE IGNITION OF A LONG FM-PROPELLANT SAMPLE IN NITROGEN.

Pictures were taken at the rate of 2000 frames per second. Twenty frames are missing between each row of pictures. The approximate position of the sample is outlined in the first and last frames. The gas flow is on about a 45° angle flowing from bottom to top. The first frame shows the first light of ignition near the sample leading edge.

than the flux farther down the sample, such behavior is consistent with the postulate that the magnitude of the heat flux controls the ignition time. Tests were conducted using gas temperatures of 760, 1000, and 1300°C and pressures of 2.9 and 7.7 atm with gas-flow-Mach numbers of 0.78 and 0.292 in the test section. Some of the tests were conducted with the sharp-edged-turbulence trip removed to allow boundary-layer transition to occur across the sample. When surfaces of FM propellant samples were roughened by sanding with a fine-grain sandpaper, ignition started essentially simultaneously along the first quarter of the propellant surface length.

Tests were conducted in which an aluminized coarse-grain propellant, XF, was used. In this case, the first flame of ignition appeared occasionally between the leading edge and half-way down the propellant sample. When the samples ignited in the center, the flame spread both upstream and downstream across the sample surface. Often, the first flame occurred at the leading edge. On occasion, samples of XF propellant ignited simultaneously at the sample center and near the leading edge.

Although the gas pressure, temperature, and velocity were varied and the sample surface conditions were purposely altered, the first evidence of ignition of the non-aluminized FM propellant in the neutral-nitrogen atmosphere always appeared near the point of maximum-heat flux. The data obtained with the aluminized propellant were inconclusive, and it is possible that, when observed, ignition away from the leading edge may have been the result of surface irregularities.

C. RAPID HEATING OF THE POLYMERIC FUEL BINDERS

Various polymer compositions were subjected to rapid heating in the convective-heat-flux furnace. All tested samples were prepared with about three per cent of a finely dispersed carbon black. The surface temperatures of the samples were monitored during heating by use of the infrared detection system. It was hoped that variations in the rate of surface temperature rise during rapid heating could be related to the energy changes associated with the endothermic decomposition reactions of the polymers. The suitability of the apparatus for such a study could be determined by comparison to the extensive data of J. T. Cheng [15] on the PBAA system.

1. Polybutadiene-Acrylic Acid Copolymer Decomposition Studies

Samples of the PC polymer, which is the copolymer of polybutadiene-acrylic acid and Epon 828 curative resin, were prepared and subjected to rapid heating by nitrogen at 760°C and 7.7 atms. A few of the PC samples tested were coated with a film of a commercial-colloidal graphite; the surface emissivity of this coating is reported to be 0.89. The same coating was used on the surface viewed in the calibration tests of the infrared-detection system (see Appendix D). Figure 26 illustrates the surface temperature histories of various PC samples. The indicated surface temperature of the coated samples was higher than that of the uncoated PC samples for surface temperatures below 400°C. This implies that either the emissivity of the PC samples was below 0.89 or that the transmissivity of the PC polymer was significant. Since the surface temperatures of both types of samples are nearing each other at high temperatures, after the depth of temperature penetration has become significant, it is believed

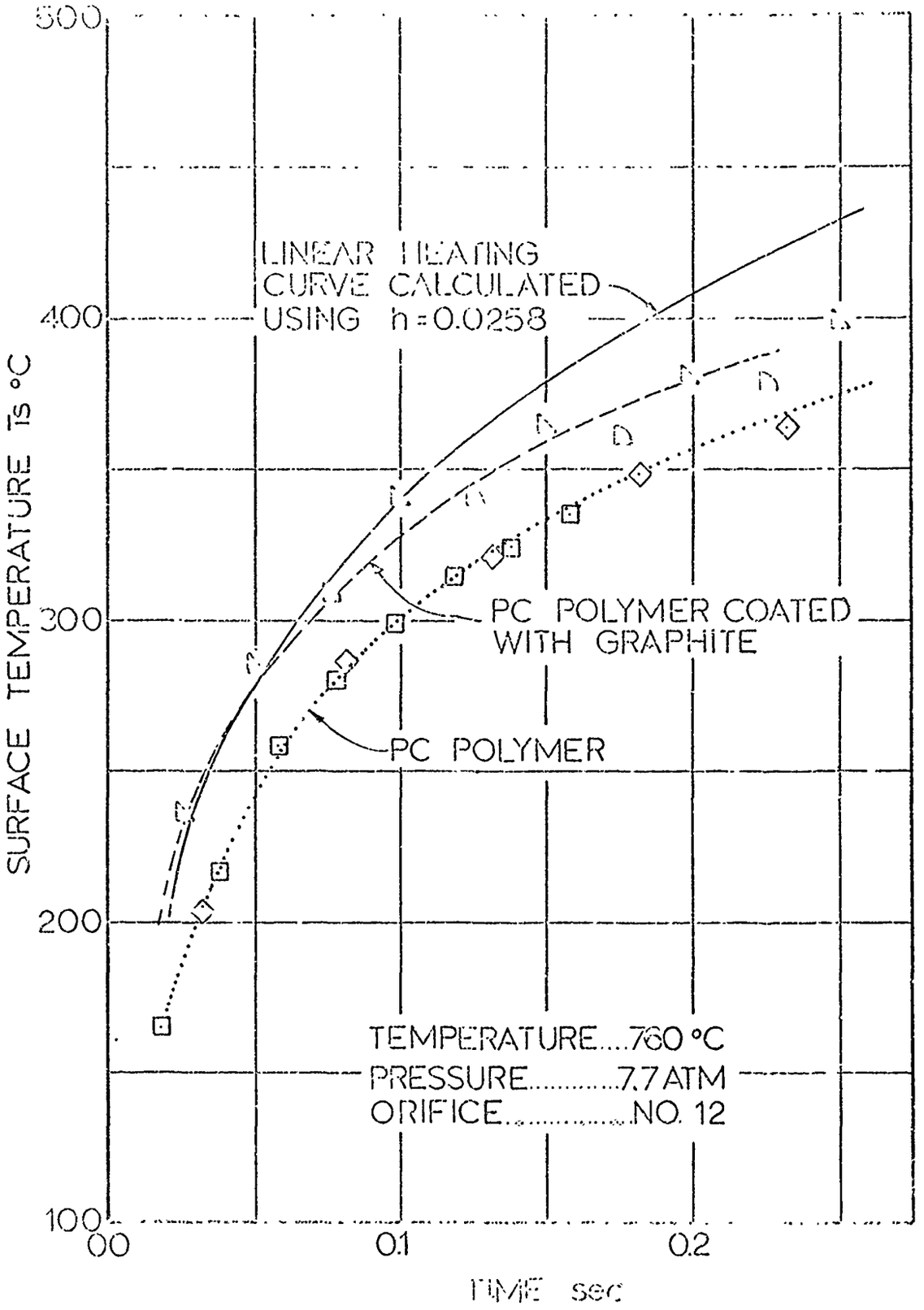

FIGURE 26. SURFACE TEMPERATURE HISTORIES OF PC AND GRAPHITE-COATED PC POLYMER SAMPLES DURING RAPID HEATING TESTS IN NITROGEN AT 760°C AND 2.9 ATM.

The indicated surface temperature of the graphite-coated polymer samples lie above the uncoated samples illustrating the effect of the surface transmissivity or decrease in emissivity.

that the surface-temperature differences are caused by differences in the transmissivity of the samples. The PC samples appeared somewhat attacked and roughened by the solvent of the colloidal graphite; and, since greatest interest was in the high-temperature conditions where both surfaces appeared to be equivalent, most tests were made with the polymer samples uncoated.

Shown in Figure 26 are temperature-time values calculated by use of the mean-heat-transfer coefficient from the GAR heat-transfer study and a thermal responsivity of .014 cal/(cm)^2(sec)$^{\frac{1}{2}}$(°C) reported by Cheng [15]. For surface temperatures of coated samples below about 340°C, the experimental values lie above the calculated values. This results because the heat-transfer coefficient is apparently decreasing with time and the instantaneous-heat-transfer coefficient at shorter times would be larger than the mean-heat-transfer coefficient used in the calculation. But, for surface temperatures around 350°C, the measured values fall below the calculated values which indicates the occurrence of an endothermic reaction.

The difference between the indicated-surface temperatures of graphite-coated samples and of uncoated samples, after long exposure, appeared to be small and, therefore, meaningful data could be obtained from the uncoated samples for long test times and at high-surface temperatures. Figure 27 shows the results of such tests for the polymer PC, where the mean-heat flux was 17.6 cal/(cm)^2(sec), and the furnace was at 1300°C and 2.9 atms. The surface temperature of the polymer rises and remains constant at about 515°C after 0.5 seconds of heating. Cheng's data indicated polymer vaporization at a temperature of 510°C and indicated some endothermic reaction

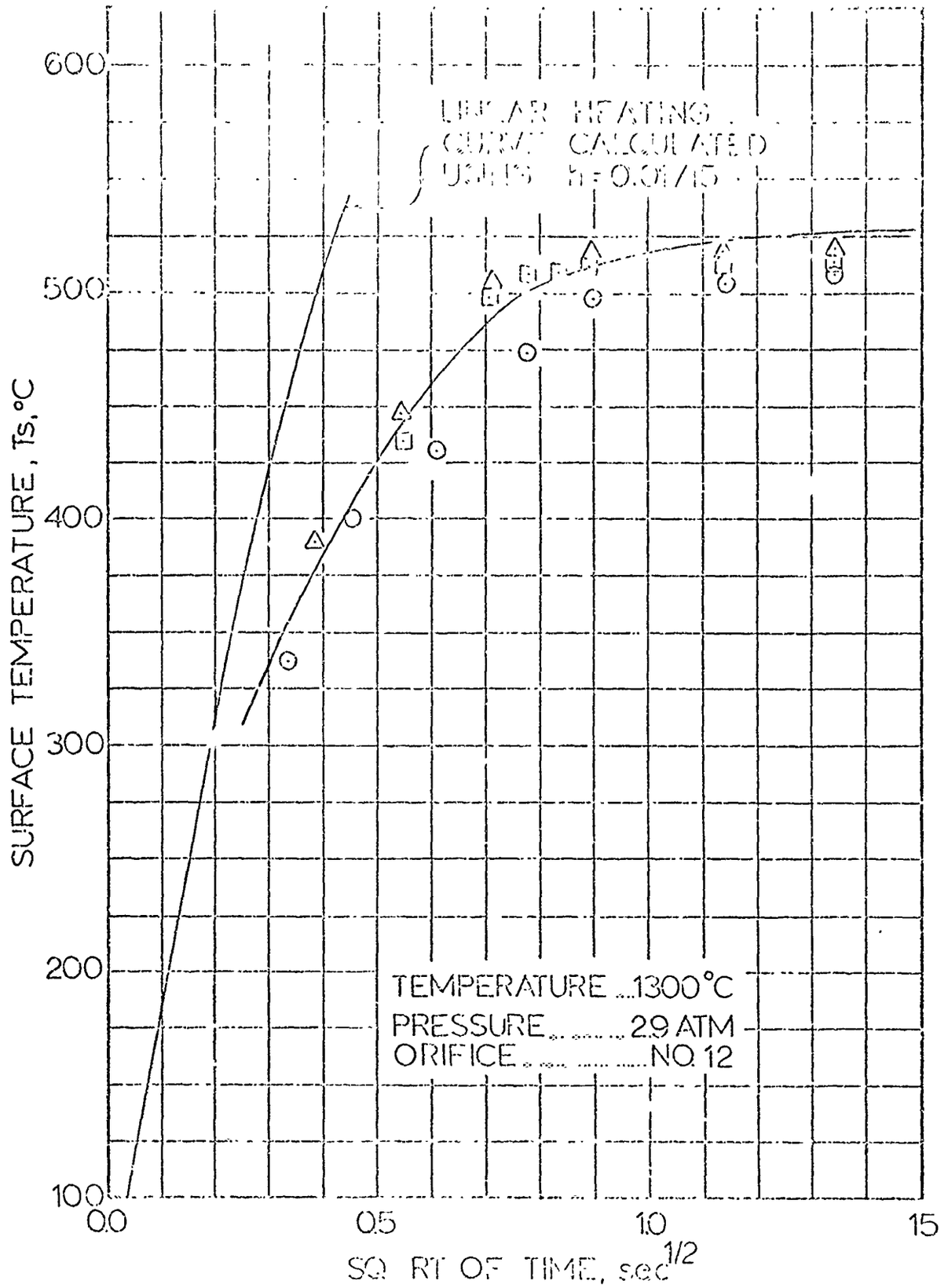

FIGURE 27. SURFACE TEMPERATURE HISTORIES OF TC POLYMER SAMPLES DURING RAPID HEATING TESTS IN NITROGEN AT 1300°C AND 2.9 ATM.

The indicated surface temperature of the polymer sample reaches a plateau near 500° where sublimation process appears to be taking place

taking place around 400°C at this pressure. Subsequent tests showed this apparent agreement to be, in part, fortuitous. The vaporization temperature reported by Cheng was shown to exhibit a predictable dependence on pressure. The constant surface temperature measured during convective heating was essentially independent of pressure (see Table XIV), and this temperature is, apparently, associated with a melting process since flow of the sample surface in the convective environment was noted (see Figure 28).

Samples were prepared by adding copper-chromite-burning rate catalyst to the PBAA polymer. These samples, labeled PCC, were tested in nitrogen pressures of 2.9 and 2.2 atm and a temperature of 1300°C with heat fluxes near 15 $cal/(cm)^2(sec)$. The surface temperature reached a plateau value around 540°C, which is about 30°C above the plateau temperature indicated for the catalyst free samples. Cheng noted a significant decrease in the decomposition temperature resulting from the addition of the catalyst. It appears likely that one effect of adding the solid catalyst was to decrease the transmissivity or increase the apparent emissivity of the polymer and, thus, to yield higher indicated surface temperatures. This effect apparently masked any decrease in decomposition temperature which might have resulted from addition of the catalyst. Samples were, also, prepared by adding small amounts of ammonium perchlorate, approximately five-weight-per cent, to the PBAA. These samples, A05, were subjected to rapid heating and the results indicated a leveling in the surface temperature to take place around 520°C for a pressure of 2.2 atm and 530°C at 2.9 atm. Again, the apparent increase in emissivity resulting from addition of solid material likely had a larger effect than reduction in decomposition

DIRECTION OF
GAS FLOW

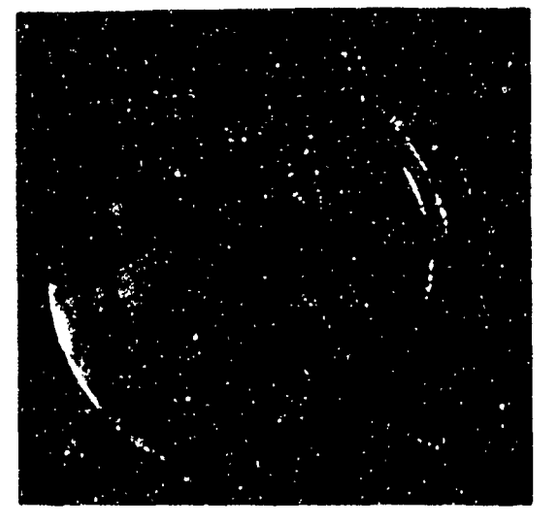

	TOP	BOTTOM
Sample:	PC	AO5
Gas Temperature:	1315°C	1307°C
Pressure:	2.9 atm	2.9 atm
Orifice Number:	12	12
Heat Flux:	17 cal/(cm)^2(sec)	17 cal/(cm)^2(sec)

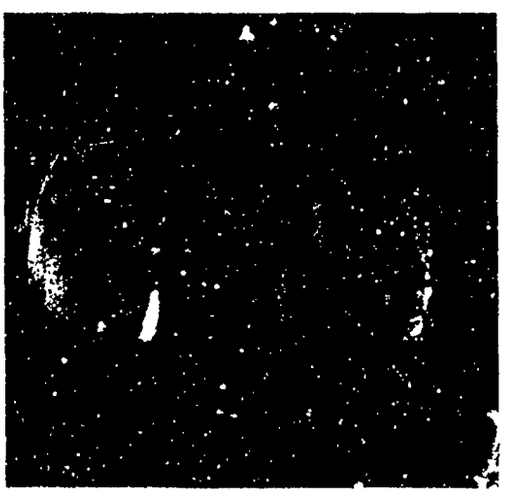

FIGURE 28. PHOTOMICROGRAPHS (5X) OF SURFACE OF PC AND AO5 POLYMER SAMPLES AFTER RAPID HEATING TESTS IN NITROGEN.

temperature resulting from the AP-polymer interaction noted by Cheng. Figure 28 is a photograph of the A05 polymer surface after a rapid-heating test.

Samples of GAR, the material similar to PC but loaded to about 50 weight per cent with fine glass beads, which was used in the heat-transfer study, were heated to anticipated decomposition temperatures in the convective apparatus. Some samples were coated with the colloidal graphite and tests were made with uncoated and blackened surfaces for comparison. Figure 29 illustrates the results of these tests. The indicated surface temperatures of both types of samples were essentially the same, but the coated surface values were,generally,slightly higher. Figure 30 is a plot of the GAR-polymer-surface temperature while heating in nitrogen at 1300°C and 7.7 atm. Also represented on the plot are calculated-surface temperatures for linear heating through a constant heat-transfer coefficient obtained from Figure 18. The GAR thermal responsivity is 0.0315 cal/$(cm)^2(sec)^{\frac{1}{2}}(°C)$. In Figure 30, the first three experimental points are below the calculated values because of inaccuracies in the correction for large background radiation from dust particles in the hot gas. At later times, when this correction is less severe, the agreement between measurement and calculation is exact. No endothermic phenomena are apparent at surface temperatures below 35[illegible]°C. Although the sample surfaces were visibly altered during these tests, it was not possible to detect this change from the surface-temperature-time records. When exposed to rapid convective heating, all the PBAA based samples reacted like passive bodies until surface temperatures of 350°C to 400°C were reached. Above this temperature, some endothermic phenomenon appeared to take place. The endo-

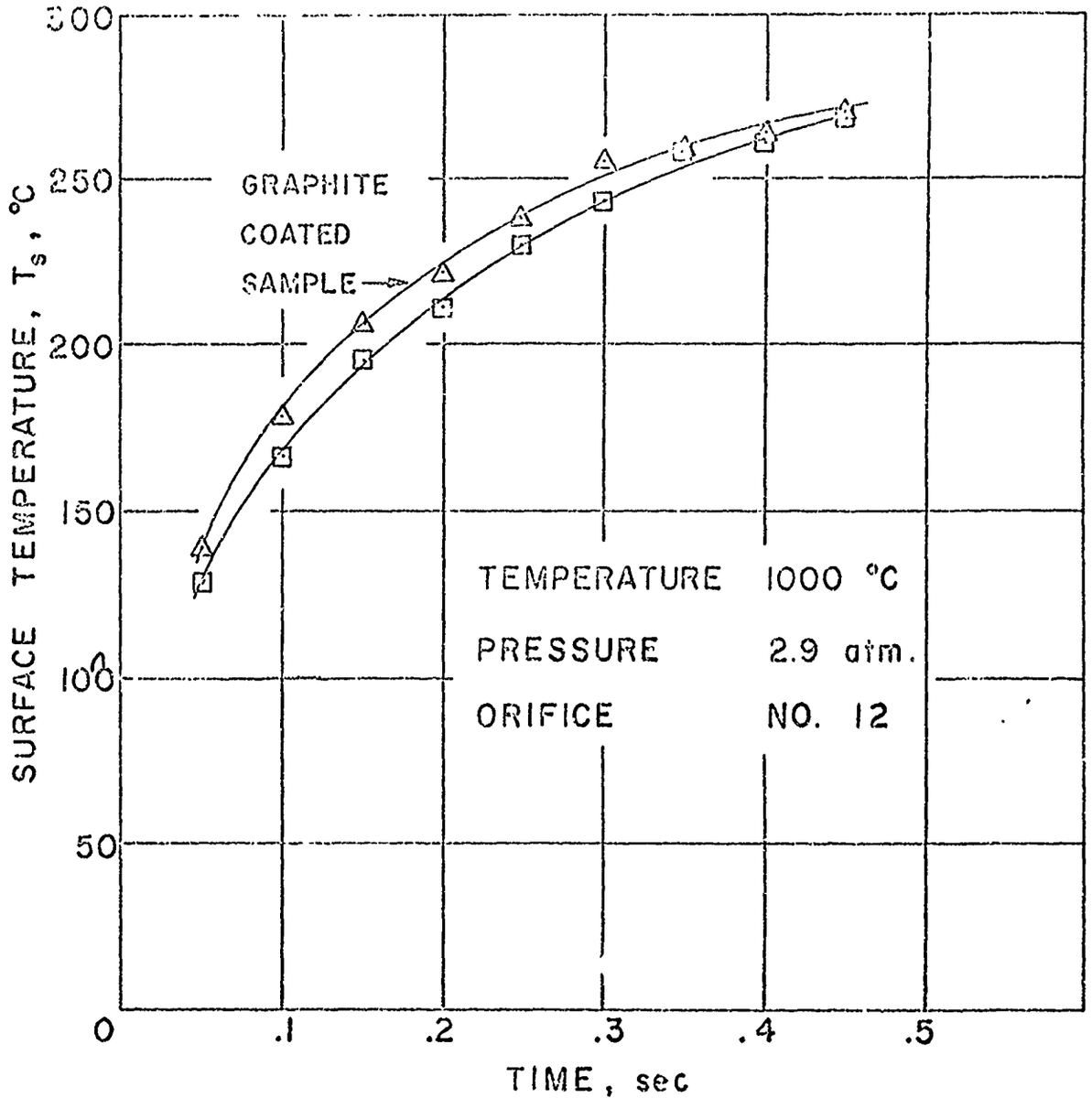

FIGURE 29. SURFACE TEMPERATURE HISTORIES OF GAR AND GRAPHITE-COATED GAR SAMPLES DURING HEAT-FLUX TESTS IN NITROGEN AT 1000°C AND 2.9 ATM.

The indicated surface temperature of the graphite coated polymer samples lie above the uncoated samples illustrating the effect of the surface transmissivity or decrease in emissivity.

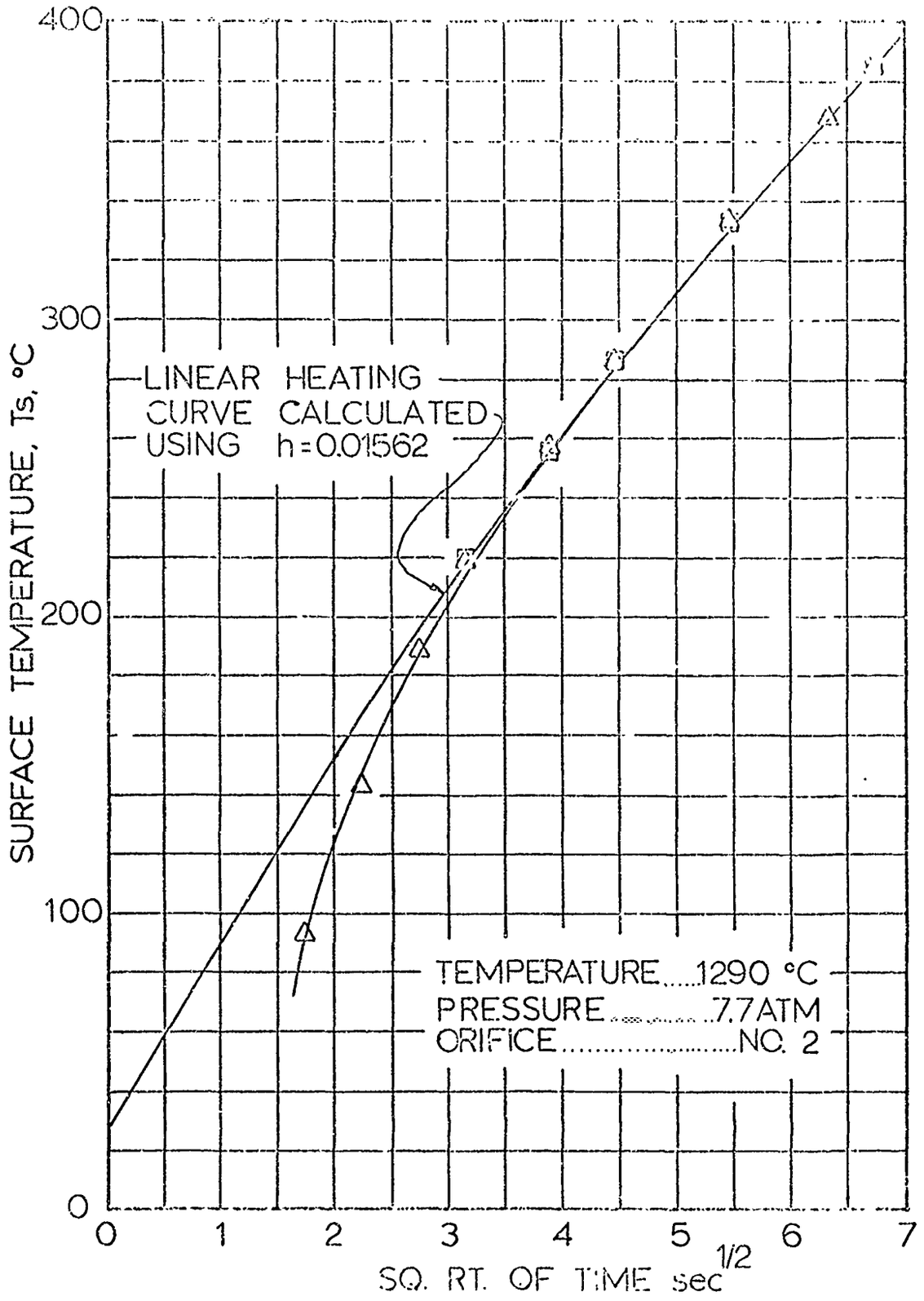

FIGURE 30. SURFACE TEMPERATURE HISTORIES OF CAR SAMPLES IN NITROGEN AT 1300°C AND 7.7 ATM.

The figure illustrates the good agreement between the experimental data and the calculated surface temperature for values above 200°C.

thermic effect observed appears to be caused by decomposition and melting of the polymer at the sample surface and may be the "first" decomposition reaction noted by Cheng. After this initial decomposition, the surface temperature then rose to values in excess of 525°C and, there, remained constant. The environmental pressure appeared to have no effect on the value of this temperature.

2. Polyurethane Polymer Decomposition Studies

A carbon-loaded-polyurethane polymer, PUC was exposed to rapid convective heating at fluxes near 10 cal/(cm)^2(sec). The results of these tests are illustrated in Figure 31 where the polymer surface temperature is plotted as a function of time. Endothermic phenomenon appear to take place when the indicated polymer surface temperature reaches a value near 380°C and separates from the calculated linear-heating temperature curve. The surface temperatures of the sample reached a plateau of around 430°C in tests for the pressures of both 2.9 and 2.2 atm. These values are uncorrected for effects of transmissivity and possible emissivity differences and may be expected to be lower than the true surface temperatures.

3. Polyflurocarbon Polymer Decomposition Studies

A polyflurocarbon, supplied by Thiokol Chemical Corporation, was tested in the convective-heat-flux furnace at heating rates near 10 cal/(cm)^2(sec) and a gas temperature of 1000°C and pressure of 2.9 atm. When both this material and polyurethane polymers (PUC) mixed with AP propellants are formed which exhibit unusually high values of the low pressure deflagration limit, P_{DL}[32]. It was hoped that some correlation would exist between the measured decomposition temperatures and the low-pressure deflagration limit of propellants produced by use of the polymers. Under normal circum-

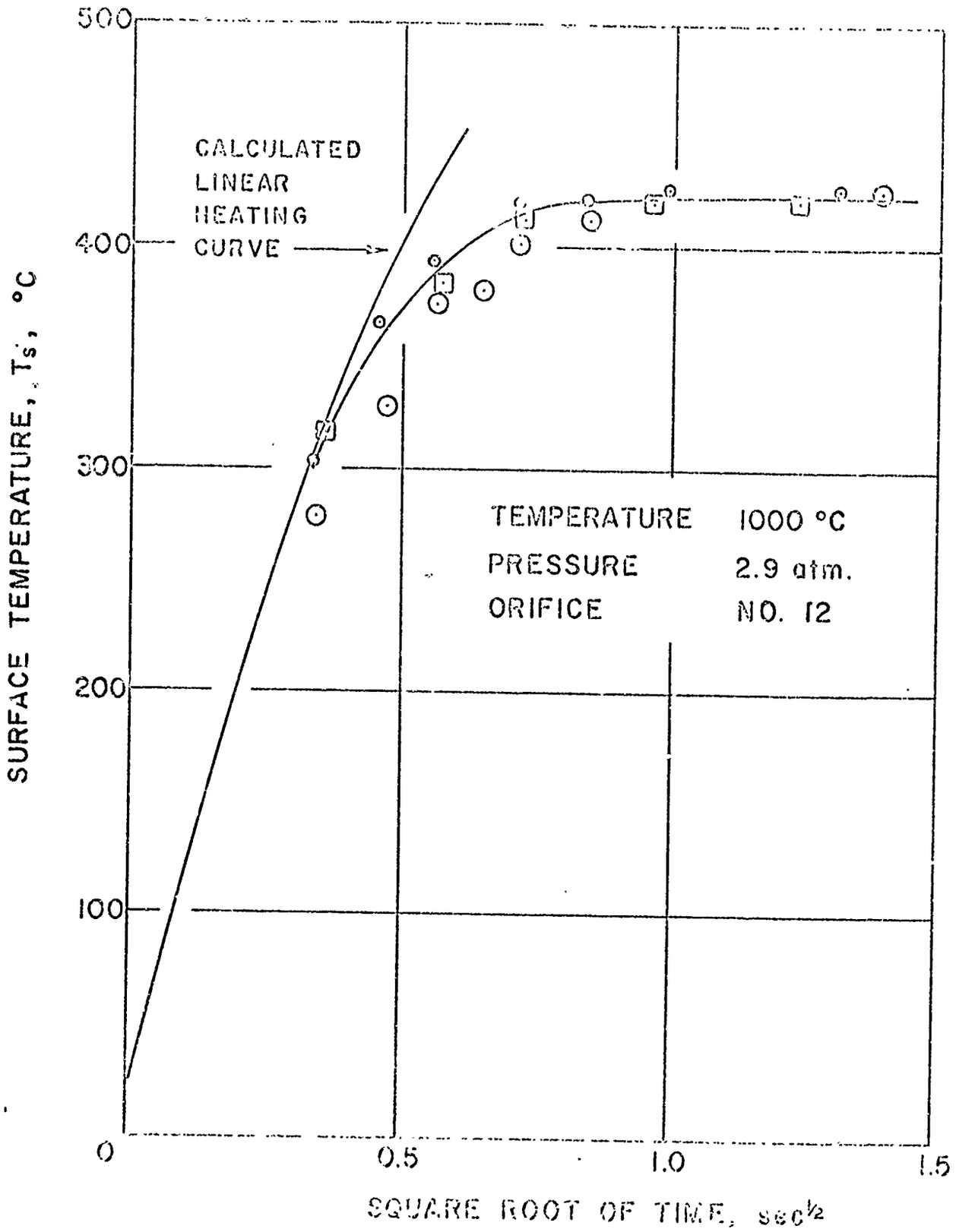

FIGURE 31. SURFACE TEMPERATURE HISTORIES OF PUC POLYMER SAMPLES DURING RAPID HEATING TESTS IN NITROGEN AT 1000°C AND 2.9 ATM.

The indicated surface temperature of the polymer sample reaches a plateau near 425°C.

stances, the deflagration limits are in the order: PBAA, polyurethane and polyflurocarbon with the polyflurocarbon propellant having the higher pressure limits.

The results of the tests on the flurocarbon are illustrated in Figure 32, where the indicated sample-surface temperature is plotted as a function of exposure time. A difference between the temperatures calculated by assuming linear heating and the measured-surface temperatures appears when temperatures near 375°C are reached. These temperatures are uncorrected for transmissivity and emissivity effects; and, although this material contained carbon black, the transmissivity effect for this polymer is likely large. The indicated polymer surface temperature was still rising at the end of the tests, even though the surface was ablating, and reached a temperature near 500°C.

If a correlation exists between polymer decomposition temperature and the low-pressure deflagration limit of the propellant produced by use of the polymer, such a correlation is not apparent from the data obtained in this study. Because of questions concerning the sample emissivity and transmissivity, these data cannot, however, be considered as conclusive.

4. Use of Convective Heat-Flux Furnace for Polymer Decomposition Studies.

The results of the polymer decomposition tests indicated that the convective-heating apparatus and the infrared-detection system may be useful for the study of polymer-decomposition reactions under conditions of rapid heating. However, before truly meaningful data can be obtained, the correction for background emission must be more accurately determined, and the effects of polymer surface emissivity and transmissivity must

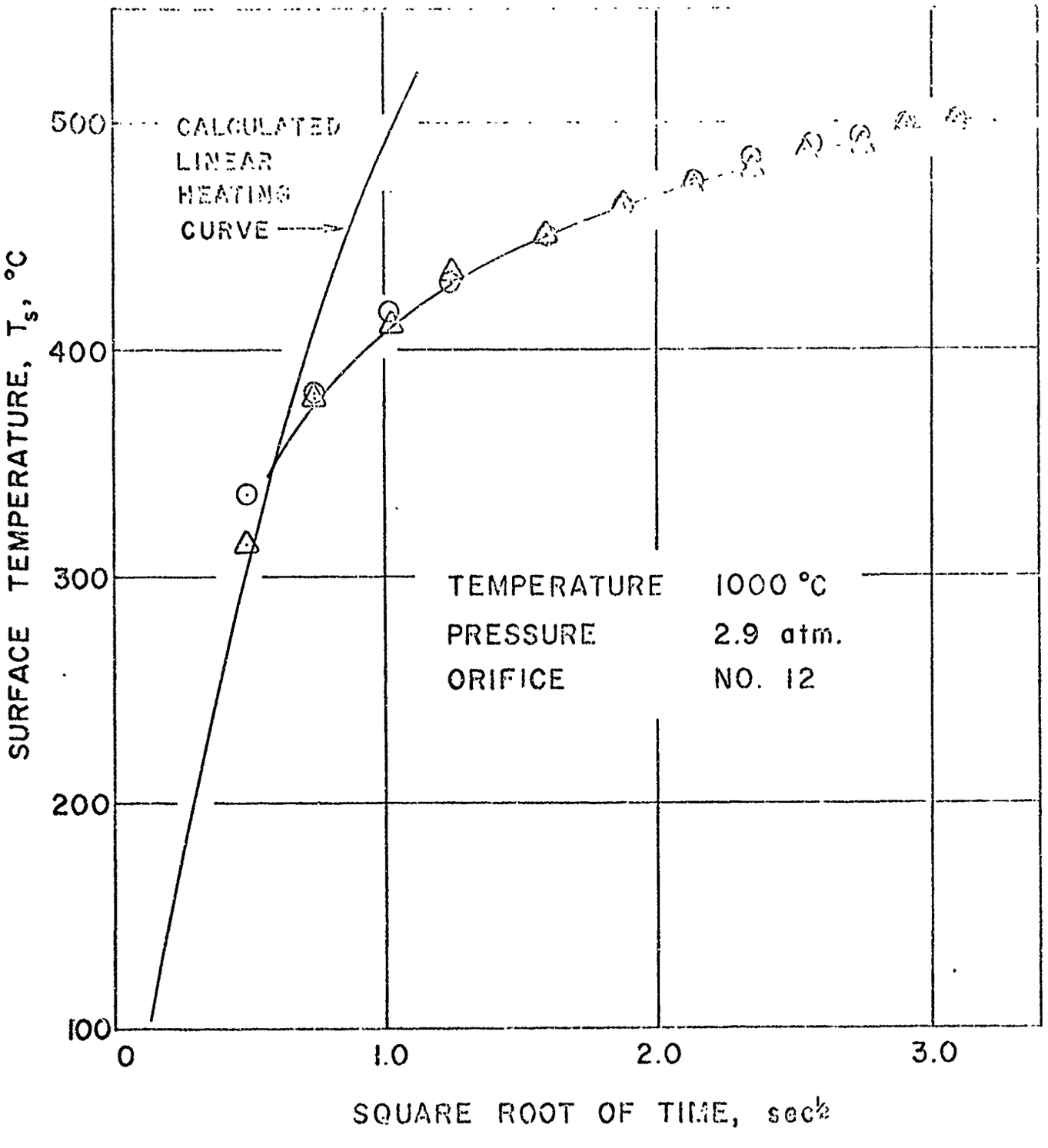

FIGURE 32. SURFACE TEMPERATURE HISTORIES OF PFC POLYMER SAMPLES DURING RAPID HEATING TESTS IN NITROGEN AT 1000°C AND 2.9 ATM.

be accounted for. The use of filters may help cut down background emission effects, and the addition of more and better dispersed carbon black could help blacken the polymer surface to account for emissivity and transmissivity effects.

CHAPTER VI

CONCLUSIONS AND RECOMMENDATIONS

A MEASUREMENT OF IGNITION TIMES

The experimental detection of the time of ignition of a solid propellant has been an unresolved problem for most studies. Often "first flame," as detected by a photo sensitive device, has been used as a convenient indication of ignition; however, even after appearance of a flame, continued application of external energy may be needed to produce a transition to steady-state burning. Tests have been made in which a "go-no-go" criterion was used by termination of the externally applied energy and waiting for consumption of the sample [48]. In this case, there can be no question about the transition to burning. The practical definition is likely the time to first reach steady-state regression rate while subjected to the igniter-heat flux.

In the study reported here, the experimental-ignition time was shown to be coincident with occurrence of the "runaway" reaction postulated by the ignition model used for interpretation of the data. In the actual tests, the propellant ignition was detected by a photocell light-sensing device. The applicability of this procedure was investigated by conducting-ignition tests where the propellant surface was simultaneously observed by an infrared-sensing device and the photodiode. The infrared detector monitored the propellant-surface temperature while the photodiode observed light emissions from the sample. The results showed that the first indication of light emission from the propellant surface occurred simultaneously with maximum rate of rise of the sample-surface temperature. Therefore, in these tests, the method of measuring propellant ignition times was chosen to be consistent with the ignition model.

B. CONVECTIVE HEAT-FLUX FURNACE

The convective heat-flux furnace was found to be useful for obtaining reproducible ignition data for solid propellants. Convective-heat fluxes in the range of 2 to 50 cal/$(cm)^2$(sec) can be obtained, and various gases can be supplied at temperatures from 600°C to 1350°C and at pressures of 2 to 10 atms. The reproducibility and precision of the data obtained from this apparatus are superior to the results from the shock tube ignition apparatus which is useful only for very short ignition times [25] and are very comparable to data derived by use of thermal radiation [7] for the same time scale. The heat-transfer characterization of this apparatus was difficult, because it was found that, under some conditions, the heat-transfer coefficients were functions of the sample surface temperature. This problem is likely the result of non-uniform flow across the flow channel. It may be desirable to use a cylindrically-shaped flow channel to avoid the possibility of non-uniform gas flow or channeling.

C. EFFECT OF HEAT-TRANSFER INTERPRETATION ON CORRELATION OF IGNITION DATA

The ignition times of solid propellants are a strong function of the rate of externally applied energy. In this study, three separate heat-transfer investigations were conducted, and the results of the ignition tests were subject to quite different interpretation when applying the results of the various heat-transfer studies. Both pyrex and alumina heat-flux gages were used in separate studies to characterize the convective heat-flux furnace for mean-surface-heat fluxes. However, when these heat-

flux values were correlated with the experimental-ignition times, inverse pressure effects on ignition and other unexplained phenomena were indicated. Although the measured-ignition times were near those observed in other test devices under supposedly comparable conditions, serious disagreement was apparent between the new and prior data. For this reason, it was difficult to draw firm conclusions concerning the ignition results. Because of possible effects on the heat-transfer process of temperature gradients across the flow channel, the transition of the boundary layer, and the variation in thermophysical properties of the heat-flux gage; another heat-flux study was made in an attempt to more nearly approach ignition test conditions. An infrared-detection system was used to measure the surface temperature of heated-simulated-propellant samples. The results of these tests were then used to further evaluate the ignition test data. Finally, a consistent and hopefully correct interpretation was generated. It must, therefore, be concluded that when convective-heat fluxes are employed in propellant-ignition studies, the characterization of the transient heat-transfer processes in the apparatus is a most critical process. Anomalies suggested by other studies may be the result of an insufficient heat-transfer characterization.

D. INTERPRETATION OF THE IGNITION TEST DATA

Ignition tests were conducted in nitrogen and helium atmospheres with furnace temperatures of 760, 1000, and 1300°C, and pressures of 2.9 and 7.7 atm. Gas-flow-Mach numbers across the sample surface were varied from 0.02 to 0.292. When experimental-ignition times of propellants were correlated

with mean-surface heat fluxes no effects of pressure or gas velocity on ignition times were observed. No detectable effect of surface roughness of the samples was noted for the range of ignition times considered from 0.0225 to 47.5 sec; although, the precision of the data was improved by use of smooth-surface samples.

The temperature of the gas phase in the boundary layer adjacent to the propellant sample apparently affected the ignition times of the propellants. Ignition tests conducted with nitrogen at 760°C yielded propellant-ignition times in very good agreement with ignition data from the thermal-radiation furnace. These data were well described by the "thermal ignition model." But ignition times where gas temperatures of 1000°C or greater were employed were 20 per cent shorter than the ignition times for the 760°C gas. It is postulated that the apparent increase in propellant ignitibility was caused by an increase in the release of energy and reactive species from the ammonium perchlorate-decomposition products in the high-temperature gas phase adjacent to the solid. This phenomenon is not predicted by the thermal ignition model. However, the model does describe the ignition behavior, if it is assumed that the gas temperature affects the pre-exponential factor of the key-surface reaction.

The correlation of the experimental-ignition times with mean-surface-heat fluxes indicated that the activation energy of the rate-controlling-surface reaction was the same for all gas temperatures and was equal to about 25,000 cal/mole. The pre-exponential factor describing the energy-release rate per unit area from the key-surface reaction was increased from 1.5×10^9 cal/$(cm)^2$(sec) when the test-gas temperature was 760°C to

6.6×10^9 cal/(cm)^2(sec) when 1000°C and 1300°C temperature gases were used.

E. IGNITION TESTS OF RELATIVELY LONG PROPELLANT SAMPLES

Motion pictures at speeds of 2000 frames per second were taken of the ignition of 1.9-cm-long samples of propellants in nitrogen. Results from tests under a variety of conditions showed that the ignition of the coarse-grain FM propellant consistently started near the leading edge of the samples near the point where the surface heat flux was expected to be the highest. Propellant samples containing aluminum ignited either near the leading edge or half way down the sample surface. Samples of surface-roughened FM propellant ignited simultaneously along the first half of the sample surface. Therefore, it may be concluded that the 1-cm-diameter propellant samples used in the ignition tests reported here, should yield data representative of larger propellant samples. Under the test conditions available, the phenomenon of convective ignition away from the point of maximum heat flux reported by Bastress [10] was not noted.

F. SURFACE TEMPERATURE MEASUREMENTS OF POLYMERIC FUEL BINDERS DURING RAPID CONVECTIVE HEATING

Samples of PBAA polymeric fuel binder were prepared with and without copper-chromite catalyst, glass beads, and small percentages of ammonium perchlorate. These samples were exposed to rapid heating and appeared to behave like passive bodies until surface temperatures of about 350°C were reached. Above this temperature, some endothermic phenomenon appeared to take place, and when the surface reached temperatures near 525°C, it was

mained constant even during additional heat exposure. The environmental pressure appeared to have no effect on the value of this high temperature plateau; and this temperature appears to be associated with a melting process.

Samples of carbon-loaded polyurethane exposed to rapid convective heating appeared to behave like a passive body until surface temperatures above 380°C were reached. The measured surface temperature became constant at about 430°C for all pressures tested.

A tested polyflurocarbon-fuel binder behaved like a passive body until a surface temperature of above 375°C was reached. The polymer surface temperature was still rising at the end of the tests, even though the surface was ablating and had reached an indicated temperature near 500°C.

The results of these tests indicated that the convective heating apparatus and the infrared detection system may be useful for the study of polymer decomposition reactions under rapid heating conditions; however, a number of improvements in the technique for sample preparation and operating procedures appear to be needed before truly meaningful data can be obtained.

REFERENCES

1. Adams, D. M. "Igniter Performance in Solid Propellant Rocket Motors." *J. Spacecraft, 4,* 1024-1029 (1967).

2. Allan, D. S., Bastress, E. K., and Smith, K. A. "Heat Transfer Processes During Ignition of Solid Propellant Rockets." *J. Spacecraft, 4,* 95-100 (1967).

3. Allen, H., Jr. and Pinns, M. L., "Relative Ignitability of Typical Solid Propellants with Chlorine Trifluoride." NASA TN D-1533 (1963).

4. Altman, D. and Grant, A. F., Jr. "Thermal Theory of Solid-Propellant Ignition by Hot Wires." *Fourth Symposium (International) on Combustion.* Williams and Wilkins Co., Baltimore, Md., 1953, 158-161.

5. Anderson, R., Brown, R. S., and Shannon, L. J. "Ignition Theory of Solid Propellant." *AIAA* Reprint No. 64-156 (January 1964).

6. Anderson, R., Brown, R. S., Thompson, G. T., and Ebeling, R. W., "Theory of Hypergolic Ignition of Solid Propellants." *AIAA* Reprint No. 63-514 (December 1963).

7. Baer, A. D., "Ignition of Composite Rocket Propellants," unpublished Ph.D. thesis, University of Utah, Department of Chemical Engineering (Salt Lake City, June 1959).

8. Baer, A. D. and Ryan, N. W. "Ignition of Composite Propellants by Low Radiant Fluxes." *AIAA J., 3,* 884-889 (1965).

9. Baer, A. D. and Ryan, N. W. "An Approximate But Complete Model for the Ignition Response of Solid Propellants." *AIAA J., 6,* 872-877 (1968).

10. Bastress, E. K. and Niessen, W. R. "Solid Propellant Ignition by Convective Heating." Arthur D. Little, Inc. Prepared Under Contract AF 49 (638) - 1120, Final report (October 1966).

11. Beyer, R. B. and Fishman, N. "Solid Propellant Ignition Studies with High Flux Radiant Energy as a Thermal Source." *Progress in Astronautical and Rocketry, Vol. I. Solid Propellant Research.* Edited by M. Summerfield (Academic Press, New York, 1960), 673-692.

12. Brown, R. S., Warrick, T. K., and Anderson, R. "Theory of Ignition and Igniter Propagation of Solid Propellants in a Flow Environment." *AIAA*, Reprint No. 64-157 (1964).

13. Carlson, L. W. and Seader, J. D. "A Study of the Heat Transfer Characteristics of Hot Gas Ignition." Air Force Rocket Propulsion Laboratory TR-66-158, Rocketdyne, North American Aviation, Inc. (June, 1965).

14. Carslaw, A. S. and Jaegar, J. C. *Conduction of Heat in Solids*, 2nd edition. London England: Oxford University Press, 1959.

15. Cheng, J. T. "Thermal Effects of Composite-propellant Reactions," unpublished Ph.D. thesis, Department of Chemical Engineering, University of Utah (Salt Lake City, August, 1967).

16. Cheng, J. T., Bouck, L. S., Keller, J. A., Gaer, A. D., and Ryan, N. W. "Ignition of Solid Propellants." Department of Chemical Engineering, University of Utah, Technical Report under Air Force Grant AFOSR 40-65 (September, 1965).

17. Eckert, E. R. G. and Drake, F. M., Jr. *Heat and Mass Transfer*, 2nd edition,New York, Toronto, London: McGraw-Hill Book Company, Inc. 1959.

18. Evans, M. W., Beyer, R. B., and McCulley, L. "Initiation of Deflagration Waves at the Surface of Ammonium Perchlorate-Copper Chromite-Carbon Pellets." *J. Chem. Phys.*, *40*, 2431-2438 (1964).

19. Hermannce, C. E., Shinnar, R., and Summerfield, M. "Ignition of an Evaporating Fuel in a Hot Stagnant Gas Containing an Oxidizer. *AIAA J.*, *3* (Sept., 1965).

20. Hicks, B. L. "Theory of Ignition Considered as a Thermal Reaction." *J. Chem. Phys. 22*, 419-429 (1959).

21. Hightower, J. D. "An Investigation of the Effect of Environmental Gases and Pressure on the Ignition of Solid Rocket Propellants." Naval Weapons Center, China Lake, California (Oct., 1967).

22. Hsu, S. T. "Determination of Thermal Conductivities of Metals by Measuring Transient Temperatures in Semi-infinite Solids." *Trans. ASME*, *79*, 1197-1203 (1957).

23. Inami, S. H., Rosser, W. A., and Wise, H. "Hot Release Kinetics of Ammonium Perchlorate in Presence of Catalyst and Fuel," Research under Navy Contract nonr-3415, Stanford Research Institute, Menlow Park, California (March, 1967).

24. Jensen, G. E., Case, D. A., Brown, R. S., MacLaren, R. O., Anderson, R., and Corcoran, W. J. "Studies in Ignition and Flame Propagation of Solid Propellants," Report No. UTC 2117-R, United Technology Center, Sunnyvale, California (June, 1966).

25. Keller, J. A. "Studies on Ignition of Ammonium Perchlorate-based Propellants by Convective Heating," unpublished Ph.D. thesis, University of Utah, Department of Chemical Engineering (Salt Lake City, August, 1965).

26. Keller, J. A. "Surface Temperature Measurements of Solid Propellants During Ignition," Department of Chemical Engineering, University of Utah, Research under Air Force Grants AFOSR 40-66 and 40-67 (August, 1967).

27. Keller, J. A., Baer, A. D., and Ryan, N. W. "Ignition and Combustion of Solid Propellants." Department of Chemical Engineering, University of Utah, Final Technical Report under Air Force Grant 40-64 (September, 1964).

28. Keller, J. A., Richardson, C. P., and Baer, A. D. "Propellant Ignition by Convective Heat Fluxes," Department of Chemical Engineering, University of Utah, Final Technical Report under Contract No. N60530-9060 U.S. Naval Ordinance Test Station (September, 1964).

29. Keller, J. A. and Ryan, N. W. "Measurements of Heat Flux from Initiators for Solid Propellants." *ARS J., 31,* 1375-1379 (1961).

30. Kling, R., Moman, A., and Brulard, J. "The Kinetics of the Ignition of Composite Solid Propellants Submitted to High Heat Fluxes." *Rech. Aerosp., No. 103,* 3-10 (1964).

31. Lukenas, L. A., Most, W. J., Stang, P. L., and Summerfield, M. "The Ignition Transient in Small Solid Propellant Rocket Motors of Practical Configurations," Aerospace and Mechanical Science Report No. 801 under Research Grant NsG 200-60, Department of Aeronautical Engineering, Princeton University (July, 1967).

32. Mantyla, R. G. "Extinguishment of Solid Propellants by First Rarefaction Waves," unpublished Master's thesis, University of Utah, Department of Chemical Engineering (Salt Lake City, June, 1968).

33. Mantyla, R. G., Cheng, J. T., Bouck, L. S., Keller, J. A., Baer, A. D., and Ryan, N. W. "Ignition and Combustion of Solid Propellants," Department of Chemical Engineering, University of Utah, Technical Report under Air Force Grant AFOSR 40-66 (September, 1966).

34. Marklund, T. "Ignition of Ammonium Perchlorate at Different Pressures," FCA 2 Report A2322-242, Ministry of Technology, Farnborough Hants 1245 (August, 1967).

35. McAlevy, R F., III, Cowan, P. L., and Summerfield, M. "The Mechanism of Ignition of Composite Solid Propellants by Hot Gases." *Progress in Astronautics and Rocketry: Bol I. Solid Propellant Rocket Research*, edited by M. Summerfield. New York: Academic Press, 1960, pp. 623-652.

36. McAlevy, R. F., and Magee, R. S. "Flame Spreading Over the Surface of Double Base Propellants." Repring No. 64-109, *AIAA J.* (January, 1964).

37. McCune, C. C. "Solid Propellant Ignition Studies in a Shock Tube," unpublished Ph.D. thesis, Department of Chemical Engineering,

38. Mitchell, R. C. "Flame Spread on Solid Propellant," unpublished Ph. D. thesis, Department of Chemical Engineering, University of Utah (Salt Lake City, 1963).

39. Mitchell, R. C., Keller, J. A., Baer, A. D., and Ryan, N. W. "Ignition and Combustion of Solid Propellants " Department of Chemical Engineering, University of Utah, Final Technical Report under Air Force Contract AF 49 (638)-170 (September, 1961).

40. Mitchell, R. C., Keller, J. A., Baer, A. D., and Ryan, N. W. "Ignition and Combustion of Solid Propellants," Department of Chemical Engineering, University of Utah, Final Technical Report under Air Force Grant 62-99 (September, 1962).

41. U. S. Department of Commerce, *Tables of Thermal Properties of Gases*, National Bureau of Standards Circular 564 (November, 1955).

42. Niessen, W. R. and Bastress, E. K. "Solid Propellant Ignition Studies," Arthur D. Little, Inc., Technical Report No. AFRPL-TR-66-32, prepared under Contract AF04 (611)-10741 (February, 1966).

43. Ohlemiller, T. J. and Summerfield, M. "A Critical Analysis of Arc-image Ignition of Solid Propellants." *AIAA J.*, *6*, 878-886 (1968).

44. Osada, H. and Karinouchi, S. "The Initiation of Ignition in Composite Solid Rocket Propellants." Technical Information and Library Services, Ministry of Aviation, Kogyo Kayaku Kyokaishi, Japan (1965).

45. Price, E. W., Bradley, H. H., Jr., Dehority, G. L., and Ibiricu, M. M. "Studies of Ignition of Solid Propellants," U.S. Naval Ordinance Test Station, China Lake, California (March, 1966).

46. Price, E. W., Bradley, H. H., Jr., Hightower, J. D., and Fleming, R. O., Jr. "Ignition of Solid Propellants." *AIAA J.*, reprint No. 64-120 (January, 1964).

47. Richardson, C. P., Ryan, N. W., and Baer, A. D. "Propellant Ignition by Convective Heat Fluxes," Department of Chemical Engineering, University of Utah, Final Technical Report under Contract No. N60530-10690, U.S. Naval Ordinance Test Station (November 1965).

48. Rosser, W. A., Fishman, N., and Wise, H. "Ignition of Simulated Propellants Based on Ammonium Perchlorate," Research under Contract Nonr-3415(00), Stanford Research Institute, Menlow Park, California (July, 1965).

49. Ryan, N. W., Baer, A. D., Keller, J. A., and Mitchell, R. C. "Ignition and Combustion of Solid Propellants," Department of Chemical Engineering, University of Utah, Technical Report under Air Force Grant 62-69, AFOSR 62-69 (September, 1962).

50. Ryan, N. W , Baer, A. D., Keller, J. A., and Mitchell, R. C. "Ignition and Combustion of Solid Propellants," Department of Chemical Engineering, University of Utah, Technical Report under Air Force Grant 40-63, AFOSR 40-63 (September, 1963).

51. Sehgal, R. "Low Pressure Combustion and Ignition of Solid Rocket Propellants." *Astronautica Aeta, 13,* 167-181 (1967).

52. Shannon, L. J. "Composite Solid Propellant Ignition Mechanism," AFOSR Scientific Report under Contract No. AF49(638)-1557, United Technology Center, Sunnyvale, California (September, 1967).

53. Soto, de, S., and Friedham, H. A. "Flame-spreading and Ignition Transients in Solid Grain Propellants." *AIAA J.*, Repreint No. 64-122 (January, 1964).

54. Vidal, R. J. "Model Instrumentation Techniques for Heat Transfer and Force Measurements in a Hypersonic Shock Tunnel," Cornell Aeronautical Laboratory Report No. AD-917-A-1, WADC-TN-56-315, (AD 97238)(1956).

55. Waldman, C. H., Cheng, S. I., and Summerfield, M. "Theoretical Search for Analytical Solutions to the Gas Phase Ignition Problem," Aerospace and Mechanical Sciences Report No. 770 under AFOSR Contract AF 49(638)-1267, Department of Aeronautical Engineering, Princeton University (August, 1963).

APPENDICES

APPENDIX A

CALIBRATION OF THE FLOW CONTROL ORIFICES

The mass-flow rate of the gas through the test section could be varied for a given gas pressure and temperature by changing the size of the flow-control orifice. Seven different orifices were used. The inlet region of each orifice was shaped to form small flow nozzles and gas velocities were sonic through the minimum aperature. Table III lists the sizes and discharge coefficients of the orifices and the gas Mach numbers in the test section produced by use of each orifice.

The effective orifice areas were determined by use of a rarefaction tube. The pressure change in the inlet to the orifice generated by bursting a diaphragm and emptying the pressurized tube was introduced into the following equation [38]:

$$\frac{A_{or}}{A_r} = (n - 1)\left(\frac{n}{n + 1}\right)^{n/2}\left(\frac{1 - \sigma_2}{\sigma_1}\right)\left[1 + (n - 1)\left(\frac{1 - \sigma_1}{\sigma_1}\right)^2\right]^{-n/2} \qquad \text{(A-1)}$$

to yield the effective area. Here,

$$n = \frac{\gamma + 1}{\gamma - 1},$$

$$\sigma_1 = (P_1/P_o)^{1/1+n};$$

where

A_r is the cross-section area of the rarefaction tube;

A_{or} is the effective area of the orifice;

P_o is the initial pressure in the tube;

P_1 is the pressure in the tube immediately following the passage of the rarefaction wave; and

γ is the ratio of specific heats for the test gas.

Pressure recordings were obtained from a Kistler Model 401 pressure transducer mounted on the high-pressure side of the orifice. The discharge pressure was atmospheric. A Model 568 charge amplifier transmitted the signal from the pressure transducer to a Tektronix Model 502 oscilloscope. After the diaphragm was ruptured, the pressure dropped as the rarefaction waves passed the pressure transducer position. The specific heat ratios used were obtained from Reference 41.

APPENDIX B

MEASUREMENTS OF CRITICAL SYSTEM PARAMETERS

A. TIME DELAY OF HOT GAS FLOW

The oscilloscope-trace photographs obtained during the GAR heat-transfer tests indicated a slight time delay between the bursting of the diaphragm and the initial-indicated temperature rise of the sample surface (see Figure 33). The bursting of the diaphragm could be seen by the sudden change in the pressure trace. At some later time, up to three per cent of the UA propellant-ignition time when orifice number two was employed, the indicated-surface temperature of the sample rose. A portion of the time delay can be accounted for by considering the gas in the nickel tube leading to the test section as cooler than the furnace gas. If the gas flowing in the tube after the bursting of the diaphragm were "plug flow," it would take about one-half of the measured-delay time for the hot furnace gas to reach the propellant sample. Therefore, it may be concluded,that the majority of the measured time delay in the sample surface temperature rise was due to the flow of cool gas at the start of each test. Since for the majority of test conditions, the time delay was relatively small, no corrections were made on the propellant-ignition times reported in the Tables.

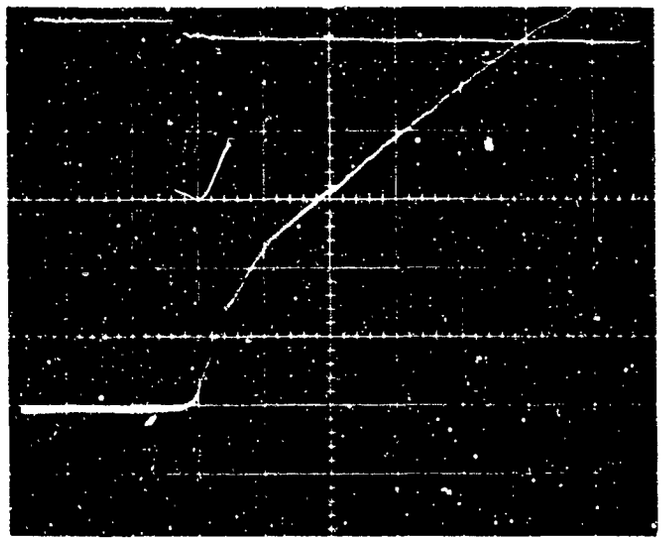

Gas Temperature: 1300°C Time Scale: 0.01 sec/div
Pressure: 2.9 atm IR Sensitivity: 250 mv/div

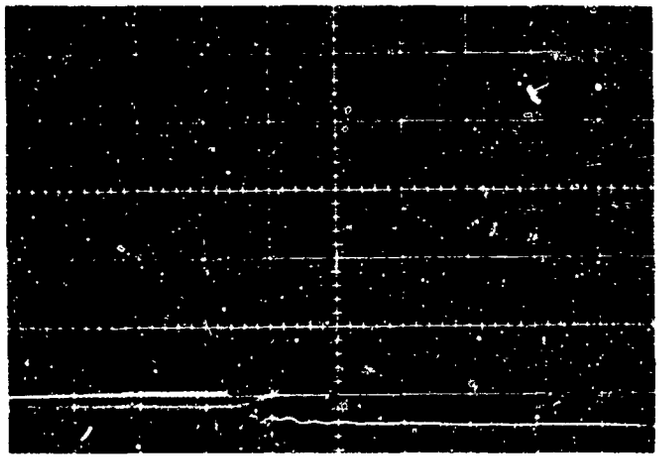

Gas Temperature: 1300°C Time Scale: 0.005 sec/div
Pressure: 7.7 atm IR Sensitivity: 250 mv/div

FIGURE 33. TYPICAL OSCILLOSCOPE RECORDS OF INDICATED GAR SURFACE TEMPERATURE RISE IN MILLIVOLTS.

The pressure trace is horizontal, then suddenly drops when the diaphragm is burst to initiate the gas flow. At some short time later, the indicated surface temperature rises.

B. GAS TEMPERATURE MEASUREMENTS

The furnace temperature and, thus, the heating gas-temperature was checked by three different methods. A well-mounted platinum-platinum-rhodium (13 per cent) thermocouple positioned in the furnace center was used as a primary indicator of furnace temperature. This thermocouple was checked against an NBS calibrated thermocouple. While operating at 1000 and 1300°C, the furnace temperature was periodically checked by use of calibrated-optical pyrometers. The temperatures measured by the optical pyrometer were found to be within 10 to 15°C of the values indicated by the platinum-platinum-rhodium thermocouple.

Direct gas-temperature measurements were made [47] by placing a 0.005-inch diameter chromel-alumel thermocouple in the test-section channel. Figure 34 shows an oscilloscope recording of the thermocouple output as a function of time during a simulated ignition test. When the results of the data were corrected for heat conduction and radiation losses from the thermocouple, the gas temperature, at the sample position, was shown to be within 15°C of the furnace temperature. The initial rise time to the steady-thermocouple temperature was the result of the flow-starting time in the channel which leads hot gas from the furnace to the test section. The overshoot of the thermocouple has not been satisfactorily explained.

C. PRESSURE IN THE TEST SECTION DURING TESTS

The monitored pressure in the test section dropped as much as 40 per cent of the initial pressure during propellant-ignition tests in which the

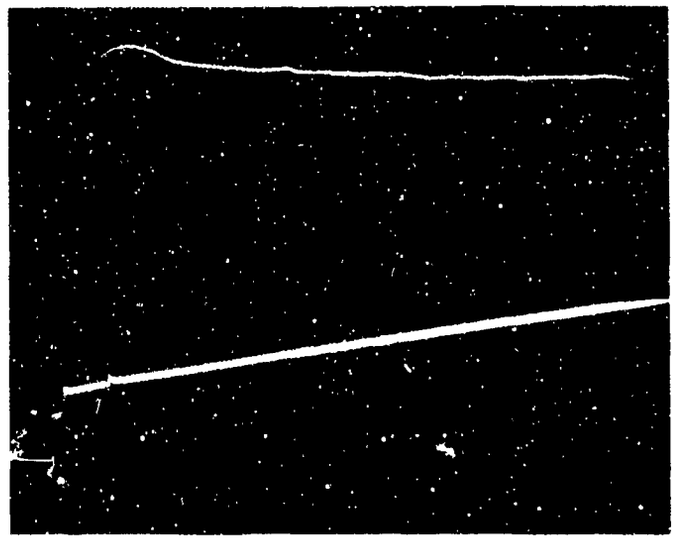

Pressure Scale:	0.204 atm/div	Time Scale:	0.5 sec/div
Temperature Scale:	5 mv/div	Orifice:	No. 12
Furnace Temperature:	755°C	T. C. Temperature:	680°C

Pressure Scale:	0.204 atm/div	Time Scale:	1.0 sec/div
Temperature Scale:	5 mv/div	Orifice:	No. 2
Furnace Temperature:	755°C	T. C. Temperature:	630°C

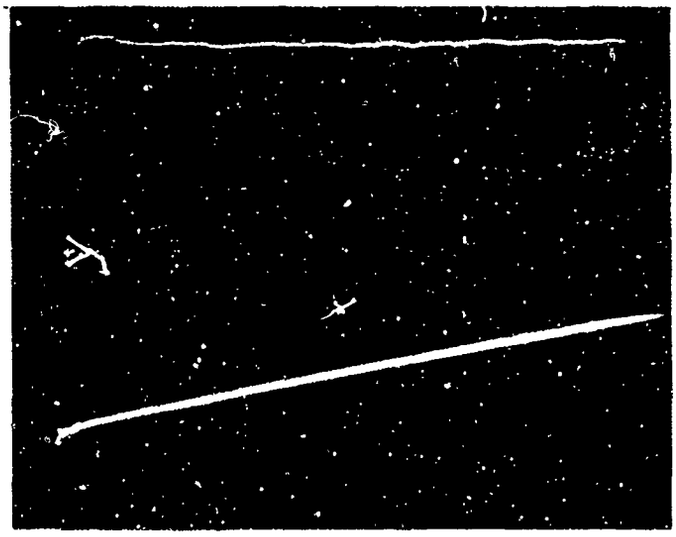

FIGURE 34. OSCILLOSCOPE RECORDS OF GAS TEMPERATURE IN THE CHANNEL OF THE TEST SECTION.

A .005-inch-diameter Chromel-Alumel thermocouple was placed in the flowing gas stream. The pressure trace is the lower trace through the whole period. In each case, the total initial pressure was 2.89 atm. The indicated thermocouple temperature was measured at the end of the test period. When corrections were made for radiation loss and conduction loss from the thermocouple, the measured gas temperatures were found to be within 20°C of the measured furnace temperature.

largest orifice, Number 12, was employed for furnace conditions of 1300°C and 7.7 atm. When the smaller orifices were employed, the pressure drop decreased; and when the smallest orifice was used, the largest pressure drop measured was only one per cent of the initial pressure. In the correlation of the heat transfer data, obtained by use of the alumina heat-flux gage, an average value for the test pressure was used in the calculation of gas mass-flow rates. These average pressures are reported in the Tables listing the propellant-ignition times and heat-transfer results.

It may be noted that the Statham 401 and Kistler 401 pressure transducers and the Champion pressure gage used in all of the tests reported herein, were calibrated by use of a Crosby Style CC-110 dead-weight pressure-gage tester. The sweep rate, horizontal amplifier, and vertical aplifier, of the Tektronix Model 502 oscilloscope employed in the tests, were periodically calibrated. The sweep rate was set with the use of a Du Mont Type 300 time calibrator, and the vertical gain was calibrated each testing day with the use of a Du Mont Type 264-B voltage calibrator.

APPENDIX C

HEAT-TRANSFER STUDY EMPLOYING PLATINUM-FILM-RESISTANT THERMOMETERS

A. HEAT FLUX GAGE CONSTRUCTION AND CALIBRATION

Heat flux gages were constructed with Pyrex 7740 and alumina (Alsimag 614) substrates (see Figure 4). Liquid Bright Platinum, No. 05-X, manufactured by the Hanovia Liquid Gold Division of Engelhard Industries, Inc., was painted and fired on to the surfaces of the substrate materials to produce thin platinum-film-resistance thermometers having response times on the order of a few microseconds.

The platinum-film resistance on the substrate surface was joined to four heavily painted platinum leads running down the side of the gage; copper leads were soldered to these four platinum leads. The substrate was then sealed into a sample holder with epoxy resin which served both as a cement and as an electrical insulator between the leads and the metal of the sample holders.

The temperature coefficients of resistance were determined for each gage by measuring the film resistances at various temperatures ranging from 0 to 95°C. The resistances of the gages were well represented by the equation:

$$R_T = R_o(1 + \beta_o T) \qquad \text{(C-1)}$$

where

R_o is the film resistance at 0°C (ohm)

T is the temperature. (°C)

β is the temperature coefficient of resistance. ohm/(ohm)(°C)

During the heat-transfer-test runs, gage-surface temperatures of 99°C for alumina and 233°C for pyrex gages were indicated. Experimental data employed in the calibration tests for the gage temperature coefficients of resistance were available only up to 95°C. For the pyrex gage, an extrapolation must be made for surface temperatures above its calibrated range.

The electrical circuitry used in conjunction with the heat-flux gages is shown in Figure 35. The sensitivity of the oscilloscope could be adjusted by employing the temperature rise simulator. This was done by turning switch A to position 1, where a predetermined resistance, R_1, simulated a set temperature rise, ΔT. In position 2, the circuit was set for normal heat-flux-test operation.

The settings for R_1, and R_2, in the circuitry of Figure 35, were determined from the following equations:

$$R_1 = \frac{R_c\left[\beta_o(\Delta T)\right]}{1 + \beta_o(T + \Delta T)} \qquad \text{(C-2)}$$

$$R_2 = R_c - R_1 - R_g \qquad \text{(C-3)}$$

where: β_o is the temperature coefficient of resistance determined for each gage for Equation (C-1). ohm/(ohm)(°C)

R_c is the total resistance in the circuit. (ohm)

R_s is the resistance of the platinum film. (ohm)

ΔT is the preset temperature rise. (°C)

T_1 is the initial uniform temperature of the gage. °C

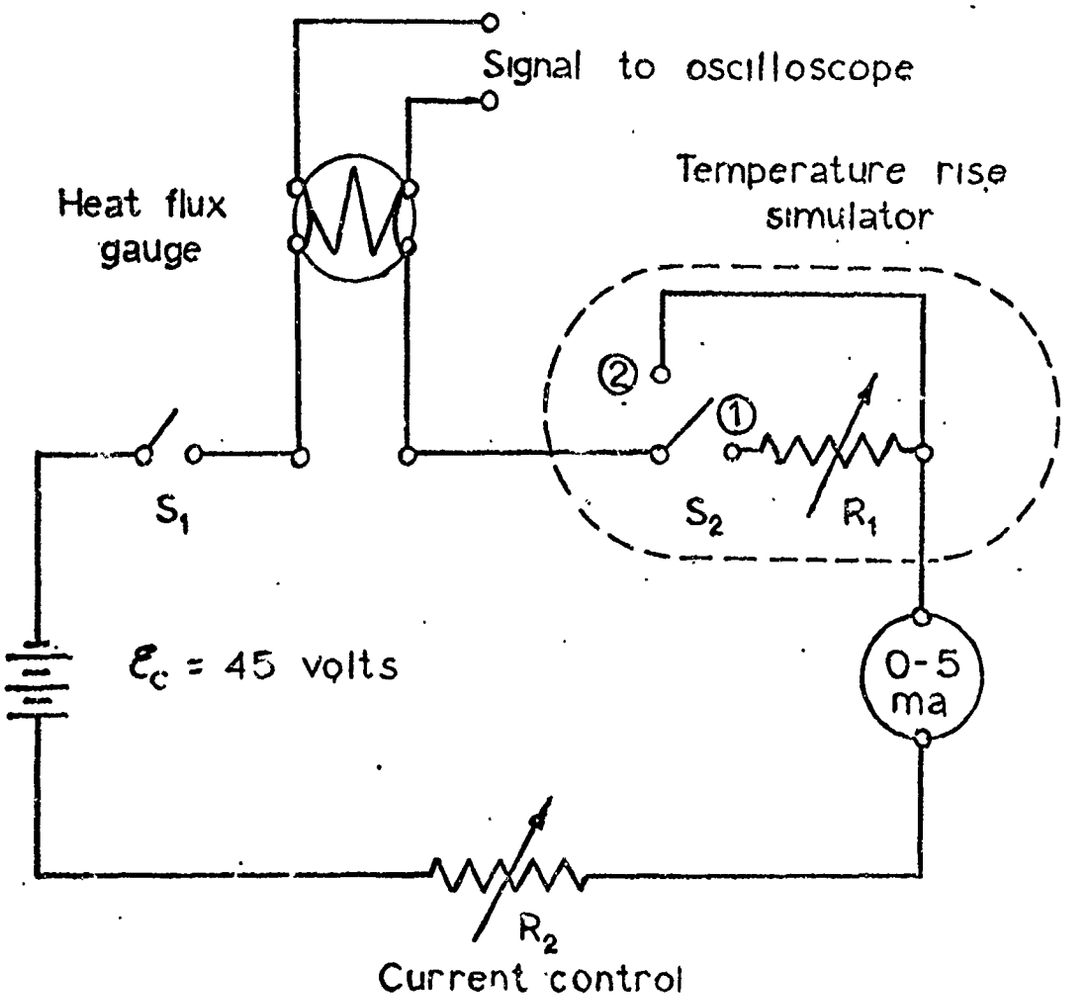

FIGURE 35. ELECTRICAL CIRCUITRY DIAGRAM FOR TEMPERATURE MEASUREMENTS WITH HEAT-FLUX GAGES.

Application of Equation (C-2) requires the assumption that the resistances controlling the current in the system were much larger than the changes in resistance of the platinum film during test operation; this condition was satisfied in these tests. Since the current was essentially constant, changes in the platinum-film resistance produced change in emf output of the gage which was linear with the surface temperature change. Current through the film was held to values less than five milliamperes to prevent significant heating of the gage surface [53].

B. HEAT FLUX TESTS

The heat-flux gage was placed in the test section and simulated-ignition tests were made. Temperature histories of the gage surface were recorded by polaroid photographs of oscilloscope traces. Several tests were made for each individual condition of gas temperature and pressure and flow-control-orifice area.

Heat-transfer coefficient values were calculated from the temperature histories of the heat-flux gage obtained during simulated ignition tests. The following is a development of the method used and the assumptions involved in the calculations. The equation describing the one-dimensional conduction in the exposed heat-flux gage, a passive body, is:

$$\frac{\partial T}{\partial t} = \alpha \frac{\partial^2 T}{\partial x^2} \qquad \text{(C-4)}$$

with boundary conditions at

$$x = 0,\ F(o,t) = -R \frac{\partial T}{\partial x}$$

$$x = +\infty\ T(t) = T_o \quad \text{for all } t \geq 0$$

$$t = 0\ \ T(x) = T_o \quad \text{for all } x \geq 0$$

where

α is the thermal diffusivity;

K is the thermal conductivity;

F(o,t) is the heat flux at the propellant surface.

In this analysis, it was assumed that the thermophysical properties were constant. However, a correction was made in calculations to compensate for changes in the properties as the temperature was elevated. This correction, which is based upon work of Keller [25], will be discussed later.

The solution of Equation (C-4) at x equals zero is that

$$F(t) = \frac{\Gamma}{(\pi)^{\frac{1}{2}}} \frac{\partial}{\partial t} \left\{ \int_0^t \frac{T_s \lambda}{(t - \lambda)^{\frac{1}{2}}} d\lambda \right\} . \qquad (C-5)$$

Here, Γ is the gage thermal responsivity, defined as $\sqrt{k\rho c}$, and

λ is a dummy variable.

If the heat fluxes to be determined approximate a constant value, it is convenient to modify Equation (C-5) to give the result that

$$F(t) = \frac{\sqrt{\pi}\,\Gamma}{2} \left\{ \frac{T_s(t)}{t^{\frac{1}{2}}} + \frac{1}{\pi t^{\frac{1}{2}}} \int_0^t \frac{\lambda^{\frac{1}{2}} T_s(t) - t^{\frac{1}{2}} T_s(\lambda)}{(t - \lambda)^{3/2}} d\lambda \right\} \qquad (C-6)$$

The mathematical development of Equation (C-6) from (C-4) may be seen in Reference 7.

At time zero, the surface temperature change, T_s, is also zero. The terms containing $t^{\frac{1}{2}}$ and $(t - \lambda)^{\frac{3}{2}}$ in the denominator are of an indeterminate form. If L'Hospital's rule is applied, the terms approach a limit of zero as time approaches zero from the right. For values of λ equal to time, t, the term in the integral becomes undefined. This difficulty is overcome by allowing the upper limit to be some value slightly larger than λ.

By use of the gage-surface-temperature histories and thermal responsivity, Equation (C-6) may be used to calculate instantaneous heat fluxes from the hot gas to the gage. Heat-transfer coefficients, h, may then be calculated from the heat flux, F(t) by:

$$h = F(t)/(T_G - T_s) \qquad (C-9)$$

where T_s is the instantaneous value. Incremental value of $T_s(t)$ and of t were introduced into Equation (C-6) and F(t) was obtained by numerical integrations. Heat-transfer coefficients were calculated by this method for approximately ten increments until about the ignition time of FM propellant for the specific conditions. Figure 40 is a flow chart of the heat transfer calculation, showing the numerical method used in the solution of equation (C-6). Table XVI contains a listing of the computer program and an explanation of the variables used.

For the case where the gage-thermophysical properties are not constant, but temperature dependent, a correction term must be added. Keller [25] showed that a correction could be made to the surface-temperature values to compensate for changes in the gage properties. For the pyrex gage, the corrected temperature is:

$$T_{sc} = T_s + 4.59 \times 10^{-4}(T_s) \qquad (C-7)$$

and for the alumina gage:

$$T_{sc} = T_s - 4.10 \times 10^{-5}(T_s) \qquad (C-8)$$

where

T_s is the gage-surface temperature,

change from T_o, the initial-uniform temperature. °C

T_{sc} is the corrected temperature change. °C

APPENDIX D

HEAT-TRANSFER STUDY WITH THE INFRARED-DETECTION SYSTEM

The infrared-detection system was used for monitoring surface temperatures of a simulated propellant subjected to rapid heating. Figure 6 is a schematic diagram of the test configuration. The simulated propellant, GAR, consisted of 45 per cent PBAA and 55 per cent fine glass beads by weight and had thermophysical properties approaching those of the FM propellant.

A. CALIBRATION OF THE INFRARED DETECTION SYSTEM

Calibration tests of the infrared detection system were made using an electrically heated copperdisc. Figure 36 is a sectional view of this disc, and the sample holder mounting. The disc was coated with colloidal graphite (thermogage) having an emissivity of 0.89. The copper disc was welded to the heating element from a Weller Model D-550 soldering gun. Heavy copper leads connected the heating element to two 6-volt automotive batteries which were coupled in parallel. The copper disc was mounted in a sample holder and placed in the test section in the normal propellant sample position. The disc temperature was monitored by a copper-constantan thermocouple which was welded onto the disc, and the thermocouple output was displayed on an oscilloscope screen. The output from the infrared detector was also displayed on the screen. Figure 37 is a photograph of typical oscilloscope trace showing the infrared detector and thermocouple responses. Tests made at various heating rates confirmed a calculation which showed

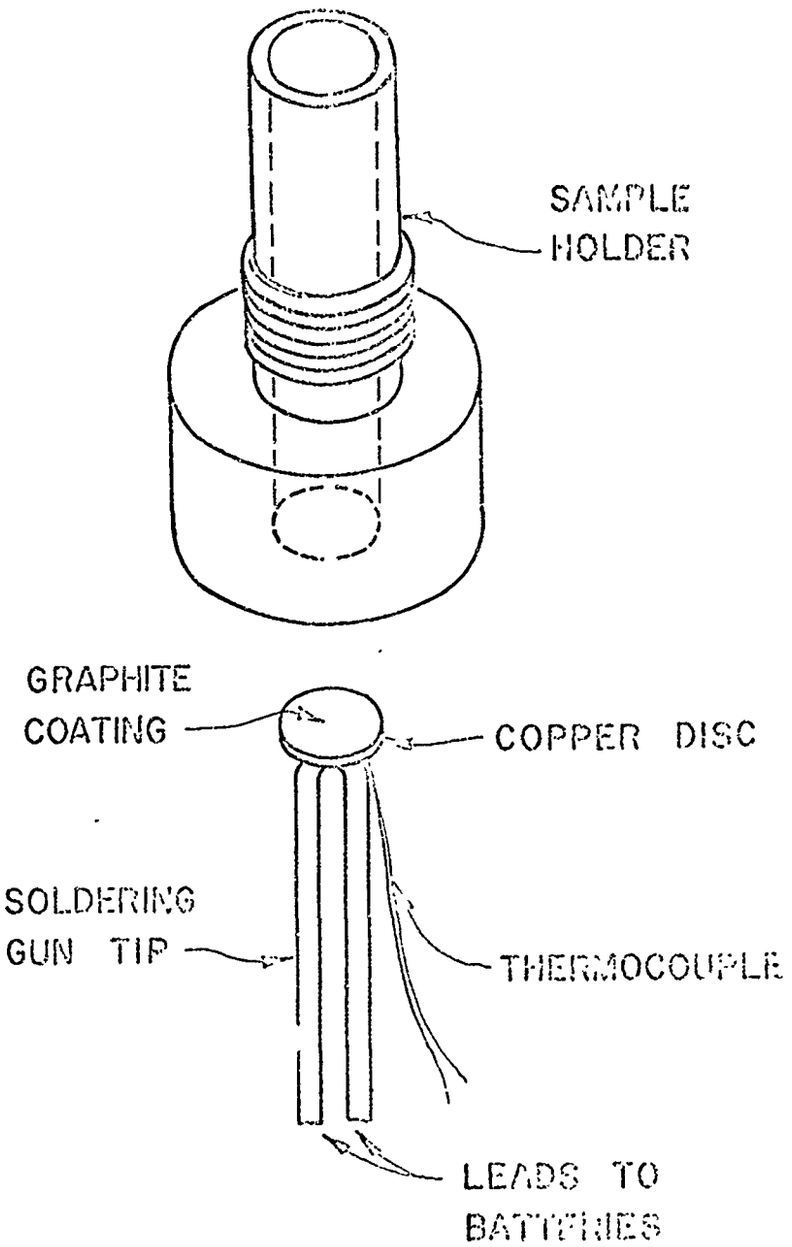

FIGURE 35. SKETCH OF INFRARED DETECTION SYSTEM CALIBRATION DISC.

The copper disc was glued into the sample holder with an epoxy resin so that it was flush with the top.

Time scale: 1.0 sec/div (left to right)
Detector sens: -500 mv/div
Thermocouple sens: +5 mv/div

FIGURE 37: TYPICAL OSCILLOSCOPE RECORD OF INFRARED DETECTOR CALIBRATION TEST.

The upper trace is the output from the infrared detector focusing on the graphite coated copper disc. The lower trace is from the output from the thermocouple in the copper disc.

that temperature gradients in the copper disc are negligible, and, thus, the thermocouple indication corresponds to the surface temperature seen by the infrared detector. Figure 38 is a plot of the surface temperature, in degrees centigrade, T_s, versus the infrared detector output in millivolts.

In a test when hot gases were in the test section, the infrared sensor responded to radiation from hot dust particles and to emission resulting from heating of the Irtran window. The magnitude of these background emissions were measured by simulating an ignition test with a sample holder filled with polished brass in place of the propellant. During such a test, the brass surface temperature remained too low to produce significant radiant energy. Several tests were made for each separate set of conditions of pressure, temperature, and flow-control-orifice size. Normally, the background radiation seen by the detector rose rapidly as hot gas entered the test section, but then increased slowly during the test as the window temperature increased.

Efforts to reduce the effect of the background radiation by use of filters to eliminate the short wavelength radiation from the hotter particles in the gas phase were not successful. A filter (Series Number 240, manufactured by Eastman Kodak Company) which essentially eliminated radiation of wavelength shorter than four microns was found to reduce the relative importance of the background radiation; however, the total detector output was so greatly reduced that problems with noise and drift nullified any bennefits gained by use of the filter, and use of the filter was discontinued.

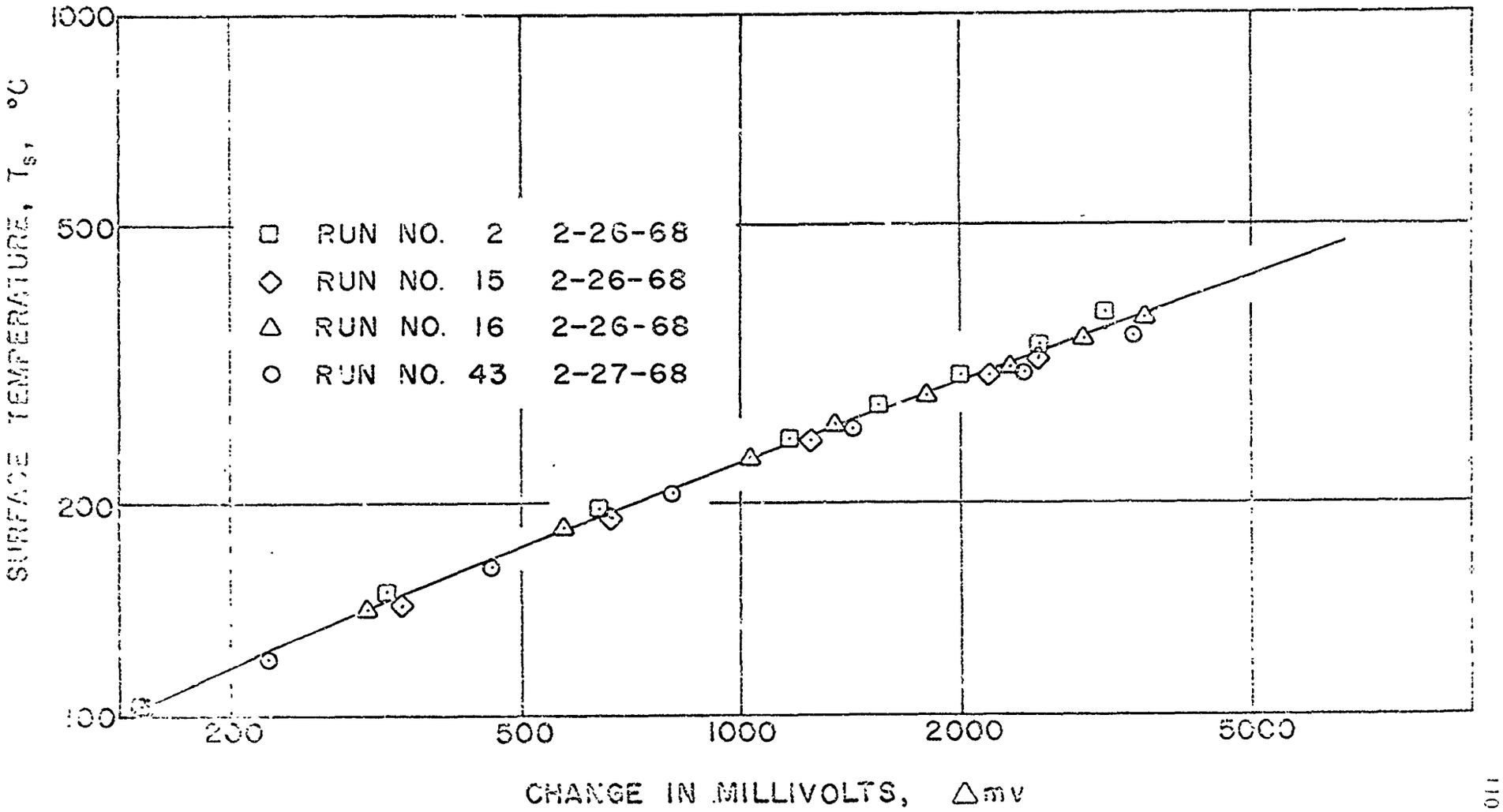

FIGURE 38. CALIBRATION CURVE FOR THE INFRARED-DETECTION SYSTEM.

The significance of reflection of radiation from the brass was checked by coating the surface with colloidal graphite and making additional tests. For several runs, the coated-brass-emittance values were slightly less than those obtained with polished brass (see Figure 39). It was concluded that the contribution to radiation seen by the detector from the polished brass, normally, could be neglected; although, some reflected radiation from the gas phase reached the detector from the polished surface.

B. HEAT-TRANSFER MEASUREMENT TESTS

Simulated ignition tests were made using GAR samples. The detector-output histories were recorded. Incremental values were taken from the oscilloscope traces and background effects for identical times were subtracted from the values. The values were then converted to surface temperatures by taking readings directly from the calibration curve (Figure 38).

At times comparable to FM-propellant-ignition times and for the maximum gas temperature employed, the background contribution was about 25 per cent of the total detector output in these GAR tests. However, for early test times where the surface temperature was below 100°C, the background was about 75 per cent of the total emission, making meaningful data reduction quite difficult for these values.

C. THERMAL RESPONSIVITY MEASUREMENTS OF SIMULATED PROPELLANT

In order to calculate heat-transfer coefficients from the GAR temperature histories, it was necessary to know the thermal responsivity, Γ, of this material. Tests were conducted in which two semi-infinite bodies

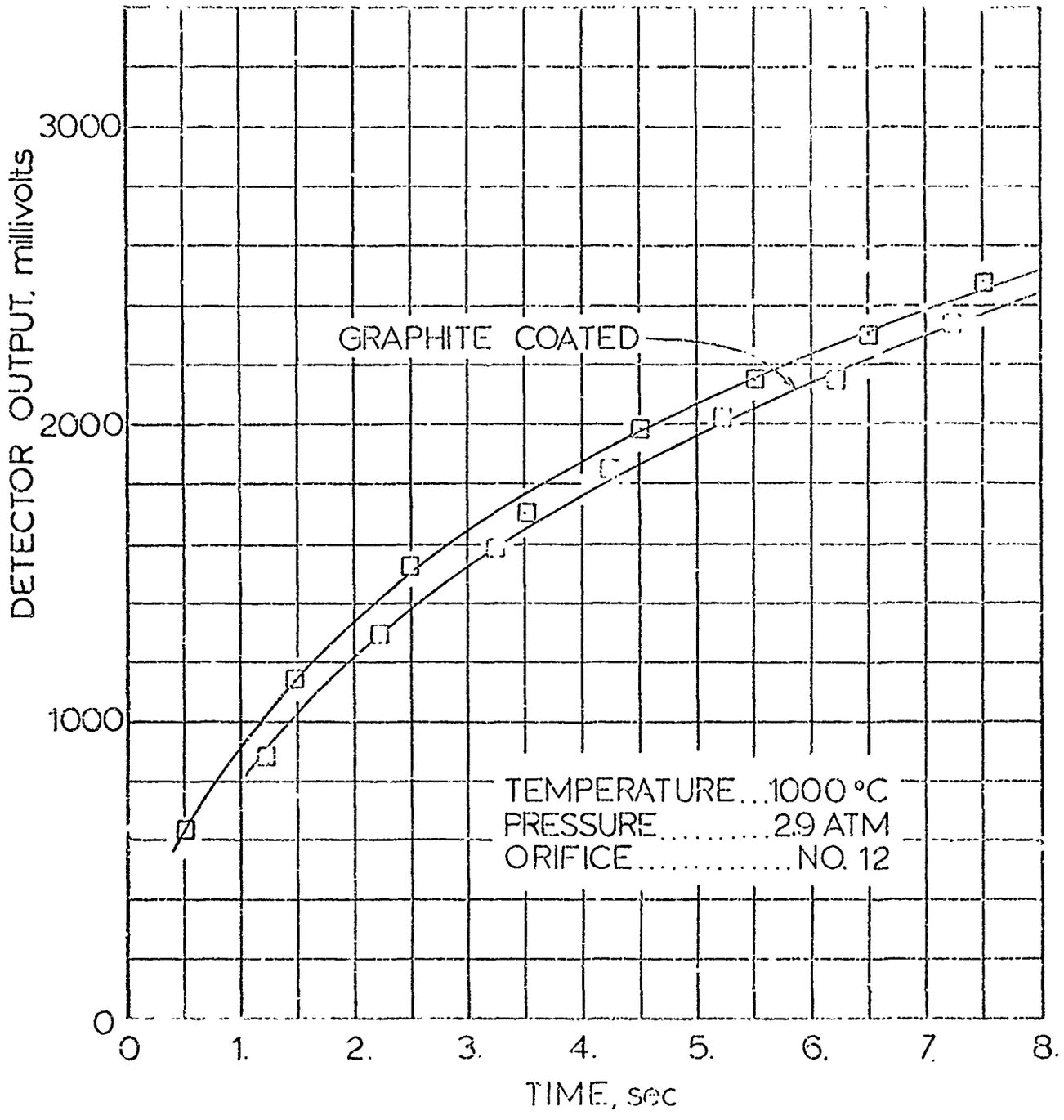

FIGURE 39. BACKGROUND EMISSIONS FROM POLISHED AND GRAPHITE-COATED BRASS PLUG DURING RAPID HEATING TESTS.

The closeness of the two curves illustrates that the emissions due to a temperature rise in the brass plug could be neglected.

of different temperatures, one of GAR and the other of FM propellant, were joined and their interface temperature was monitored. The interfacial temperature becomes constant for a period, and the change in surface temperature of each solid may be used to determine the thermal responsivity ratio of the solids. This technique, for solids, is described by McCune [37] and Hsu [22]. The responsivity ratio is

$$\frac{\Gamma_{GAR}}{\Gamma_{FM}} = \frac{T_i - T_{FM}}{T_{GAR} T_i} \qquad \text{(D-1)}$$

where, Γ_{GAR} is the thermal responsivity of GAR;

Γ_{FM} is the thermal responsivity of FM propellant and is equal to 0.0212 $\text{cal}/(\text{cm})^2(\text{sec})^{\frac{1}{2}}(°\text{K})$;

T_i is the temperature of the interface;

T_{FM} is the initial uniform temperature of the FM propellant; and

T_{GAR} is the initial uniform temperature of GAR.

Tests were conducted with the FM side at the higher temperature and then with the GAR side at the higher temperature. A 0.005-inch diameter thermocouple measured the interfacial temperature. Measured values of the thermal responsivity for the GAR varied from 0.0295 to 0.0340. The average value for eight tests was 0.0315. These data are summarized in Tables XV.

D. CALCULATION OF THE HEAT-TRANSFER COEFFICIENTS

Heat-transfer coefficients were calculated from the solution of the one-dimensional, semi-infinite heat-conduction equation for heating of a semi-infinite body. Here

$$\theta = \frac{T_s - T_o}{T_G - T_o}, \text{ by definition; and} \tag{D-2}$$

$$\theta = 1 - e^{N^2} \operatorname{erfc}(N); \text{ when} \tag{D-3}$$

$$N = h\, t_i^{1/2}/\Gamma \tag{D-4}$$

Thus,

$$h = N\Gamma/t_i^{1/2}. \tag{D-5}$$

Here,

t_i is the propellant-ignition time, and

T_s is the GAR-surface temperature at the propellant-ignition time, t_i.

Since the thermal responsivity of GAR was greater than that of the propellant, Equation (D-3) predicts higher surface temperatures for the UA propellant than for the GAR material. At some time, t_e, when the surface temperature of GAR has reached a value equal to the propellant-linear-ignition temperature, T_{si}^{L}, the values in Equation (D-2) are identical.

$$\theta_{GAR} = \theta_P \tag{D-6}$$

and, therefore,

$$N_{GAR} = N_P . \tag{D-7}$$

From Equation (D-7), if the heat-transfer coefficients for the GAR and UA ignition tests are considered equal, the time, when the GAR surface temperature was equal to T_{si}^{L}, was

$$t_e = \left(\frac{\Gamma_{GAR}}{\Gamma_P}\, t_i^{1/2}\right)^2 \tag{D-8}$$

In using extrapolated surface temperatures of GAR at time t_e and substituting t_e into Equations (D-2), (D-3), and (D-5), heat-transfer coefficients

were calculated for conditions where the GAR-surface temperature was equal to the calculated-propellant-linear-ignition temperature.

TABLE I

COMPOSITION OF PROPELLANTS AND POLMERIC FUEL BINDERS

Propellant or Polymer Code Name	Weight Percent of Ingredients					Ammonium Perchlorate Particle Size, micron (e)
	Fuel Binder		Copper Chromite Catalyst (c)	Philblack (d)	Ammonium Perchlorate	
	PBAA (a)	Estane (b)				
AR	25.00	---	2.00	3.00	70.00	15
FM	18.00	---	2.00	----	40.00 40.00	15 200
G	18.00	---	----	----	41.00 41.00	15 200
UA	23.00	---	2.00	----	75.00	15
A05	92.23	---	----	2.91	2.43 2.43	15 200
PC	97.09	---	----	2.91	----	---
PCC	87.38	---	9.71	2.91	----	---
PUC	---	96.97	----	3.03	----	---
PUG	---	61.34	----	1.92	36.74(f)	38
GAR	43.91	---	----	1.32	54.77(f)	38

(a) The fuel binder used in these propellants consisted of 85.0 per cent of a liquid polybutadiene-acrylic-acid copolymer cured with 15.0 per cent Epon 828.

(b) The fuel binder used in these cases consisted of 92.85 per cent of Estane and 7.15 per cent of a special curative.

(c) Copper Chromite Catalyst CU-0202 P obtained from Harshaw Chemical Company and contains approximately 82 per cent CuO and 17 per cent Cr_2O_3. The weight-average particle-diameter of the copper chromite is 3.7 microns.

(d) A rubber-reinforcing carbon black obtained from Phillips Petroleum Company. Philblack E has a surface area of 142 square meters per gram.

(e) Ammonium perchlorate of the designated-particle size means that 50 weight per cent of the particles have diameters less than the value indicated. A screen analysis was used to determine particle diameter

(continued)

TABLE I

COMPOSITION OF PROPELLANTS AND POLMERIC FUEL BINDERS

Propellant or Polymer Code Name	Weight Percent of Ingredients					Ammonium Perchlorate Particle Size, micron (e)
	Fuel Binder		Copper Chromite Catalyst (c)	Philblack (d)	Ammonium Perchlorate	
	PBAA (a)	Estane (b)				
AR	25.00	---	2.00	3.00	70.00	15
FM	18.00	---	2.00	----	40.00	15
					40.00	200
G	18.00	---	----	----	41.00	15
					41.00	200
UA	23.00	---	2.00	----	75.00	15
A05	92.23	---	----	2.91	2.43	15
					2.43	200
PC	97.09	---	----	2.91	----	---
PCC	87.38	---	9.71	2.91	----	---
PUC	---	96.97	----	3.03	----	---
PUG	---	61.34	----	1.92	36.74(f)	38
GAR	43.91	---	----	1.32	54.77(f)	38

(a) The fuel binder used in these propellants consisted of 85.0 per cent of a liquid polybutadiene-acrylic-acid copolymer cured with 15.0 per cent Epon 828.

(b) The fuel binder used in these cases consisted of 92.85 per cent of Estane and 7.15 per cent of a special curative.

(c) Copper Chromite Catalyst CU-0202 P obtained from Harshaw Chemical Company and contains approximately 82 per cent CuO and 17 per cent Cr_2O_3. The weight-average particle-diameter of the copper chromite is 3.7 microns.

(d) A rubber-reinforcing carbon black obtained from Phillips Petroleum Company. Philblack E has a surface area of 142 square meters per gram.

(e) Ammonium perchlorate of the designated-particle size means that 50 weight per cent of the particles have diameters less than the value indicated. A screen analysis was used to determine particle diameter

(continued)

Table I (continued)

for particle sizes greater than 35 microns. For particles less than 15 microns in diameter, particle sizes were determined microscopically by first dispersing ammonium perchlorate in dry carbon tetrachloride with the aid of a wetting agent and then measuring diameters of 200 to 300 particles. All the AP was supplied by American Potash and Chemical Corporation.

(f) Fine glass beads replaced the ammonium perchlorate.

TABLE II

THERMOPHYSICAL PROPERTIES OF PROPELLANTS, INGREDIENTS, AND POLYMER FUEL BINDERS AT 60°C.

Material	Heat Capacity cal/(gm)(°K)	Density gm/(cm)^3	Thermal Diffusivity (cm)^2/(sec)	Thermal Conductivity cal/(cm)(sec)(°K)	Thermal Responsivity cal/(cm)^2(sec)$^{\frac{1}{2}}$(°K)
Ammonium Perchlorate(1)	0.275	1.950	2.220×10^{-3}	1.190×10^{-3}	2.520×10^{-2}
Copper Chromite(1)	0.146	6.150	2.417	2.170	1.470
Carbon black(1)	0.204	1.880	0.407	0.156	0.774
FM(1)	0.316	1.630	1.700	0.876	2.120
G (1)	0.311	1.600	1.710	0.851	2.060
UA(1)	0.316	1.580	1.650	---	2.030
AO5(2)	0.449	0.999	0.989	0.443	1.409
PC(2)	0.457	0.970	0.974	0.432	1.380
PCC(2)	0.418	1.123	0.988	0.464	1.480
GAR(3)	---	---	---	---	3.150

(1) These constants were taken from reference [25].

(2) These constants were taken from reference [15].

(3) The determination of GAR thermal responsibity is discussed in Appendix D.

TABLE III

FLOW RATES AND FLOW-CONTROL ORIFICE DATA

Orifice Number	Orifice Area $(cm)^2$	Gas Mach Number in Test Section	Mass Flow Rate in Test Section $gm/(cm)^2(sec)$ Furnace Conditions					
			760°C 2.9 atm	760°C 7.7 atm	1000°C 2.9 atm	1000°C 7.7 atm	1350°C 2.9 atm	1350°C 7.7 atm
1*	1.792×10^{-2}	0.020	1.174	3.1083	1.063	2.815	0.941	2.493
2	6.979	0.078	4.726	12.511	4.280	11.330	3.790	10.030
3	9.981	0.113	6.950	18.396	6.294	16.660	5.574	14.750
6	4.653	0.053	3.208	8.491	2.905	7.690	2.573	6.810
8	13.608	0.155	9.477	25.088	8.583	22.720	7.601	20.120
10	20.554	0.239	14.316	37.897	12.965	34.320	11.480	30.390
12	24.697	0.292	17.195	45.515	15.572	41.220	13.790	36.500

* Missing orifice numbers were orifices not used in tests.

TABLE IV

SUMMARY OF FM PROPELLANT IGNITION TESTS IN NITROGEN

Flow Control Orifice	Furnace Conditions			Ignition Time		Mean Surface Heat Flux	
	Temp. °C	Initial Press atm	Average Press atm	t_i sec	$t_i^{\frac{1}{2}}$ $sec^{\frac{1}{2}}$	$\bar{F}_s(1)$ $cal/(cm)^2(sec)$	$\bar{F}_s(2)$ $cal/(cm)^2(sec)$
12	1307.	2.9	2.4	0.102	0.319	16.662	17.813
12	1303.	2.9	2.4	0.081	0.285	16.924	18.144
12	1312.	2.9	2.4	0.082	0.286	17.048	18.252
12	1309.	2.9	2.4	0.091	0.302	16.859	18.037
12	1306.	2.9	2.4	0.136	0.368	16.232	17.278
12	1301.	2.9	2.4	0.084	0.290	16.915	18.057
10	1311.	2.9	2.6	0.111	0.333	15.223	---
10	1307.	2.9	2.6	0.106	0.326	15.237	---
8	1307.	2.9	2.7	0.150	0.387	11.966	---
8	1305.	2.9	2.7	0.212	0.461	11.597	---
8	1303.	2.9	2.7	0.158	0.398	11.877	---
3	1305.	2.9	2.8	0.250	0.500	9.649	---
3	1305.	2.9	2.8	0.260	0.510	9.617	---
2	1303.	2.9	2.8	0.535	0.731	7.400	8.222
2	1301.	2.9	2.8	0.608	0.780	7.298	8.097
6	1301.	2.9	2.9	1.078	1.038	5.544	---
6	1306.	2.9	2.9	1.096	1.047	5.556	---
1	1301.	2.9	2.9	4.400	2.098	2.862	2.435
1	1302.	2.9	2.9	4.000	2.000	2.892	2.457
12	1307.	7.7	5.9	0.028	0.167	32.656	36.027
12	1300.	7.7	5.9	0.033	0.182	31.965	35.199
10	1310.	7.7	6.1	0.034	0.186	29.120	---
10	1308.	7.7	6.1	0.037	0.192	28.884	---
8	1306.	7.7	7.2	0.050	0.224	22.793	---
8	1310.	7.7	7.2	0.049	0.221	22.903	---
8	1328.	7.7	7.3	0.044	0.210	23.482	---
3	1309.	7.7	7.4	0.091	0.302	18.355	---
3	1308.	7.7	7.4	0.064	0.253	18.923	---

(continued)

TABLE IV (continued)

Flow Control Orifice	Furnace Conditions			Ignition Time		Mean Surface Heat Flux	
	Temp., °C	Initial Press atm	Average Press atm	t_i sec	$t_i^{1/2}$ $sec^{1/2}$	$\bar{F}_s(1)$ $cal/(cm)^2(sec)$	$\bar{F}_s(2)$
3	1308.	7.7	7.4	0.090	0.300	18.361	---
2	1311.	7.7	7.5	0.155	0.394	14.385	15.890
2	1311.	7.7	7.5	0.163	0.404	14.309	15.798
6	1307.	7.7	7.5	0.327	0.572	10.684	---
6	1308.	7.7	7.5	0.300	0.548	10.789	---
1	1308.	7.7	7.6	1.704	1.305	5.363	4.636
1	1307.	7.7	7.6	1.434	1.197	5.469	4.714
12	1004.	2.9	2.5	0.255	0.505	11.597	10.591
12	1004.	2.9	2.5	0.221	0.470	11.818	10.773
10	1004.	2.9	2.6	0.260	0.510	10.655	---
10	1002.	2.9	2.6	0.309	0.556	10.396	---
8	1002.	2.9	2.7	0.542	0.736	7.990	---
8	1002.	2.9	2.7	0.520	0.721	8.035	---
3	996.	2.9	2.8	0.755	0.869	6.542	---
3	994.	2.9	2.8	0.872	0.934	6.402	---
2	1002.	2.9	2.8	1.140	1.068	5.230	5.419
2	1006.	2.9	2.8	1.360	1.166	5.129	5.310
6	1008.	2.9	2.9	2.275	1.508	3.928	---
6	1007.	2.9	2.9	2.420	1.556	3.891	---
1	997.	2.9	2.8	9.320	3.053	1.988	1.480
12	974.	7.7	6.6	0.074	0.272	21.667	19.673
12	974.	7.7	6.6	0.102	0.319	20.645	18.837
12	957.	7.7	6.6	0.102	0.319	20.282	18.500
8	970.	7.7	7.3	0.189	0.435	14.484	---
8	970.	7.7	7.3	0.211	0.459	14.282	---

(continued)

TABLE IV (continued)

Furnace Conditions				Ignition Time		Mean Surface Heat Flux	
Flow Control Orifice	Temp. °C	Initial Press atm	Average Press atm	t_i sec	$t_i^{1/2}$ $sec^{1/2}$	$\bar{F}_s(1)$ $cal/(cm)^2(sec)$	$\bar{F}_s(2)$
2	982.	7.7	7.5	0.530	0.728	9.204	8.214
2	982.	7.7	7.5	0.480	0.693	9.350	8.328
1	984.	7.7	7.6	3.470	1.863	3.650	2.745
1	985.	7.7	7.6	3.740	1.934	3.609	2.767
12	761.	2.9	2.4	0.984	0.992	6.851	6.156
12	760.	2.9	2.4	1.030	1.015	6.773	6.093
8	762.	2.9	2.7	1.750	1.323	4.923	---
8	762.	2.9	2.7	1.860	1.364	4.860	---
2	763.	2.9	2.8	3.950	1.987	3.214	2.872
2	761.	2.9	2.8	4.950	2.225	3.056	2.746
2	761.	2.9	2.8	3.720	1.929	3.245	2.895
6	761.	2.9	2.8	11.600	3.406	2.152	1.988
6	762.	2.9	2.8	9.640	3.105	2.249	2.070
12	761.	7.7	6.5	0.304	0.551	12.975	11.630
12	762.	7.7	6.5	0.325	0.570	12.803	11.486
8	764.	7.7	7.2	0.600	0.775	9.122	---
8	764.	7.7	7.2	0.650	0.806	8.954	---
2	764.	7.7	7.5	1.460	1.208	5.870	4.800
2	763.	7.7	7.5	1.500	1.225	5.825	4.770
2	763.	7.7	7.5	1.880	1.371	5.518	4.569
1	764.	7.7	7.5	27.750	5.268	1.717	1.186
1	766.	7.7	7.5	22.250	4.717	1.840	---

(1) These mean-surface-heat fluxes were calculated using heat-transfer results from the alumina gage heat-flux study.

(2) These mean-surface-heat fluxes were calculated using heat-transfer results from the GAR-infrared detector heat-flux study.

TABLE V

SUMMARY OF G PROPELLANT IGNITION TESTS IN NITROGEN

Flow Control Orifice	Furnace Conditions			Ignition Time		Mean Surface Heat Flux	
	Temp. °C	Initial Press atm	Average Press atm	t_i sec	$t_i^{1/2}$ $sec^{1/2}$	$\bar{F}_s(1)$ $cal/(cm)^2(sec)$	$\bar{F}_s(2)$
12	1330.	2.9	2.5	0.142	0.377	16.347	17.391
12	1330.	2.9	2.5	0.150	0.388	16.249	17.280
8	1329.	2.9	2.7	0.262	0.512	11.477	---
8	1327.	2.9	2.7	0.259	0.509	11.473	---
8	1328.	2.9	2.7	0.317	0.563	11.234	---
2	1330.	2.9	2.8	0.620	0.787	7.413	8.210
2	1330.	2.9	2.8	0.620	0.787	7.413	8.210
1	1333.	2.9	2.8	7.180	2.680	2.740	2.364
1	1331.	2.9	2.8	6.250	2.500	2.785	2.396
12	1329.	7.7	6.5	0.036	0.191	31.962	35.346
12	1329.	7.7	6.5	0.041	0.202	31.555	34.847
8	1327.	7.7	7.3	0.062	0.248	22.647	---
8	1328.	7.7	7.3	0.076	0.276	22.178	---
2	1329.	7.7	7.5	0.151	0.389	14.553	16.057
2	1332.	7.7	7.5	0.190	0.436	14.241	15.674
2	1332.	7.7	7.5	0.133	0.365	14.761	16.308
1	1332.	7.7	7.6	1.160	1.077	5.672	4.876
1	1330.	7.7	7.6	1.300	1.140	5.594	4.817
12	1001.	2.9	2.4	0.470	0.686	10.398	9.612
12	1000.	2.9	2.4	0.420	0.648	10.589	9.772
8	999.	2.9	2.7	0.770	0.877	7.476	---
8	1004.	2.9	2.7	0.718	0.847	7.597	---
2	1003.	2.9	2.8	1.880	1.371	4.817	4.991
2	1003.	2.9	2.8	1.770	1.330	4.863	5.041
1	1001.	2.9	2.9	13.500	3.674	1.883	1.416
1	1001.	2.9	2.9	11.400	3.376	1.936	1.445

(continued)

TABLE V (continued)

Flow Control Orifice	Furnace Conditions: Temp. °C	Furnace Conditions: Initial Press atm	Furnace Conditions: Average Press atm	Ignition Time: t_i sec	Ignition Time: $t_i^{1/2}$ $sec^{1/2}$	Mean Surface Heat Flux: $\bar{F}_s(1)$ $cal/(cm)^2(sec)$	Mean Surface Heat Flux: $\bar{F}_s(2)$ $cal/(cm)^2(sec)$
12	1007.	7.7	6.5	0.097	0.312	21.204	19.459
12	1008.	7.7	6.5	0.085	0.292	21.679	19.856
8	1006.	7.7	7.3	0.190	0.436	14.872	---
8	1005.	7.7	7.3	0.200	0.447	14.737	---
2	1006.	7.7	7.5	0.520	0.721	9.377	8.373
2	1004.	7.7	7.5	0.561	0.749	9.241	8.264
1	1004.	7.7	7.6	4.400	2.098	3.531	2.720
1	1004.	7.7	7.6	4.500	2.121	3.516	2.712
12	760.	2.9	2.4	1.700	1.304	5.8[illegible]	5.400
12	759.	2.9	2.4	1.480	1.217	6.102	5.568
8	764.	2.9	2.5	4.700	2.168	3.738	---
8	764.	2.9	2.5	2.550	1.597	4.377	---
8	764.	2.9	2.5	2.200	1.483	4.527	---
8	764.	2.9	2.6	2.850	1.688	4.317	---
8	764.	2.9	2.6	2.700	1.643	4.375	---
2	761.	2.9	2.7	5.600	2.366	2.909	2.659
2	761.	2.9	2.7	7.240	2.691	2.725	2.506
2	761.	2.9	2.7	6.280	2.506	2.820	2.586
6	761.	2.9	2.7	12.600	3.550	2.070	1.927
6	761.	2.9	2.7	13.400	3.661	2.038	1.900
12	760.	7.7	6.5	0.700	0.837	10.182	9.410
12	760.	7.7	6.5	0.780	0.883	9.857	9.137
8	760.	7.7	7.2	0.980	0.990	7.908	---
8	759.	7.7	7.2	0.990	0.995	7.876	---
2	759.	7.7	7.4	2.390	1.546	5.058	4.270
2	760.	7.7	7.4	2.900	1.703	4.803	4.093
1	760.	7.7	7.2	39.500	6.285	1.492	---

(continued)

TABLE V (continued)

(1) These mean-surface-heat fluxes were calculated using heat-transfer results from the alumina gage heat-flux study.

(2) These mean-surface-heat fluxes were calculated using heat-transfer results from the GAR-infrared detector heat-flux study.

TABLE VI

SUMMARY OF UA PROPELLANT IGNITION TESTS IN NITROGEN

Flow Control Orifice	Furnace Conditions			Ignition Time		Mean Surface Heat Flux	
	Temp. °C	Initial Press atm	Average Press atm	t_i sec	$t_i^{1/2}$ $sec^{1/2}$	$\bar{F}_s(1)$ $cal/(cm)^2(sec)$	$\bar{F}_s(2)$
12	1302.	2.9	2.7	0.098	0.313	17.566	17.662
10	1304.	2.9	2.8	0.116	0.341	15.609	---
10	1305.	2.9	2.8	0.123	0.351	15.609	---
8	1305.	2.9	2.9	0.230	0.480	11.639	---
8	1305.	2.9	2.9	0.175	0.418	11.947	---
3	1305.	2.9	2.9	0.260	0.510	9.664	---
3	1304.	2.9	2.9	0.215	0.464	9.792	---
2	1302.	2.9	2.9	0.440	0.663	7.544	8.327
2	1301.	2.9	2.9	0.360	0.600	7.681	8.495
6	1302.	2.9	2.7	0.900	0.949	5.628	---
6	1304.	2.9	2.7	0.950	0.975	5.603	---
6	1302.	2.9	2.7	0.680	0.825	5.774	---
1	1304.	2.9	2.9	3.825	1.956	2.893	2.452
1	1311.	2.9	2.9	2.980	1.726	2.980	2.516
12	1308.	7.7	6.5	0.035	0.187	31.486	34.830
12	1303.	7.7	6.5	0.035	0.187	31.366	34.695
10	1306.	7.7	6.8	0.042	0.205	28.320	---
10	1305.	7.7	6.8	0.049	0.222	27.795	---
8	1303.	7.7	7.3	0.078	0.279	21.672	---
8	1301.	7.7	7.3	0.074	0.272	21.751	---
8	1302.	7.7	7.2	0.060	0.245	22.110	---
3	1301.	7.7	7.5	0.069	0.263	18.557	---
3	1303.	7.7	7.5	0.074	0.272	18.470	---
2	1301.	7.7	7.5	0.165	0.406	14.059	15.506
2	1302.	7.7	7.5	0.155	0.394	14.160	15.629
6	1304.	7.7	7.6	0.229	0.479	10.944	---
6	1302.	7.7	7.6	0.310	0.557	10.598	---

(continued)

TABLE VI (continued)

Flow Control Orifice	Furnace Conditions: Temp °C	Furnace Conditions: Initial Press atm	Furnace Conditions: Average Press atm	Ignition Time: t_i sec	Ignition Time: $t_i^{1/2}$ $sec^{1/2}$	Mean Surface Heat Flux: $\bar{F}_s(1)$ $cal/(cm)^2(sec)$	Mean Surface Heat Flux: $\bar{F}_s(2)$ $cal/(cm)^2(sec)$
1	1302.	7.7	7.6	0.960	0.980	5.635	4.832
1	1302.	7.7	7.6	1.150	1.072	5.530	4.756
12	1013.	2.9	2.5	0.278	0.527	11.414	10.458
12	1015.	2.9	2.5	0.264	0.514	11.516	10.545
8	1016.	2.9	2.7	0.455	0.675	8.191	---
8	1010.	2.9	2.7	0.480	0.693	8.084	---
8	1001.	2.9	2.7	0.510	0.714	7.960	---
8	1002.	2.9	2.7	0.480	0.693	8.034	---
2	1010.	2.9	2.8	1.110	1.054	5.234	5.419
2	1014.	2.9	2.8	1.140	1.068	5.236	5.421
1	1017.	2.9	2.8	8.700	2.950	2.027	1.507
1	1017.	2.9	2.8	10.500	3.240	1.971	1.477
12	996.	7.7	6.5	0.098	0.313	20.875	19.142
12	1001.	7.7	6.5	0.087	0.295	21.380	19.571
8	1001.	7.7	7.3	0.177	0.421	14.893	---
8	994.	7.7	7.3	0.170	0.412	14.886	---
2	988.	7.7	7.5	0.430	0.656	9.446	8.406
2	1000.	7.7	7.5	0.530	0.728	9.246	8.264
1	1001.	7.7	7.6	3.400	1.844	3.668	2.794
1	1001.	7.7	7.6	3.600	1.897	3.632	2.774
12	761.	2.9	2.4	1.090	1.044	6.580	5.927
12	761.	2.9	2.4	1.050	1.025	6.644	5.973
8	760.	2.9	2.7	1.850	1.360	4.764	---
8	760.	2.9	2.7	1.750	1.323	4.821	---
2	760.	2.9	2.8	4.600	2.145	3.037	2.735
2	760.	2.9	2.8	4.320	2.078	3.079	2.769
6	764.	2.9	2.8	7.280	2.698	2.366	2.157

(continued)

TABLE VI (continued)

Control Orifice	Furnace Conditions: Temp. °C	Furnace Conditions: Press atm	Furnace Conditions: Press atm	Ignition Time: t_i sec	Ignition Time: $t_i^{1/2}$ $sec^{1/2}$	Mean Surface Heat Flux: $\bar{F}_s(1)$ $cal/(cm)^2(sec)$	Mean Surface Heat Flux: $\bar{F}_s(2)$ $cal/(cm)^2(sec)$
1	764.	2.9	2.7	47.500	2.892	1.066	---
12	757.	7.7	6.5	0.340	0.583	12.270	11.091
12	758.	7.7	6.5	0.420	0.648	11.644	10.589
12	758.	7.7	6.5	0.395	0.628	11.831	10.740
8	760.	7.7	7.2	0.710	0.843	8.529	---
8	760.	7.7	7.2	0.765	0.875	8.372	---
3	761.	7.7	7.4	1.000	1.000	7.083	---
3	760.	7.7	7.4	1.210	1.100	6.745	---
3	760.	7.7	7.4	1.020	1.010	7.039	---
6	759.	7.7	7.5	3.750	1.936	3.920	---
6	760.	7.7	7.5	3.450	1.857	4.012	---
1	758.	7.7	7.5	20.750	4.555	1.819	1.224

(1) These mean-surface-heat fluxes were calculated using heat-transfer results from the alumina gage heat-flux study.

(2) These mean-surface-heat fluxes were calculated using heat-transfer results from the GAR-infrared detector heat-flux study.

TABLE VII

SUMMARY OF FM PROPELLANT ITNITION DATA IN HELIUM

Flow Control Orifice	Furnace Conditions			Ignition Time		Mean Surface Heat Flux
	Temp. °C	Initial Press atm	Average Press atm	t_i sec	$t_i^{\frac{1}{2}}$ $sec^{\frac{1}{2}}$	$\bar{F}_s$ $cal/(cm)^2(sec)$
12	992.	2.9	2.8	0.082	0.286	25.187
12	979.	2.9	2.8	0.090	0.300	24.375
8	980.	2.9	2.8	0.174	0.417	18.218
8	982.	2.9	2.8	0.170	0.412	18.340
8	982.	2.9	2.8	0.125	0.354	19.352
2	986.	2.9	2.8	0.500	0.707	10.808
2	986.	2.9	2.8	0.588	0.767	10.479
2	986.	2.9	2.8	0.410	0.640	11.200
6	992.	2.9	2.8	0.796	0.892	7.899
6	992.	2.9	2.8	0.800	0.894	7.893
1	989.	2.9	2.8	6.620	2.573	3.222
12	987.	7.7	7.5	0.030	0.175	46.201
12	992.	7.7	7.5	0.021	0.145	49.799
12	992.	7.7	7.5	0.019	0.130	50.653
12	991.	7.7	7.5	0.030	0.173	46.816
12	987.	7.7	7.5	0.035	0.187	45.477
8	992.	7.7	7.6	0.036	0.191	36.473
8	991.	7.7	7.6	0.041	0.202	35.716
2	992.	7.7	7.6	0.098	0.313	23.305
2	992.	7.7	7.6	0.092	0.303	23.562
1	992.	7.7	7.6	1.160	1.077	7.466
1	992.	7.7	7.6	1.140	1.068	7.491
12	758.	2.9	2.8	0.650	0.806	11.364
12	759.	2.9	2.8	0.560	0.748	11.914
12	769.	2.9	2.8	0.520	0.721	12.363
12	765.	2.9	2.8	0.540	0.735	12.153

(continued)

TABLE VII (continued)

Furnace Conditions			Ignition Time		Mean Surface Heat Flux
Flow Control Orifice	Temp. °C	Initial Press atm	Average Press atm	t_i sec	$t_i^{1/2}$ $sec^{1/2}$	$\bar{F}_s$ $cal/(cm)^2(sec)$
8	760.	2.9	2.8	0.748	0.865	9.650
8	759.	2.9	2.8	0.864	0.930	9.248
8	759.	2.9	2.8	0.800	0.894	9.455
2	760.	2.9	2.8	2.300	1.517	5.548
2	761.	2.9	2.8	2.970	1.723	5.157
6	761.	2.9	2.9	3.500	1.871	4.151
12	756.	7.7	7.4	0.085	0.292	21.231
8	758.	7.7	7.6	0.180	0.424	19.334
2	756.	7.7	7.6	0.400	0.632	12.405
1	752.	7.7	7.6	3.150	1.775	4.595
1	754.	7.7	7.6	3.150	1.775	4.609

TABLE VIII

SUMMARY OF G PROPELLANT IGNITION DATA IN HELIUM

Flow Control Orifice	Furnace Conditions			Ignition Time		Mean Surface Heat Flux
	Temp. °C	Initial Press atm	Average Press atm	t_i sec	$t_i^{\frac{1}{2}}$ $sec^{\frac{1}{2}}$	$\bar{F}_s$ $cal/(cm)^2(sec)$
12	991.	2.9	2.8	0.230	0.480	20.018
8	990.	2.9	2.8	0.370	0.608	15.498
2	989.	2.9	2.8	0.900	0.949	9.434
1	986.	2.9	2.8	5.200	2.280	3.318
12	995.	7.7	7.5	0.052	0.228	41.359
8	988.	7.7	7.6	0.075	0.274	31.277
2	992.	7.7	7.6	0.140	0.374	21.554
1	992.	7.7	7.6	1.320	1.149	7.205
12	764.	2.9	2.8	0.830	0.911	10.398
12	764.	2.9	2.8	0.764	0.874	10.687
12	758.	2.9	2.8	1.010	1.005	9.643
12	760.	2.9	2.8	.776	.881	10.571
8	761.	2.9	2.8	1.334	1.155	7.975
8	761.	2.9	2.8	1.284	1.133	8.074
2	759.	2.9	2.8	4.610	2.147	4.391
2	758.	2.9	2.8	3.800	1.949	4.672
6	757.	2.9	2.9	6.550	2.559	3.404
12	753.	7.7	7.5	0.240	0.490	19.430
8	758.	7.7	7.6	0.375	0.612	15.215
8	758.	7.7	7.6	0.360	0.600	15.420
2	756.	7.7	7.6	0.900	0.949	9.621
1	755.	7.7	7.6	3.400	1.844	4.446

TABLE IX

SUMMARY OF UA PROPELLANT IGNITION DATA IN HELIUM

Flow Control Orifice	Furnace Conditions: Temp. °C	Furnace Conditions: Initial Press atm	Furnace Conditions: Average Press atm	Ignition Time: t_i sec	Ignition Time: $t_i^{1/2}$ $sec^{1/2}$	Mean Surface Heat Flux: $\bar{F}_s$ $cal/(cm)^2(sec)$
12	992.	2.9	2.8	0.105	0.324	23.670
12	992.	2.9	2.8	0.115	0.339	23.248
8	990.	2.9	2.8	0.170	0.412	18.217
8	990.	2.9	2.8	0.160	0.400	18.427
2	991.	2.9	2.8	0.468	0.684	10.631
2	991.	2.9	2.8	0.506	0.711	10.672
1	993.	2.9	2.8	5.120	2.263	3.347
1	992.	2.9	2.8	5.920	2.433	3.250
12	986.	7.7	7.5	0.027	0.166	46.299
12	987.	7.7	7.5	0.024	0.154	47.653
12	986.	7.7	7.5	0.022	0.150	48.093
12	985.	7.7	7.5	0.023	0.152	47.842
8	987.	7.7	7.6	0.034	0.184	36.160
8	985.	7.7	7.6	0.051	0.226	33.533
8	981.	7.7	7.6	0.034	0.185	35.865
2	987.	7.7	7.6	0.084	0.290	23.438
2	992.	7.7	7.6	0.082	0.286	23.676
1	985.	7.7	7.6	1.620	1.273	6.780
1	991.	7.7	7.6	.990	.995	2.561
1	988.	7.7	7.6	.884	.940	7.695
12	753.	2.9	2.8	0.540	0.735	11.629
12	755.	2.9	2.8	0.505	0.711	11.903
6	760.	2.9	2.8	3.190	1.786	4.151
6	755.	2.9	2.9	2.850	1.688	4.238
12	754.	7.7	7.5	0.243	0.493	19.182
12	754.	7.7	7.5	0.390	0.624	16.187
12	754.	7.7	7.5	0.220	0.469	19.843
2	758.	7.7	7.6	0.360	0.600	12.503
2	760.	7.7	7.6	0.385	0.620	12.321
1	760.	7.7	7.6	2.850	1.688	4.668

TABLE X

SUMMARY OF ALUMINA GAGE* HEAT TRANSFER STUDY IN NITROGEN

Flow Control Orifice	Furnace Conditions			Gas Mass Flow Rate G gm/(cm)^2(sec)	Gas Flow Reynolds No. Re $Dv\rho/\mu$	Heat Transfer Coefficient h cal/(cm)^2(sec)(°K)	Nusselt Number Divided by Prandtl Number to the 0.3 $Nu/Pr^{0.3}$
	Temp °C	Initial Press atm	Average Press atm				
12	1309.	2.9	2.5	13.97	17.88×10^3	1.558×10^{-2}	54.25
12	1314.	2.9	2.5	13.95	17.85	1.573	54.77
10	1302.	2.9	2.6	11.65	14.92	1.457	50.73
10	1306.	2.9	2.6	11.64	14.90	1.461	50.87
8	1303.	2.9	2.7	7.71	9.87	1.114	38.79
8	1305.	2.9	2.7	7.71	9.87	1.108	38.58
3	1307.	2.9	2.8	5.65	7.23	0.952	33.15
3	1303.	2.9	2.8	5.66	7.24	0.937	32.63
2	1304.	2.9	2.8	3.95	5.06	0.731	25.45
2	1306.	2.9	2.8	3.59	5.06	0.735	25.59
6	1308.	2.9	2.8	2.63	3.37	0.526	18.32
6	1308.	2.9	2.8	2.63	3.37	0.525	18.28
1	1306.	2.9	2.8	1.02	1.30	0.300	10.43
1	1306.	2.9	2.8	1.02	1.30	0.302	10.51
12	1302.	7.7	6.5	37.06	47.44	3.095	107.77
12	1302.	7.7	6.5	37.06	47.44	3.074	107.04
10	1301.	7.7	6.9	30.86	39.49	2.867	99.83

(continued)

* The thermal responsivity of the alumina gage is 0.208 cal/(cm)^2(sec)$^{\frac{1}{2}}$(°K).

TABLE X (continued)

Flow Control Orifice	Furnace Condition: Temp °C	Initial Press atm	Average Press atm	Gas Mass Flow Rate G gm/(cm)^2(sec)	Gas Flow Reynolds No. Re $Dv\rho/\mu$	Heat Transfer Coefficient h cal/(cm)^2(sec)(°K)	Nusselt Number Divided by Prandtl Number to the 0.3 $Nu/Pr^{0.3}$
10	1304.	7.7	6.9	30.83	39.46×10^3	2.854×10^{-2}	99.38
8	1302.	7.7	7.3	20.42	26.14	2.161	75.25
8	1303.	7.7	7.3	20.42	26.13	2.153	74.97
3	1305.	7.7	7.4	14.96	19.15	1.792	62.40
3	1300.	7.7	7.4	14.99	19.18	1.777	61.88
2	1305.	7.7	7.5	10.41	13.39	1.333	46.42
2	1306.	7.7	7.5	10.46	13.39	1.354	47.15
6	1301.	7.7	7.6	6.99	8.94	0.995	34.65
6	1301.	7.7	7.6	6.99	8.94	1.001	34.85
1	1305.	7.7	7.6	2.70	3.45	0.556	19.36
1	1295.	7.7	7.6	2.71	3.46	0.551	19.18
12	996.	2.9	2.5	15.60	22.93	1.545	63.96
12	997.	2.9	2.5	15.59	22.92	1.538	63.67
10	998.	2.9	2.6	12.97	19.07	1.436	59.45
10	998.	2.9	2.6	12.97	19.07	1.426	59.04
8	998.	2.9	2.7	8.92	13.11	1.101	45.58
8	997.	2.9	2.7	8.92	13.11	1.087	45.00
3	996.	2.9	2.8	6.30	9.27	0.910	37.67
3	995.	2.9	2.8	6.31	9.27	0.904	37.43

(continued)

TABLE X (continued)

Flow Control Orifice	Furnace Conditions			Gas Mass Flow Rate G	Gas Flow Reynolds No. Re	Heat Transfer Coefficient	Nusselt Number Divided by Prandtl Number to the 0.3
	Temp °C	Initial Press atm	Average Press atm	gm/(cm)^2(sec)	$Dv\rho/\mu$	cal/(cm)^2(sec)(°K)	$Nu/Pr^{0.3}$
2	996.	2.9	2.8	4.41	6.48×10^3	0.711×10^{-2}	29.44
2	996.	2.9	2.8	4.41	6.48	0.704	29.15
6	999.	2.9	2.8	2.94	4.31	0.517	21.40
6	997.	2.9	2.8	2.94	4.32	0.511	21.16
1	999.	2.9	2.8	1.14	1.67	0.234	9.69
1	996.	2.9	2.8	1.14	1.67	0.235	9.73
12	1000.	7.7	6.5	41.23	60.60	3.280	135.79
12	1004.	7.7	6.5	41.16	60.51	3.229	133.68
10	1001.	7.7	6.8	34.30	50.42	2.851	118.03
10	1002.	7.7	6.8	34.28	50.40	2.806	116.17
8	1002.	7.7	7.3	22.70	33.36	2.172	89.92
8	1000.	7.7	7.3	22.72	33.39	2.157	89.30
3	1001.	7.7	7.4	16.65	24.48	1.747	72.32
3	1001.	7.7	7.4	16.66	24.50	1.718	71.13
2	1004.	7.7	7.5	11.63	17.10	1.344	55.64
2	1006.	7.7	7.5	11.62	17.08	1.340	55.48
6	1003.	7.7	7.5	7.76	11.40	0.979	40.53
6	1004.	7.7	7.5	7.76	11.40	0.974	40.32
1	1002.	7.7	7.6	3.00	4.41	0.534	22.11
1	1005.	7.7	7.6	3.00	4.41	0.524	21.69

TABLE XI

SUMMARY OF ALUMINA GAGE* HEAT TRANSFER STUDY IN HELIUM

Flow Control Orifice	Furnace Conditions		Gas Mass Flow Rate G $gm/(cm)^2(sec)$	Gas Flow Reynolds No. Re $Dv\rho/\mu$	Heat Transfer Coefficient h $cal/(cm)^2(sec)(°K)$	Nusselt Number Divided by Prandtl Number to the 0.3 $Nu/Pr^{0.3}$
	Temp. °C	Initial Press atm / Average Press atm				
12	1008.	2.9 / 2.8	6.24	8.21×10^3	3.899×10^{-2}	33.06
12	1007.	2.9 / 2.8	6.24	8.21	3.921	33.25
8	1007.	2.9 / 2.8	3.44	4.52	2.988	25.34
8	1005.	2.9 / 2.8	3.44	4.53	2.976	25.24
2	1006.	2.9 / 2.8	1.76	2.32	1.740	14.76
2	1006.	2.9 / 2.8	1.76	2.32	1.777	15.07
1	1006.	2.9 / 2.8	0.45	0.60	0.551	4.67
1	1006.	2.9 / 2.8	0.45	0.60	0.544	4.61
12	1005.	7.7 / 7.4	16.53	21.75	7.634	64.74
12	1002.	7.7 / 7 4	16.54	21.77	7.877	66.80
12	1002.	7.7 / 7.4	16.54	21.77	7.856	66.19
8	1005.	7.7 / 7.6	9.11	11.98	5.565	47.19
8	1002.	7.7 / 7.6	9.12	12.00	5.984	50.74
2	1005.	7.7 / 7.6	4.67	6.15	3.611	30.62
2	1005.	7.7 / 7.6	4.67	6.15	3.684	31.24

(continued)

*The thermal responsivity of the alumina heat-flux gage is 0.208 $cal/(cm)^2(sec)^{\frac{1}{2}}(°K)$

TABLE XI (continued)

Flow Control Orifice	Furnace Conditions		Gas Mass Flow Rate G gm/(cm)^2(sec)	Gas Flow Reynolds No. Re $dv\rho/\mu$	Heat Transfer Coefficient h cal/(cm)^2(sec)(°K)	Nusselt Number Divided by Prandtl Number to the 0.3 $Nu/Pr^{0.3}$
	Temp. °C	Initial Press atm / Average Press atm				
1	1005.	7.7 / 7.6	1.20	1.58×10^3	1.249×10^{-2}	10.59
1	1005.	7.7 / 7.6	1.20	1.58	1.226	10.37
12	755.	2.9 / 2.7	6.96	10.64	3.790	37.33
12	755.	2.9 / 2.7	6.96	10.64	3.752	36.96
8	755.	2.9 / 2.8	3.84	5.86	2.768	27.46
8	755.	2.9 / 2.8	3.84	5.86	2.753	27.12
2	752.	2.9 / 2.8	1.97	3.01	1.668	16.43
2	751.	2.9 / 2.8	1.97	3.01	1.608	15.84
1	753.	2.9 / 2.8	0.51	0.77	0.456	4.49
12	752.	7.7 / 7.4	18.45	28.21	7.441	73.29
12	753.	7.7 / 7.4	18.44	28.20	7.473	73.61
8	755.	7.7 / 7.6	10.15	15.52	5.470	53.88
8	753.	7.7 / 7.6	10.16	15.54	5.472	53.90
2	752.	7.7 / 7.6	5.21	7.97	3.379	33.28
2	752.	7.7 / 7.6	5.21	7.97	3.331	33.81
1	755.	7.7 / 7.6	1.34	2.04	1.330	13.10
1	757.	7.7 / 7.6	1.34	2.04	1.306	12.86

TABLE XII

HEAT-TRANSFER STUDY IN NITROGEN EMPLOYING THE INFRARED-DETECTION SYSTEM AND SIMULATED PROPELLANT GAR

Flow Control Orifice	Furnace Conditions			Gas Mass Flow Rate G gm/(cm)^2(sec)	Ignition Time t_i sec	GAR Surface Temperature T_s °C	Mean Heat Transfer Coefficient	
	Temp °C	Initial Press atm	Average Press atm				$\bar{h}(1)$ cal/(cm)^2(sec)(°K)	$\bar{h}(T^*)^{0.3}(2)$ cal/(cm)^2(sec)(°K)
12	1305.	2.9	2.7	13.97	0.098	246.	1.715×10^{-2}	1.610×10^{-2}
2	1308.	2.9	2.9	3.95	0.400	234.	0.806	0.757
1	1315.	2.9	2.9	1.02	3.390	196.	0.230	0.216
12	1295.	7.7	6.5	37.06	0.035	275.	3.520	3.304
2	1295.	7.7	7.5	10.46	0.160	264.	1.562	1.466
1	1305.	7.7	7.6	2.70	1.052	213.	0.453	0.425
12	1015.	2.9	2.5	15.57	0.270	239.	1.415	1.415
2	1014.	2.9	2.8	4.28	1.125	252.	0.746	0.746
1	1007.	2.9	2.8	1.06	9.580	200.	0.190	0.190
12	994.	7.7	6.5	41.22	0.093	258.	2.740	2.740
2	1002.	7.7	7.5	11.33	0.479	254.	1.178	1.178
1	1005.	7.7	7.6	2.82	3.500	229.	0.376	0.376
12	765.	2.9	2.4	17.20	1.070	282.	1.322	1.543
2	767.	2.9	2.8	4.73	4.460	266.	0.590	0.689
6	762.	2.9	2.8	3.21	7.275	263.	0.459	0.536
12	762.	7.7	6.5	45.52	0.383	309.	2.580	3.011
2	755.	7.7	7.5	12.51	1.970	282.	0.993	1.159
1	760.	7.7	7.5	3.11	20.800	250.	0.257	0.300

(continued)

TABLE XII (continued)

(1) Mean surface heat transfer coefficients, $\bar{h}$, were calculated using the GAR surface temperature, T_s, measured at ignition time, t_i, and Equation 5. The thermal responsivity, Γ, of GAR is 0.0315.

(2) T^* is equal to 1273°K divided by the gas temperature in degrees Kelvin.

TABLE XIII

SUMMARY OF 1.9 CM LONG PROPELLANT SAMPLE IGNITION TESTS IN NITROGEN

Propellant Sample Code Name	Flow Control Orifice	Furnace Conditions		Position Fraction of Sample Length
		Gas Temp °C	Initial Press atm	
FM	2	1050.	2.9	1/4
FM	2	1050.	2.9	1/6
FM	2	1050.	2.9	1/8
FM	2	1050.	2.9	1/10
FM	12	1013.	2.9	1/5
FM	12	1013.	2.9	1/5
FM	12	1013.	2.9	1/5
FM	12	750.	7.7	1/8
FM	2	1361.	2.9	1/8
FM	2	1361.	2.9	1/5
FM(1)	2	1305.	2.9	1/10
FM	2	1301.	2.9	1/10
SFM(2)	2	1298.	2.9	0-1/4
SFM	2	1298.	2.9	0-1/3
SFM	2	1298.	2.9	0-1/2
FM	2	1298.	2.9	1/3
XF(3)	12	764.	7.7	1/2
XF	12	764.	7.7	1/8
XF	12	761.	7.7	1/2
XF	12	758.	7.7	1/5

(1) For this test and those reported below, the rectangular orifice turbulence trip was removed.

(2) SFM is FM propellant roughened by 400 grain sandpaper.

(3) XF is similar to FM propellant but contains 10 per cent aluminum.

TABLE XIV

POLYMERIC FUEL BINDER DECOMPOSITION STUDIES

Polymer Code Name	Flow Control Orifice	Furnace Conditions Gas Temp °C	Furnace Conditions Initial Press atm	Sample Surface Temp. at Plateau T_s °C
PC	12	1315.	2.9	515.
PC	12	1319.	2.9	512.
PC	12	1315.	2.9	519.
PCC	12	1315.	2.9	540.
PCC	12	1313.	2.9	532.
PCC	12	1315.	2.9	542.
PCC	12	1317.	2.2	525.
PUC	12	1008.	2.9	423.
PUC	12	1008.	2.9	426.
PUC	12	1009.	2.9	423.
PUC	12	1011.	2.2	436.
PUC	12	1011.	2.2	427.
PUC	12	1014.	2.2	435.
PCC	12	1309.	2.2	542.
PCC	12	1309.	2.2	540.
PCC	12	1309.	2.2	540.
PC	12	1311.	2.2	510.
PC	12	1310.	2.2	502.
PC	12	1308.	2.2	505.
A05	12	1310.	2.2	549.
A05	12	1310.	2.2	522.
A05	12	1306.	2.2	522.
A05	12	1307.	2.9	522.
A05	12	1307.	2.9	545.
A05	12	1308.	2.9	530.

(continued)

TABLE XIV (continued)

Polymer Code Name	Flow Control Orifice	Furnace Conditions Gas Temp. °C	Furnace Conditions Initial Press atm	Sample Surface Temp. at Plateau T_s °C
PCC	2	1308.	2.9	533.
PUC	12	1311.	7.7	426.
PUC	12	1311.	7.7	426.
PUC	2	1310.	2.9	430.
AO5	2	1012.	2.9	475.*
AO5	12	1016.	2.9	476.*
AO5	12	1016.	2.9	478.*
PUG	12	1006.	2.9	373.*
PUG	12	1006.	2.9	367.*
AO5	12	1004.	2.9	510.*
AO5	12	1004.	2.9	506.*
PFC**	12	1009.	2.9	499.*
PFC	12	1009.	2.9	500.*
PFC	12	1007.	2.9	482.*

* The sample surface temperature was still rising at the end of these tests.

** PFC is made from a polyflurocarbon.

TABLE XV

DATA FROM GAR THERMAL-RESPONSIVITY MEASUREMENTS (1)

Initial Temperature		Interface Temperature	Thermal Responsivity
GAR °C	FM °C	T_i °C	$cal/(cm)^2(sec)^{\frac{1}{2}}(°K)$
24.4	81.8	52.15	0.0304
25.2	81.0	47.20	0.0326
25.3	81.0	48.60	0.0295
81.0	25.2	57.20	0.0285
80.5	25.3	59.30	0.0340
80.5	25.3	58.85	0.0328
80.5	25.3	58.93	0.0331

(1) Thermal responsivity of FM propellant is 0.0212 (25).

APPENDIX F

THE HEAT-TRANSFER COMPUTER PROGRAM

A. PROGRAM DESCRIPTION

The program is written in Fortran IV language and is designed for use on a UNIVAC 1108 computer system.

The program calculates instantaneous heat-transfer coefficients from surface temperature-time data by an integration of Equation (C-6).

B. DEFINITION OF PROGRAM VARIABLE NAMES

F	Instantaneous heat flux
HTC	Instantaneous heat-transfer coefficient
HTCA	Average heat-transfer coefficient
NUM	Number of data points in set
ORI	Orifice number
PRESS	Gas pressure
RT	Temperature in cm
SENS	Temperature, °C, per cm
SPOG	Thermal responsivity divided by two times the square root of pi
TIME	Time, sec, per cm
TG	Gas temperature
X	Time in cm

APPENDIX F (continued)

TABLE XVI

LISTING OF HEAT-TRANSFER PROGRAM

```
      DIMENSION X(40), T(40), RT(40), SX(40), SG(40), F(40), V(40),
     HTC(40), SUM(40)
66    FORMAT (3E15.5, I2, J2)
77    FORMAT (2E15.5)
88    FORMAT (5E20.5)
89    FORMAT (1HO, 9HGAS TEMP=,E15.8,5X,6H PRESS=, E15.8, 5X, 7H ORIFICE,
     I3, 5X, 8HAVG HTC HTC=, E15.8)
99    READ 66, SPOG, TG, PRESS, NUM, ORI
      READ 77, SENS, TIME
      NU = NUM + 1
      DO 21 J=2, NU
      READ 77, (X(J)*SENS
      RT(J)=RT(J)*SENS
      X(J) = X(J) * TIME
      SX(J) = SQRT(X(J))
21    T(J) = RT (J) - .000410*RT(J)*RT(J)
      RT(1) = 0.
      SX(1) = 0.
      T(1) = 0.
      X(1) = 0.
      SUM(2) = 0.
      RNUM = NUM
      DO 30 I = 2, NU
      PS5 = 0.0
      PS1 = 3.14159 * T(I)
      PS2 = (T(I)*SX(I-1)-T(I-1)*SX(I))/SQRT(X(I)-X(I-1))
      IF (J-1) 41, 41, 42
42    DO 31 N=2, J
```

(continued)

APPENDIX F (continued)

```
      PS3 = (T(I)*SX(N)-T(N)*SX(J))/((X(I)-X(N)*SQRT(X(I) - X (N)))
      V(N) = (PS3 + PS4)*0.5*(X(N) - X(N-1))
31    PS5 = PS5 + V(N)
41    GF(I) = (PS1+PS2+PS5)/SX(I)
      F(I) = GF(I)*SPOG
      HTC(I) = F(I)/(TG-RT(I)-19.)
30    SUM(I) = SUM(J)+HTC(I)
      HTCA = SUM(NU)/RNUM
      PRINT 89, TG, PRESS, ORI, HTCA
      PRINT 88, (X(K), RT(K), T(K), F(K), HTC(K), K=2, NU)
      GO TO 99
```

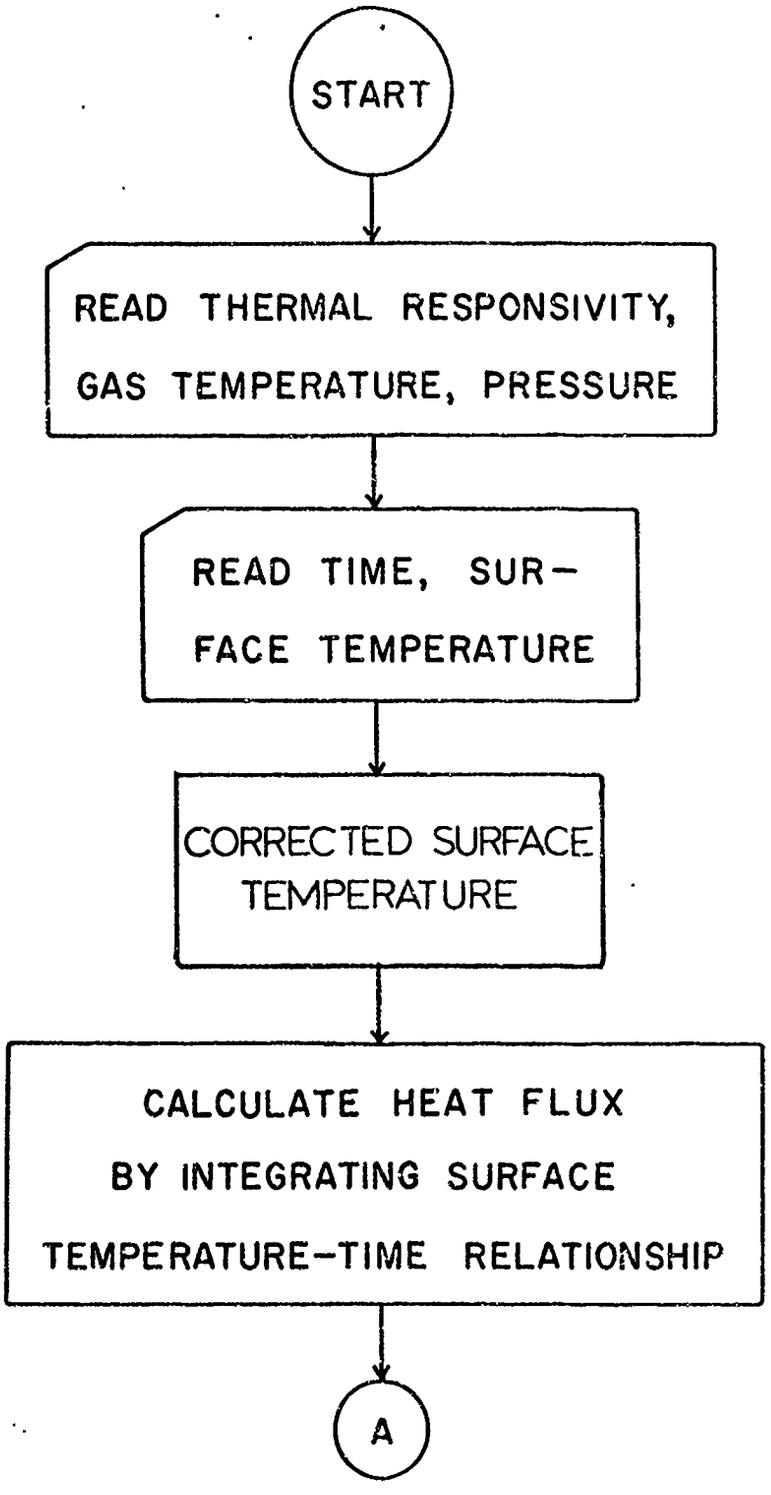

FIGURE 40. PROGRAM-FLOW CHART OF HEAT-TRANSFER COEFFICIENT CALCULATIONS.

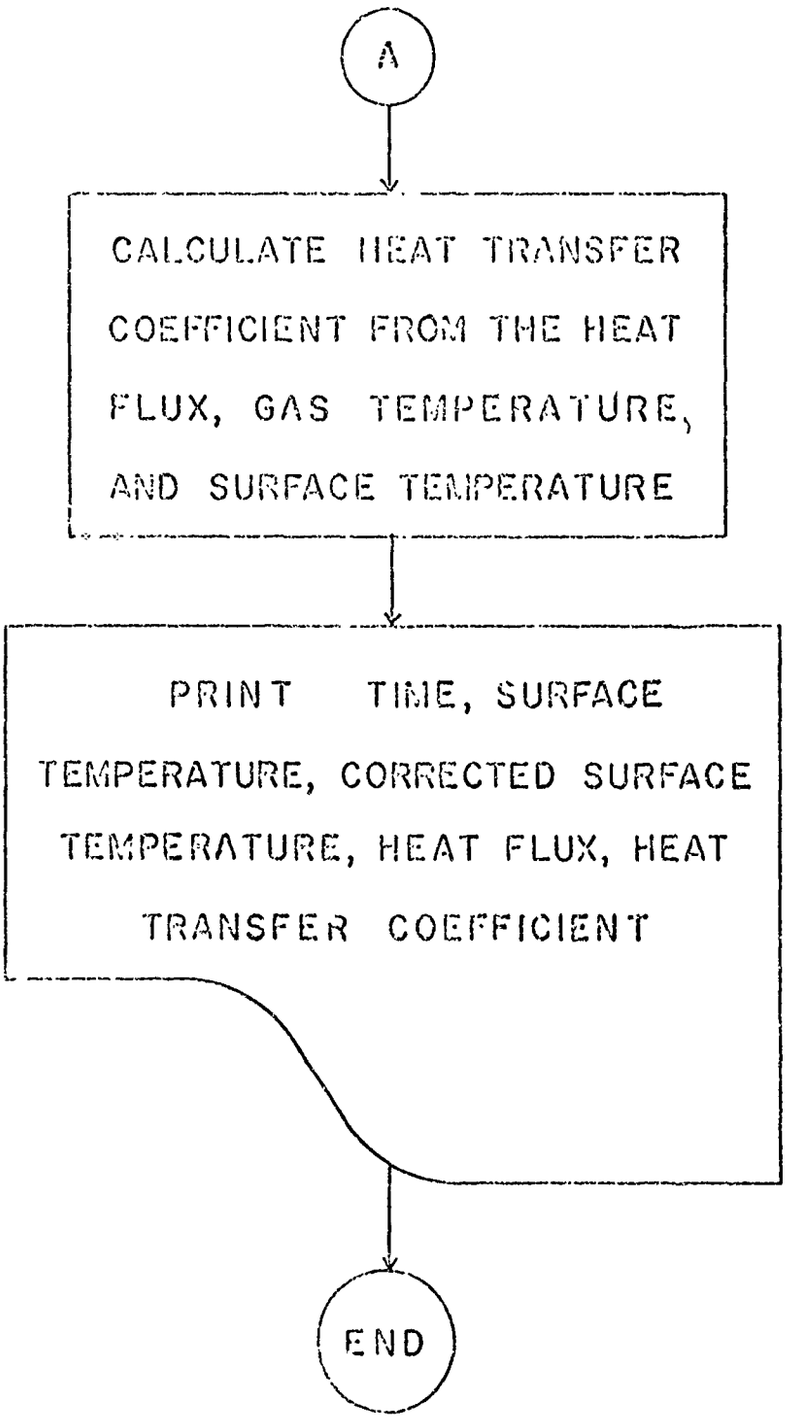

FIGURE 40. (continued)

APPENDIX G

NOMENCLATURE

Symbol	Definitions	Units
B	Product of frequency factor, z, and energy released at the propellant surface per unit area	$cal/(cm)^2(sec)$
C	Heat capacity	cal/(g)(°K)
D	Hydraulic diameter of flow channel: four times the cross-sectional area divided by the wetted perimeter of the channel	cm
E_a	Activation energy for key ignition reaction	cal/mole
F	Heat flux	$cal/(cm)^2(s\ c)$
F_s	Surface heat flux	$cal/(cm)^2(sec)$
$\bar{F}_s$	Mean surface heat flux	$cal/(cm)^2(sec)$
F_t	Total heat flux at the propellant surface	$cal/(cm)^2(sec)$
G	Mass flow rate of test gas through flow channel	$gm/(cm)^2(sec)$
h	Convective heat transfer coefficient	$cal/(cm)^2(sec)(°K)$
$\bar{h}$	Mean convective heat transfer coefficient	$cal/(cm)^2(sec)(°K)$
$\bar{h}^+$	Mean convective heat transfer coefficient calculated at linear ignition temperature	$cal/(cm)^2(sec)(°K)$
k	Thermal conductivity	cal/(cm)(sec)(°K)
N	$N = \frac{h\ (t)^{\frac{1}{2}}}{r}$	dimensionless
N_u	Nusselt number (h D/k)	dimensionless
P_r	Prandtl number (cμ/k)	dimensionless

APPENDIX G (continued)

Symbol	Definitions	Units
Q_s	Energy released at the propellant surface by key ignition reaction	$cal/(cm)^2(sec)$
R	Gas constant (1.987)	cal/(mole)(°K)
Re	Reynolds number of fluid stream, based on hydraulic diameter of test section channel, $(Dv\rho/\mu)$	dimensionless
S	Slope of line that represents ignition data plotted in the form $\log (\bar{F}_s)$ versus $\log (t_i)^{\frac{1}{2}}$	---
t	Time	sec
t_i	Ignition time	sec
t_e	Time when GAR surface temperature reaches propellant linear ignition temperature	sec
T	Temperature	°C
T_G	Gas temperature	°C
T_o	Initial temperature	°C
T_s	Surface temperature	°C
T_{si}^L	Linear ignition temperature	°C
T^*	1273°C divided by T_G in degrees Kelvin	dimensionless
v	Linear velocity of gas in test section	cm/sec
x	Distance into solid measured from the surface	cm
α	Thermal diffusivity	$(cm)^2/sec$
Γ	Thermal responsivity; the square root of the product of thermal conductivity, density, and heat capacity	$cal/(cm)^2(sec)^{\frac{1}{2}}(°K)$
ρ	Density	$gm/(cm)^3$
μ	Viscosity	(gm)(cm)/sec

UNCLASSIFIED

Security Classification

DOCUMENT CONTROL DATA - R & D

68-1665

(Security classification of title, body of abstract and indexing annotation must be entered when the overall report is classified)

1. ORIGINATING ACTIVITY (Corporate author)	2a. REPORT SECURITY CLASSIFICATION
University of Utah Chemical Engineering Department Salt Lake City, Utah 84112	UNCLASSIFIED 2b. GROUP

3. REPORT TITLE

AMMONIUM PERCHLORATE-BASED PROPELLANT IGNITION BY LOW-CONVECTIVE HEAT FLUXES

4. DESCRIPTIVE NOTES (Type of report and inclusive dates)

Scientific Technical

5. AUTHOR(S) (First name, middle initial, last name)

Charles P. Richardson, Norman W. Ryan, Alva D. Baer

6. REPORT DATE	7a. TOTAL NO. OF PAGES	7b. NO. OF REFS
1 August 1968	151	55

8a. CONTRACT OR GRANT NO	9a. ORIGINATOR'S REPORT NUMBER(S)
AF-AFOSR 40-67 and 67-40A	
b. PROJECT NO. 9711-01	
c. 61445014	9b. OTHER REPORT NO(S) (Any other numbers that may be assigned this report)
d. 681308	AFOSR 68-1665

10. DISTRIBUTION STATEMENT

2. This document is subjected to special export controls and each transmittal to foreign governments of foreign nationals must be made only with prior approval of AFOSR (SRGO).

11. SUPPLEMENTARY NOTES	12. SPONSORING MILITARY ACTIVITY
Tech, Other	AF Office of Scientific Research (SREP) 1400 Wilson Boulevard Arlington, Virginia 22209

13. ABSTRACT

The ignition response to convective heating of a series of ammonium perchlorate-based composite propellants was determined. Surface-heat fluxes in the range of 2-50 cal/(cm)^2(sec) were employed at pressures of 2-10 atmospheres of nitrogen or helium. Ignition times were determined by use of photoconductive detectors which indicated the appearance of first flame in the dark convective heating environment. The light signal was shown to correspond in time to the rapid rise of surface temperature measured by means of infrared radiation from the surface.

Close agreement was found between ignition data derived from these tests when a gas temperature of 750°C was used and previously reported data from the thermal radiation heating of the same propellants. When convective heating-gas temperatures above 1000°C were used, it was found that the ignition times were about 80 per cent of the values observed at the same mean-heat flux for radiative heating and for tests at lower gas temperatures. In all cases, it was possible to represent the ignition data in terms of a thermal ignition model which considers a single, exothermic, Arrhenius type surface reaction. The indicated activation energy for this reaction is 25-30 kcal/gm mole under all conditions; however, the pre-exponential factor is higher by a factor of five when the higher temperature convective heating gases were employed than under other conditions. It is postulated that reactions in the thin high-temperature boundary layer yield additional energy or reactive species which feed energy back to the surface. Since the activation energy is unchanged, it is presumed that the decomposition reaction of the ammonium perchlorate limits the initial reactive species.

DD FORM 1 NOV 65 1473

UNCLASSIFIED

Security Classification

14 KEY WORDS	LINK A		LINK B		LINK C	
	ROLE	WT	ROLE	WT	ROLE	WT
Solid Propellant Ignition						
Ammonium Perchlorate Propellants						
Convective Heating						
Heat transfer						
Surface Temperature Measurements						
Composite Propellants						